ornl

OAK
RIDGE
NATIONAL
LABORATORY

UNION
CARBIDE

NUREG/CR-1159
ORNL/NUREG/TM-367

MASTER

Mathematical Phantoms Representing Children of Various Ages for Use in Estimates of Internal Dose

M. Cristy

Prepared for the
U.S. Nuclear Regulatory Commission
Office of Nuclear Regulatory Research
Under Interagency Agreement DOE 40-550-75

HEALTH AND SAFETY RESEARCH DIVISION
OAK RIDGE NATIONAL LABORATORY

OPERATED BY
UNION CARBIDE CORPORATION
FOR THE UNITED STATES
DEPARTMENT OF ENERGY

Printed in the United States of America. Available from
National Technical Information Service
U.S. Department of Commerce
5285 Port Royal Road, Springfield, Virginia 22161

Available from
GPO Sales Program
Division of Technical Information and Document Control
U.S. Nuclear Regulatory Commission
Washington, D.C. 20555

NUREG/CR-1159
ORNL/NUREG/TM-367
Dist. Category RH

Contract No. W-7405-eng-26

Health and Safety Research Division

MATHEMATICAL PHANTOMS REPRESENTING CHILDREN OF VARIOUS AGES FOR USE IN ESTIMATES OF INTERNAL DOSE

M. Cristy

NUREG/CR--1159

TI86 000170

Manuscript Completed: March 1980

Date Published: June 1980

NOTICE This document contains information of a preliminary nature. It is subject to revision or correction and therefore does not represent a final report.

Prepared for the
U.S. Nuclear Regulatory Commission
Office of Nuclear Regulatory Research
Washington, D.C. 20555
Under Interagency Agreement DOE 40-550-75
NRC FIN No. B0410-8

Prepared by the
OAK RIDGE NATIONAL LABORATORY
Oak Ridge, Tennessee 37830
operated by
UNION CARBIDE CORPORATION
for the
DEPARTMENT OF ENERGY

CONTENTS

Page

HIGHLIGHTS

In the mid-1960's, Fisher and Snyder developed a mathematical phantom of an adult human for use in internal dose estimations in conjunction with a Monte Carlo transport code for photons. Simple equations defining the boundaries of the body and the principal organs were given for this phantom. To estimate dose in children, Snyder and co-workers employed phantoms that were transformations of the adult phantom. Equations for major body sections were given explicitly, with the internal organs defined implicitly through similitude transformation equations. The major shortcoming of these derivative phantoms was that the organ sizes and bone marrow distributions were not always realistic.

To overcome this shortcoming, a series of distinct phantoms representing children of ages 0, 1, 5, 10, and 15 years has been developed. All equations for boundaries of organs are explicitly defined with realistic sizes. In addition, the regional distributions of hematopoietically active bone marrow and inactive fatty marrow have been assigned for each phantom, using the method of Cristy.

Because detailed anatomical data for organ shapes and locations are not available for children, the "Similitude Rule" was used to determine the shape and the location of most of the organs. This rule is consistent with drawings depicting developmental trends of organs in the trunk. Known exceptions to the rule were adjusted appropriately. The organ volumes were assigned such that organ masses at the various ages conform closely with the data presented in International Commission on Radiological Protection Publication 23.

INTRODUCTION

Fisher-Snyder Adult Phantom and its Similitudes

In the mid-1960's Fisher and Snyder developed a mathematical phantom representing an adult human, which was used in conjunction with a Monte Carlo transport code to estimate dose from internal sources of photons (Fisher and Snyder 1967; 1968). Simple equations are given for the major body sections and the principal organs. Into the Monte Carlo code are programmed three tissue densities — a low density for lung tissue, a high density for skeletal tissue, and a near unit density for all other tissues. The latest version of this phantom can be found in Snyder et al. (1974).

To estimate dose in children, Snyder and co-workers employed so-called "similitude phantoms" (Snyder and Cook 1971; Hilyer, Snyder, and Warner 1972; Snyder and Ford 1973; Warner, Poston, and Snyder 1974; Poston, Snyder, and Warner 1975; Snyder et al. 1976). These phantoms were obtained by transforming the adult phantom. Three orthogonal scaling factors were chosen for each body section so that the size and shape of each section could be designed to approximate the dimensions of a child of a given age. The dimensions chosen for ages 0-, 1-, 5-, 10-, and 15-year-old children in one of these studies (Snyder et al. 1976) are given in Fig. 1. (Age 0 years is the newborn.) The scaling factors for the trunk are thus seen to be A_T (given age)/A_T (adult), B_T (given age)/B_T (adult), and C_T (given age)/C_T (adult). The head dimension B_H is set equal to B_T; and in the legs region, the radius of each leg is set equal to 0.5 A_T at the top and 0.1 A_T at the bottom. These constraints mean that only two dimensions for the head and one dimension for the legs region are chosen independently. Thus, although there are nine scaling factors, only six are independent.

The Monte Carlo transport code can be used in conjunction with a "similitude phantom" (i.e., a phantom whose major body sections are each a similitude of the corresponding body section in the adult phantom), even though there are no explicit equations for the individual body organs but only explicit equations describing the three major body

ORNL–DWG 79-19953

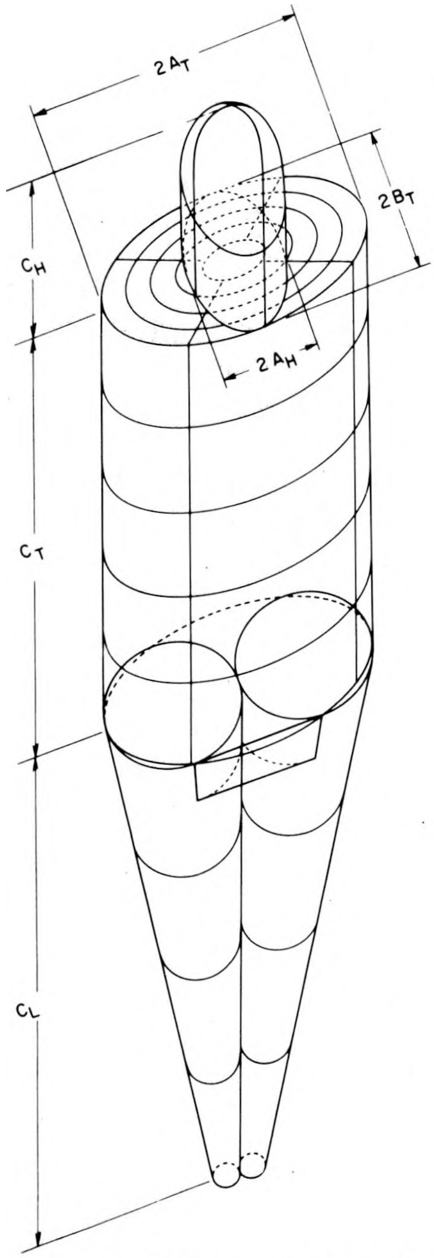

THE ADULT HUMAN PHANTOM

AGE (yr)	WEIGHT (kg)	C_T (cm)	C_H (cm)	C_L (cm)	A_T (cm)	B_T (cm)	A_H (cm)
0	3.148	23	13	16	5.5	5	4.5
1	9.112	33	16	28.8	8	7	6.5
5	18.12	45	20	46	11	7.5	6.5
10	30.57	54	22	64	14	8	6.5
15	53.95	65	23	78	18	9	7
ADULT	69.88	70	24	80	20	10	7

Fig. 1. Dimensions of adult phantom and of similitude phantoms used by Snyder et al. (1976). The subscripts H, T, and L refer to head, trunk, and legs, respectively.

sections. To determine whether a point in a phantom for a given age lies in a particular organ, one uses the adult organ equation and the scaling factors for the appropriate body section. The advantage of this procedure is that one has to provide only the dimensions of the body sections to spawn a phantom with all of the internal organs of the adult phantom. The disadvantage, of course, is that the volumes, shapes, and positions of the internal organs are all determined by the scaling factors and may not be realistic for a particular organ. A review of the treatise on developmental anatomy by Scammon (1953) revealed that, for most organs, the shapes and positions are not seriously different from the shapes and positions in a similitude phantom; this can be seen by studying Scammon's Figs. 26-28 and 30-34. In other words, during development, the shapes of the organs often follow body shape, and the relative positions of organs are generally the same. This observation is embodied formally in the Similitude Rule: for many organs, a similitude transformation of the adult phantom into a child phantom gives a good first approximation to the shapes and the locations of the organs.

The accuracy of the organ volumes in similitude phantoms is another matter. Cristy and Warner (unpublished data) compared similitude organ volumes with mean value organ volumes in the newborn child; agreement was fair to good for some organs and poor for others. These data are summarized in Table 1. Another problem with the similitude technique is that the distribution of active bone marrow is not accurately portrayed.

Pediatric Phantoms of Hwang and Co-workers

Hwang and co-workers developed a series of pediatric phantoms. Descriptions of mathematical phantoms representing ages 0, 1, 5, and 15 years were reported (Hwang et al. 1976; Hwang, Shoup, and Poston 1976a,b; Jones et al. 1976). Although a phantom representing age 10 was also developed, the description was not published (Hwang, personal communication). These phantoms are similar to the Fisher-Snyder adult phantom in that the basic types of equations for the body sections and organs are the same (e.g., the liver is represented by an elliptical cylinder cut by an oblique plane in all phantoms). These phantoms purport to

Table 1. Ratio of newborn similitude phantom volumes to corresponding mean value newborn volumes[a] for selected organs

Organ	Similitude volume: Mean value volume
Adrenals	0.13
Urinary bladder wall	0.81
Stomach wall	1.18
Heart	0.55
Kidneys	0.64
Liver	0.66
Lungs	0.95
Ovaries	1.30
Pancreas	1.09
Spleen	0.96
Thymus	0.10
Thyroid	2.98
Uterus	0.86
Skeleton as whole	1[b]
Intestines as whole	0.66-1[c]

[a]Given by ICRP Publication 23 (1975).

[b]Reliable data for the individual parts of the skeleton were not available. The value of 1 given here is based on a statement by Scammon (1953, p. 37) that postnatal growth of the skeleton proceeds with that of the body as a whole.

[c]The lower value is based on Scammon (1953, p. 43); the higher value is based on ICRP Publication 23 (1975, p. 135).

have organ size, shape, and position determined from anatomical references and thus to be an improvement over the similitude phantoms (Hwang et al. 1976, pp. 3, 19, and 23; Poston 1976, p. 105). A careful analysis of the phantom descriptions revealed, however, that for most organs, such as the lungs, the shape in a given pediatric phantom is the same as in the adult phantom, even though the trunk shapes are different in the two cases (by "same shape" is meant, for example, that two ellipsoids have the same shape if one ellipsoid can be transformed into the other by multiplying all three axis lengths by the same factor). Some organs in their descriptions, such as the liver and the ribs, conform to the Similitude Rule.

Having been designed with the same shape as in the adult, the lungs took up a disproportionate length of the trunk in the younger age phantoms. This error resulted apparently from an effort to attain correct lung volumes. Because the lungs were too long and because most adult organ shapes were retained while adult trunk shape was not, severe fitting problems were encountered in the lower trunk. The result was that organs in the lower trunk had to be shifted around and crowded together, but not in a manner which reflected actual anatomical trends.

Pediatric Phantoms of This Report

In designing the adult phantom, Fisher relied heavily upon the excellent cross-section anatomy of adults by Eycleshymer and Schoemaker (1911). Too few cross-sectional studies have been done with children to permit the design of pediatric phantoms in the same way. What is known are sizes of organs (ICRP 1975) and general developmental trends, discussed by Scammon (1953). The Similitude Rule was used extensively in designing the pediatric phantoms for ages 0, 1, 5, 10, and 15 years given in this report.

With the Similitude Rule, the design procedure became simple and straightforward: (1) the dimensions of the trunk, the head, and the legs were determined from anthropological data (references are given later); (2) organ shapes and locations were determined by the Similitude Rule; (3) organ volumes were determined using masses and specific gravities from ICRP Publication 23 (1975); (4) overlapping of organs was eliminated by changing shape, location, or size, depending upon interpretations of drawings and text in *Morris' Human Anatomy* (Schaeffer 1953) or upon constraints imposed by the simplicity of the phantom design; (5) exceptions to the Similitude Rule were handled individually (e.g., the thymus); and (6) the active marrow distributions were determined. The use of an improved method for estimating the distribution of the active bone marrow for each age (Cristy 1980) is a new feature in these pediatric phantoms. This change is noteworthy because the blood-forming organ is important in the assessment of radiological risk.

With the exception of the newborn, direct information on the distribution of active marrow or total marrow (hematopoietically active marrow plus fatty, inactive marrow) is not known for children. In response to this lack of data, Atkinson (1962) derived an approximate method to estimate the distribution of active marrow in children. He assumed that the distribution of the total marrow spaces in the adult (Mechanik 1926) could be used as an approximation to the distribution of total marrow spaces in children. He then applied age-dependent cellularity factors to the Mechanik data to obtain age-dependent distributions of active marrow (cellularity is defined as the fraction of marrow in a given bone that is active).

The newer method of Cristy (1980) is a modification of Atkinson's method that is simple, yet has numerically large effects at early ages. Factors have been added which take into account that in children the head is proportionately larger and the legs are proportionately smaller than in adults. This method predicts that, in the newborn, 27.8% of the active marrow resides in the skull and 20.7% resides in the lower limbs. By contrast, Atkinson's method predicts 7.0% in the skull and 38.9% in the lower limbs. According to the data of Hudson (1965) on the skeletons of 16 late-term fetuses and newborns, 29.5% (±4.2%) of the active marrow resides in the skull, and 23.7% (±2.2%) resides in the lower limbs. The newer method is clearly an improvement.

Snyder (1977) pointed out that in considering doses to the active marrow in the newborn and 1-year-old, the doses given for the *total marrow compartment* in the similitude phantoms for these ages could be used, since essentially all of the marrow in infants is active. With regard to the marrow distribution, the similitude technique automatically includes the factors for the relative sizes of the body sections, but does not include cellularity factors. Following the example of Atkinson, Hwang and co-workers failed to include correction factors for relative body section size. Thus, ironically, the procedure suggested by Snyder employing similitude phantoms would give more meaningful estimates of dose to the active marrow for ages 0-1 year than would using values generated employing Hwang's phantoms.

Another important change in the phantoms presented here is the addition of female breast tissue, a tissue known to be radiosensitive (ICRP 1977). Female breast tissue appears to be at greatest risk from ionizing radiation during adolescence and early adult life; the breast tissue in female infants and children appears to be at risk also, but the magnitude of this risk is uncertain (UNSCEAR 1977, pp. 385-394). For prudence' sake, female breast tissue has been included for all ages.

During the development of these pediatric phantoms, several changes were made in the adult phantom. Female breast tissue was added to the trunk, and the improved heart model of Coffey (1978) was fitted into the trunk. The lungs had to be redesigned to accommodate the new heart; the difference in size between right and left lungs — not represented in the Fisher-Snyder phantom — was incorporated into the new design. The head was redesigned to incorporate the ideas of Hwang, Shoup, and Poston (1976b), including a change in position of the thyroid. A modification of the descending colon was made to eliminate a small overlap with the pelvic skeleton and to make the wall thickness uniform. Other minor changes were made so that the adult phantom would be consistent with the manner in which certain organs were fitted into the pediatric phantoms: the position of the adrenals, the position of the gall bladder, the size of the pancreas, and the shape and position of the thymus were all changed for this reason. The gall bladder design was also simplified slightly. The modified adult phantom is included in the description that follows.

DESCRIPTION OF THE MATHEMATICAL PHANTOMS

The phantom descriptions will follow the format of Snyder et al. (1974) and even include language and diagrams used therein (without formal attribution in many cases) so that the reader will not have to refer to that publication constantly to fill in missing information.

Each phantom consists of three major sections: (1) an elliptical cylinder representing the trunk and arms; (2) two truncated circular cones representing the legs and feet; and (3) an elliptical cylinder capped by half an ellipsoid representing the head and neck. Attached to the legs section is a small region with a plain front surface to contain the testes. Attached to the trunk are portions of two ellipsoids representing the female breasts.

The exterior of the adult phantom is depicted in Fig. 2. The arms are not separated from the trunk, and minor appendages such as fingers, feet, chin, and nose are omitted. The dimensions of the pediatric phantoms and the dimensions of the adult head, which was revised, were chosen after considering data on body and body section dimensions and volumes and ratios of dimensions. The data used were from the following sources: Figs. 6 and 10 of ICRP Publication 23 (ICRP 1975), Tables 10A-10D of Watson and Lowrey (1967), Charts I and K and Table K of Bardeen (1920), Figs. 13 and 14 of Scammon (1953), and Figs. 26 and 27 of Krogman (1941, p. 101). It was impossible to assign dimensions for the width (side to side) and the depth (front to back) of the trunk and of the head directly because of disagreement within the literature. Values for these dimensions were calculated using the ratio of width to depth (for which there was agreement), the volume, and the height. This procedure, after Hayes (1960, p. 4), ensures proper shape of the trunk and the head.

Three-dimensional perspective drawings depicting the external features of all the phantoms are shown in Figs. 3 and 4.

Composition of the Phantoms

Each phantom consists of skeletal, lung, and other soft tissue. The composition and density of each type used by Snyder et al. (1974) for

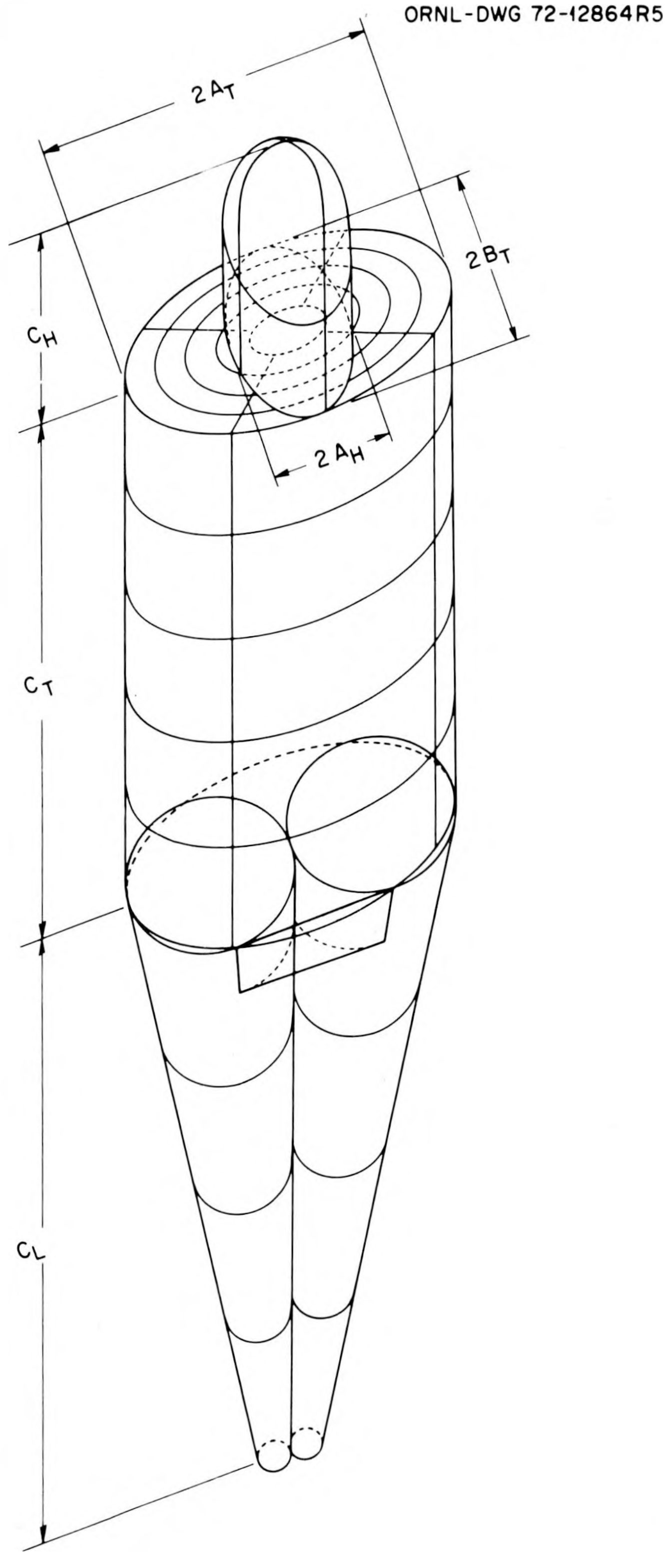

Fig. 2. The adult human phantom. Breasts are not shown.

ORNL-DWG 79-19955

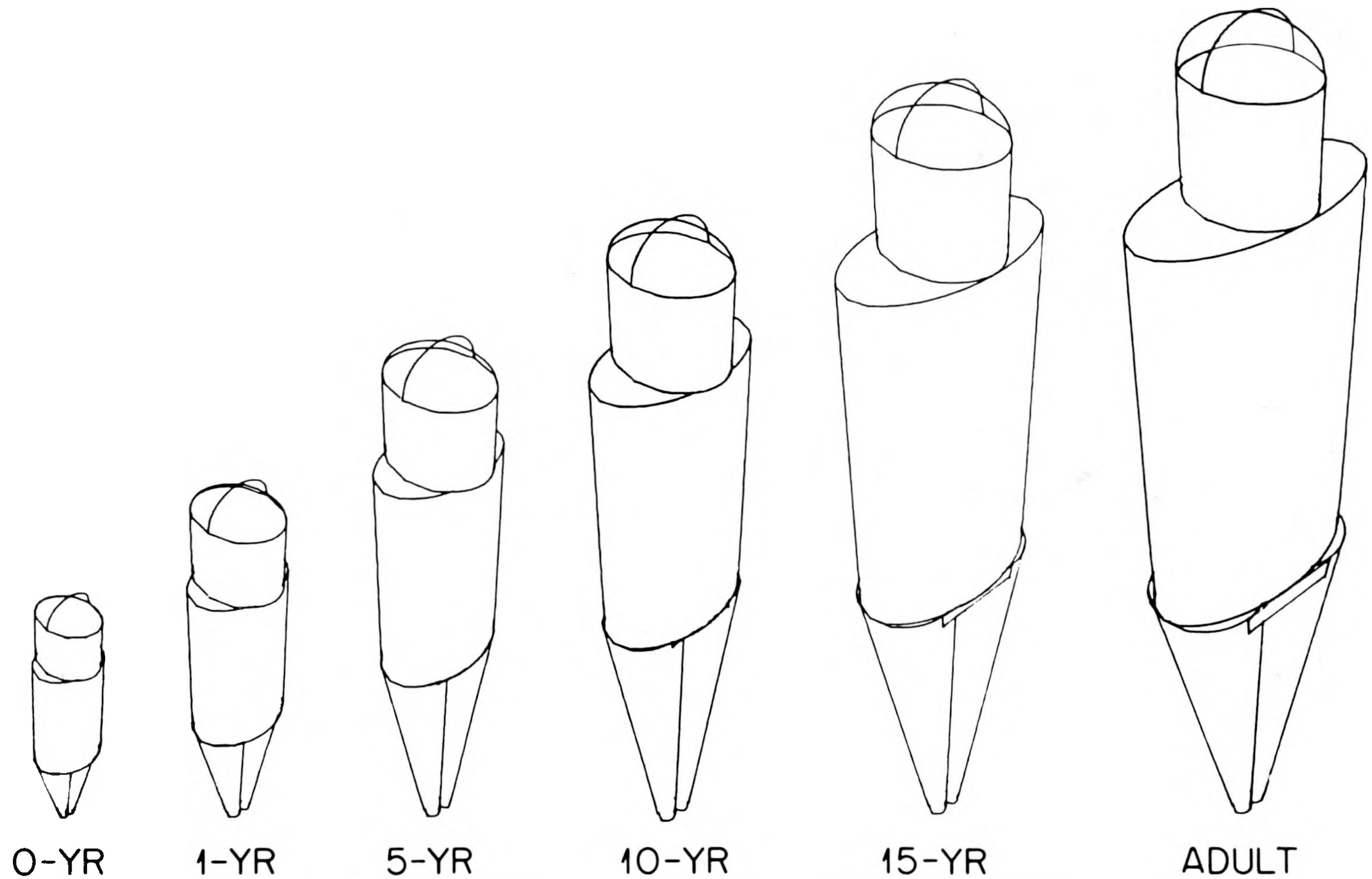

Fig. 3. Computer-drawn three-dimensional perspective drawings showing external views of the phantoms. In the younger-age phantoms, the head is relatively larger, the legs are relatively smaller, and the trunk is relatively thicker. The view is from above and to one side of each phantom. Breasts are not shown.

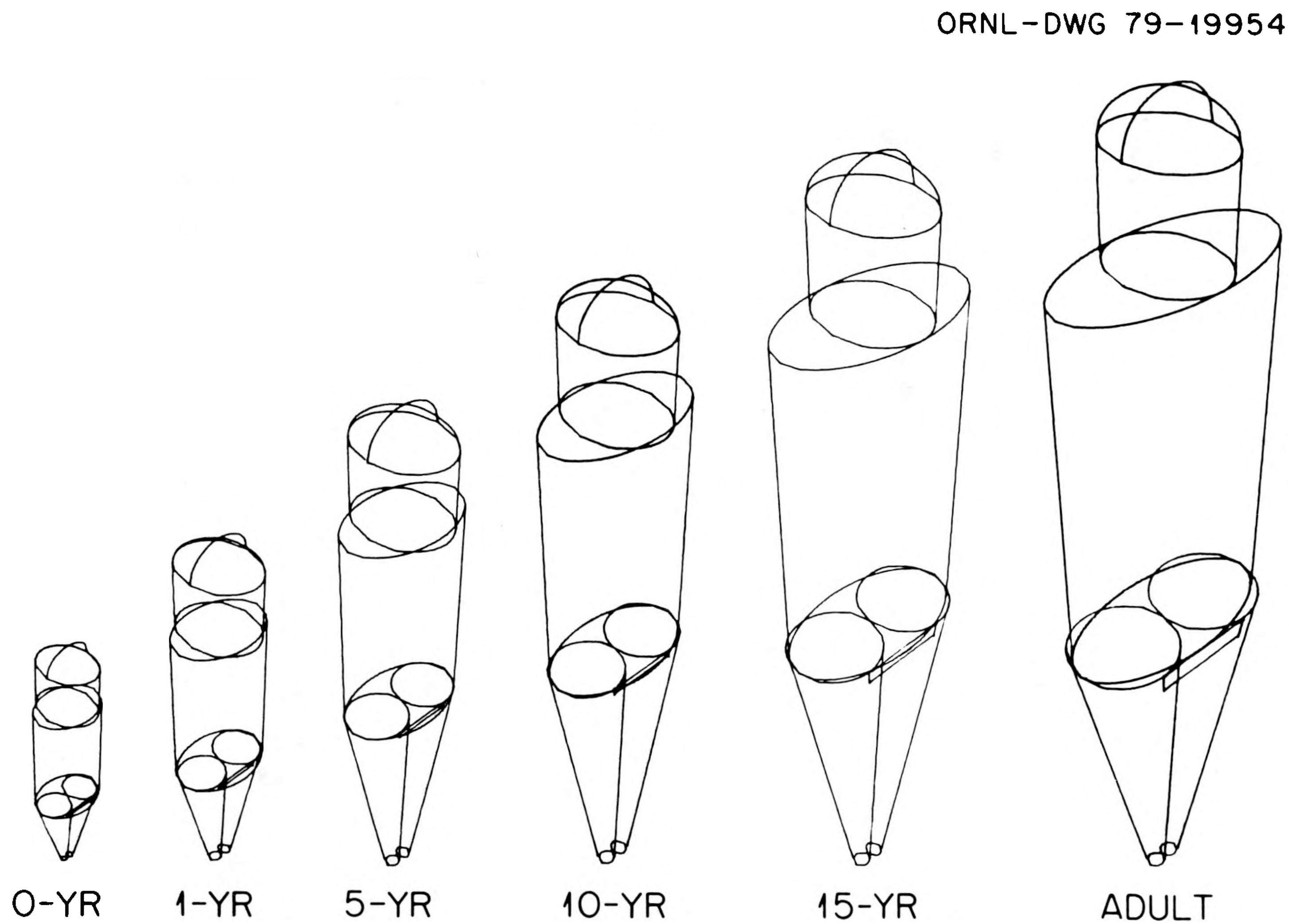

Fig. 4. Computer-drawn three-dimensional perspective drawings showing hidden lines.

the adult are used for the pediatric phantoms; these compositions and densities are given in Table 2. The skeletal system represents the total content of the intact skeleton and thus includes both bone and bone marrow. This material is considered to be homogeneously distributed in the skeleton. This is clearly a compromise due to our present inability to represent more accurately the bone and marrow spaces. The tissue composition shown in Table 2 can only be regarded as an average and is not representative of the different portions of the skeleton but only of the total.

The three tissue types used are composed principally of hydrogen, carbon, nitrogen, and oxygen. In the skeleton, additional elements amount to about 18% of the total mass, with calcium and phosphorus accounting for most of this. In the lungs, the composition is somewhat different from that of other soft tissues in the phantom, probably because the lungs contain almost no fat and a larger fraction of blood than most organs. The densities of the skeletal region (bone plus marrow), lungs, and the remainder of the phantom are approximately 1.5, 0.30, and 0.99 g/cm^3, respectively. The values for the composition were obtained from Tipton, Snyder, and Cook (1966), who have analyzed tissue specimens obtained from autopsies of 150 grossly normal U.S. adults. They analyzed these specimens for a wide variety of trace elements and selected values for the major chemical elements from the literature to be consistent with physiological data on content of fat, water, and other constituents of these organs.

Description of the Phantoms and Organs

The pediatric phantoms have been designed to form a developmentally consistent family with the existing Fisher-Snyder adult phantom. The exterior of each phantom has approximately the form of the human body; but, as in the adult phantom, there has been no attempt to introduce small variations which would be presumed to have only a small effect on the scattering of photons. Similarly, the description of the interior organs, while approximately correct as to size, shape, position, composition and density, are simplified to provide formulas which are readily

Table 2. Elemental composition of different tissues of the phantom (% by weight)

Element	Skeletal tissue[a]	Lung tissue[b]	Total body minus skeleton and lungs[c]
H	7.0	10	10
C	23	10	23
N	3.9	2.8	2.3
O	49	76	63
Na	0.32	0.19	0.13
Mg	0.11	7.4×10^{-3}	0.015
P	6.9	0.081	0.24
S	0.17	0.23	0.22
Cl	0.14	0.27	0.14
K	0.15	0.20	0.21
Ca	9.9	7.0×10^{-3}	0
Fe	8.0×10^{-3}	0.037	6.3×10^{-3}
Zn	4.8×10^{-3}	1.1×10^{-3}	3.2×10^{-3}
Rb	0	3.7×10^{-4}	5.7×10^{-4}
Sr	3.2×10^{-3}	5.9×10^{-6}	3.4×10^{-5}
Zr	0	0	8.0×10^{-4}
Pb	1.1×10^{-3}	4.1×10^{-5}	1.6×10^{-5}

[a] Density 1.5 g/cm^3 .

[b] Density 0.30 g/cm^3 .

[c] Density 0.99 g/cm^3 .

Source: Snyder et al. (1974).

calculated on a digital computer. The exact specifications of the phantom and the internal organs are given below. See Fig. 5 for a schematic view of the principal organs.

Another perspective of the organs in the trunk is given in Figs. 6-23. For each phantom, these figures show superimposed cross-sections within the upper trunk, the middle trunk, or the lower trunk. Some information on organ shapes, positions, and sizes (relative to the trunk) can be gleaned from these views.

Exterior of each phantom

The body is represented as erect with the positive z-axis directed upward toward the head. The x-axis is directed to the phantom's left (the reader's right in Fig. 2), and the y-axis is directed toward the posterior side of the phantom. The origin is taken at the center of the base of the trunk section of the phantom.

In general, the dimensions (in centimeters) are given to two decimal places. The use of two decimal places does not imply that the average dimensions in some human population are known to such precision. This use is for convenience in designing the organs with correct volumes and spatial relationships.

Trunk. The trunk, exclusive of the female breasts, is represented by a solid elliptical cylinder specified by

$$\left(\frac{x}{A_T}\right)^2 + \left(\frac{y}{B_T}\right)^2 \leq 1 \text{ and } 0 \leq z \leq C_T \quad .$$

The values of A_T, B_T, and C_T for each phantom are given in the table below. The equation used to calculate the volume follows the table.

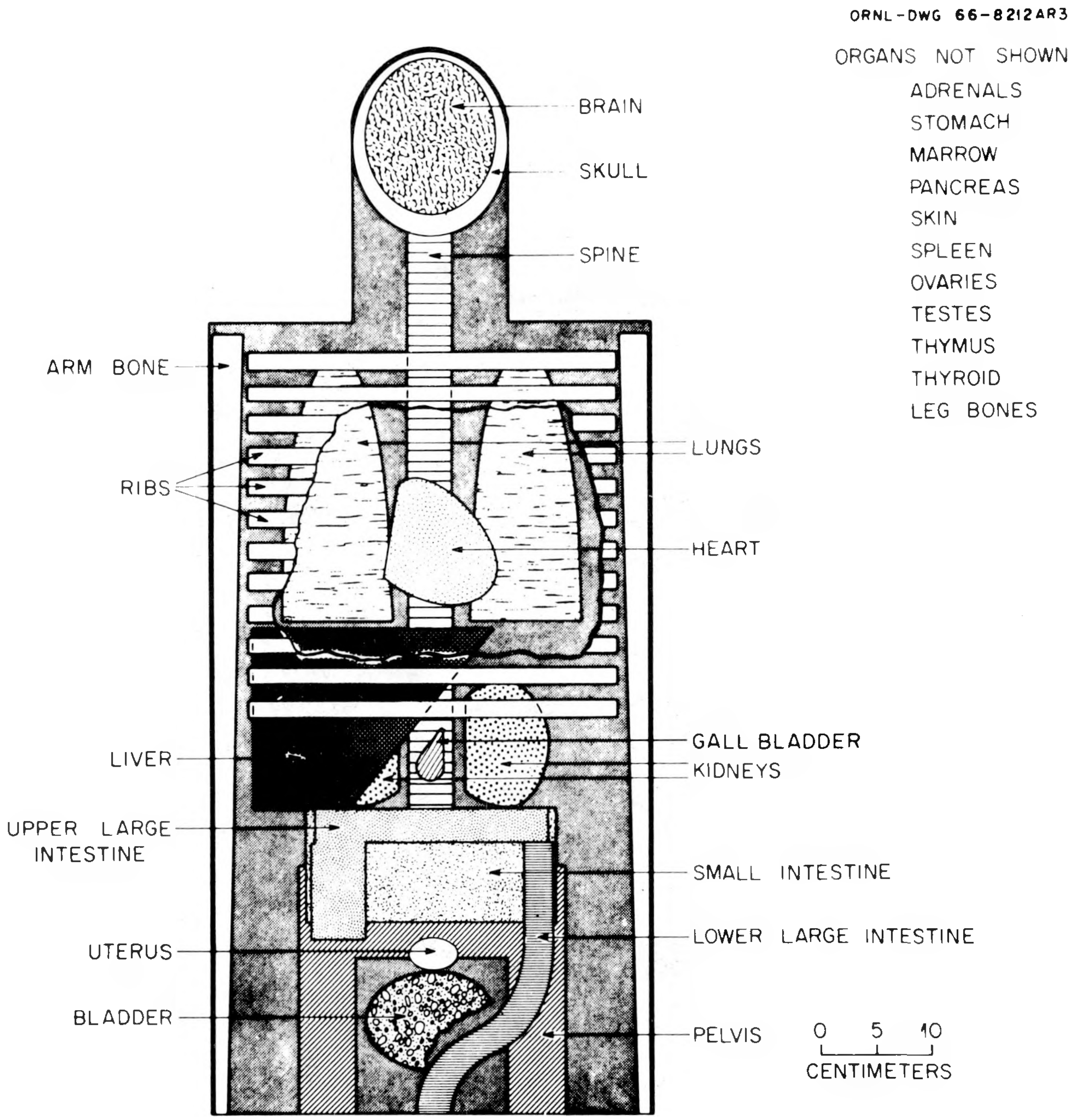

Fig. 5. Anterior view of the principal organs in the head and trunk of the adult phantom developed by Snyder et al. (1974). Although the heart and head have been modified in this report, this schematic illustrates the simplicity of the geometries of the organs.

ORNL-DWG 79-13269R

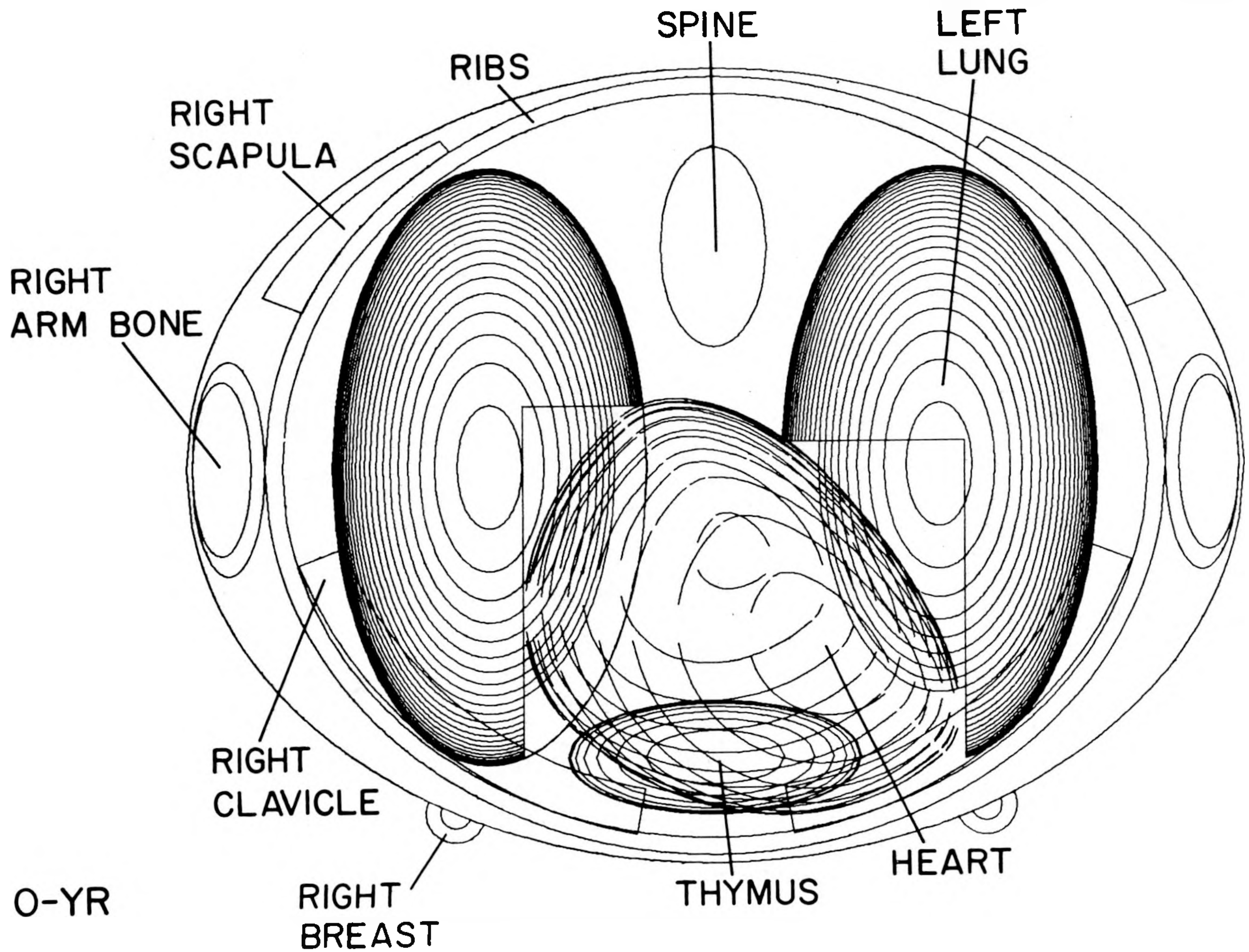

Fig. 6. Superimposed cross-sections within the upper trunk of the newborn phantom. Figs. 6-11 depict the upper trunk of each phantom, defined here as the space from the bottom of the lungs to the top of the trunk. For the adult (Fig. 11), cross-sections of the organs are drawn at 1-cm intervals. For the other phantoms, cross-sections are drawn at intervals designed to give the same number of superimposed cross-sections as in the adult. Additional cross-sections of individual organs are drawn as necessary to incorporate the largest cross-section of that organ.

ORNL-DWG 79-13268R

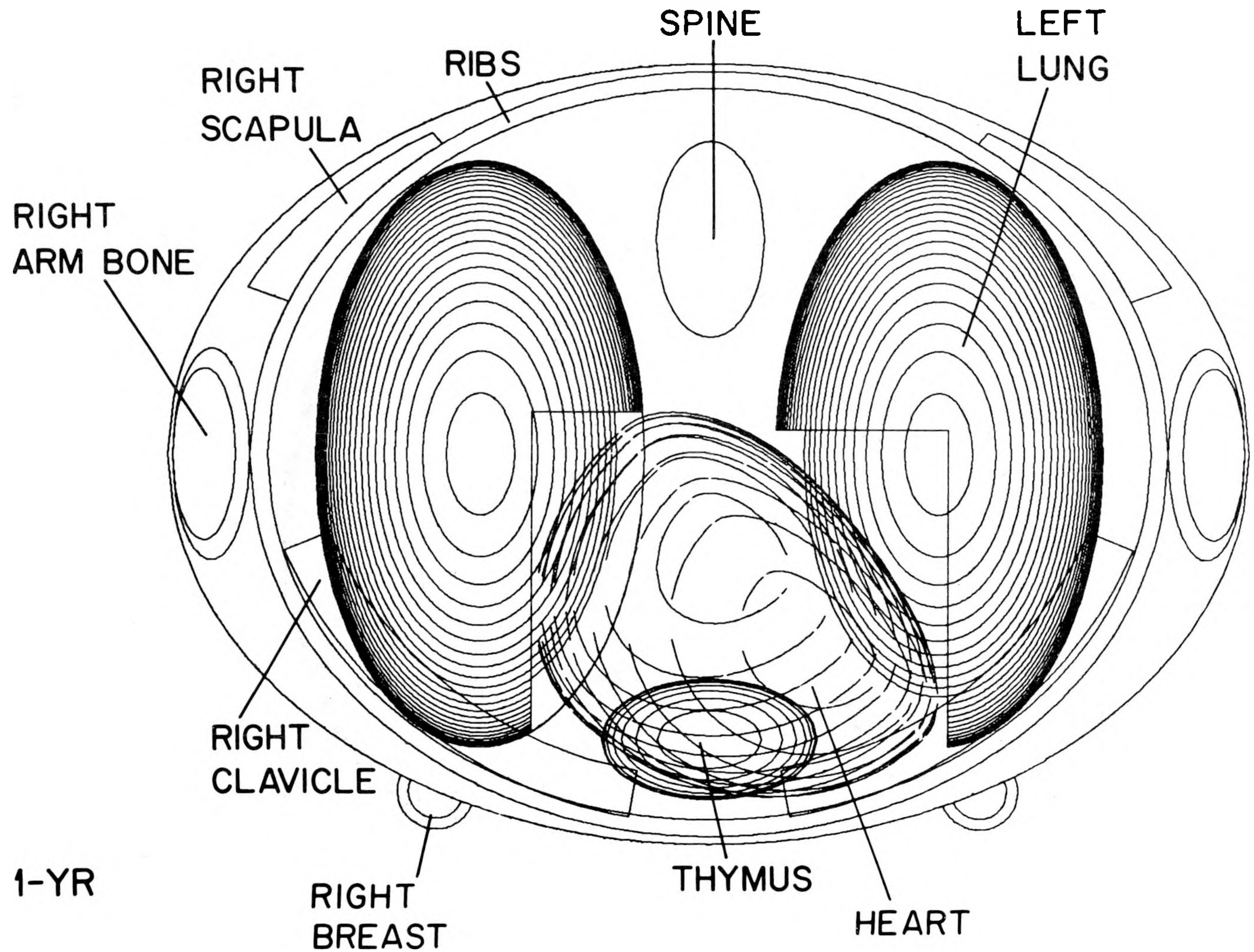

Fig. 7. Superimposed cross-sections within the upper trunk region of the phantom representing the 1-year old. See Fig. 6.

ORNL-DWG 79-13267R

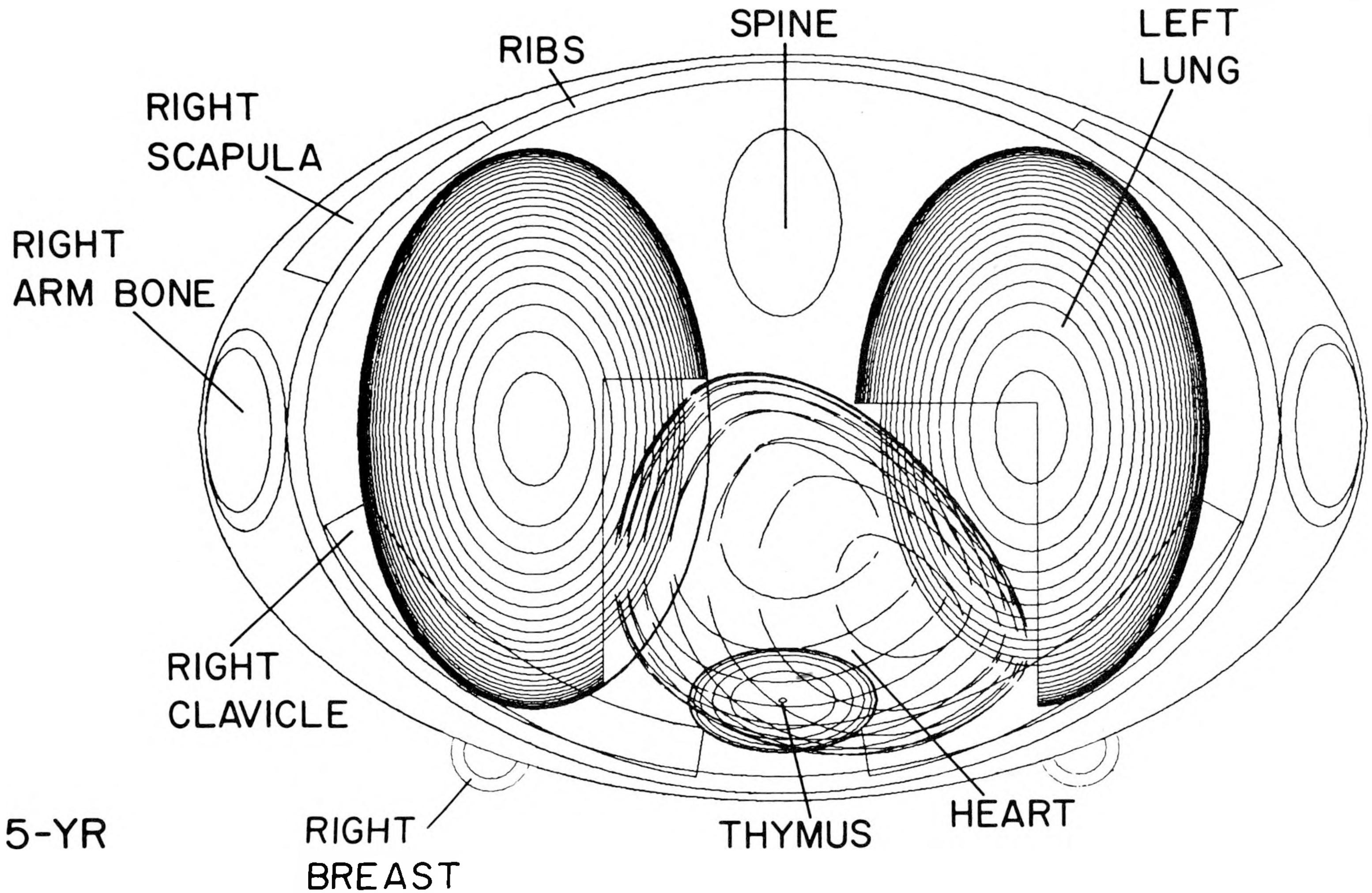

Fig. 8. Superimposed cross-sections within the upper trunk region of the phantom representing the 5-year old. See Fig. 6.

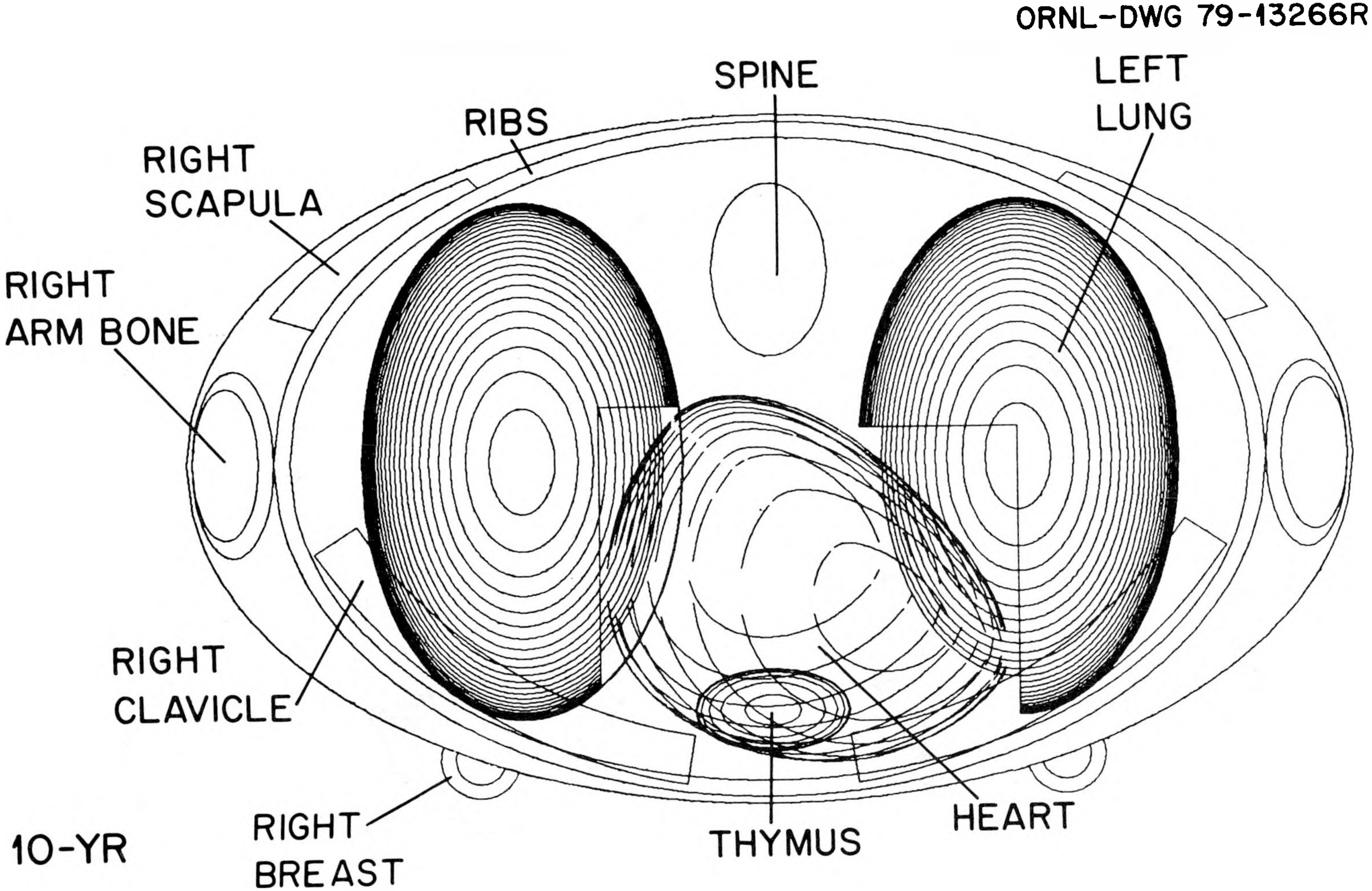

Fig. 9. Superimposed cross-sections within the upper trunk region of the phantom representing the 10-year old. See Fig. 6.

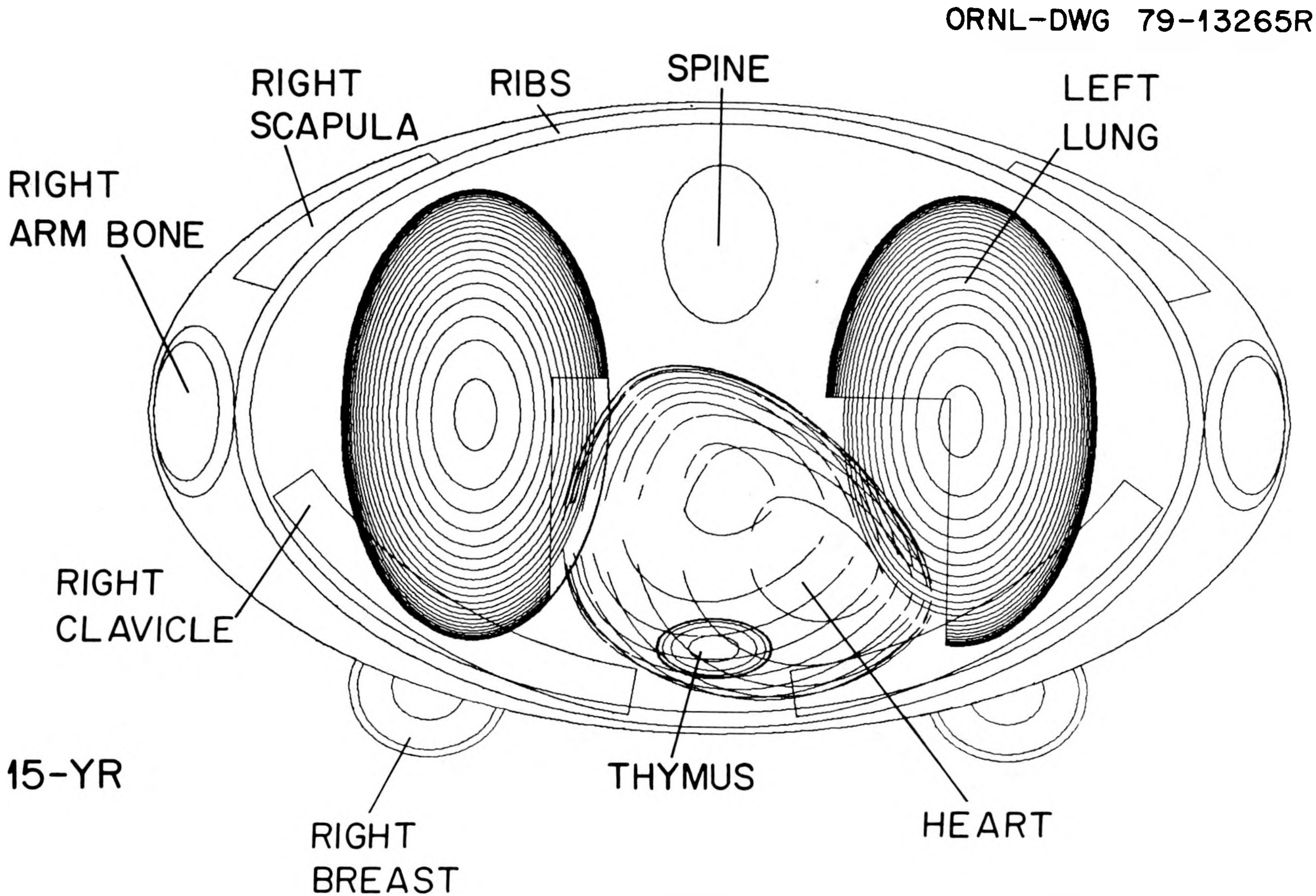

Fig. 10. Superimposed cross-sections within the upper trunk region of the phantom representing the 15-year old. See Fig. 6.

ORNL-DWG 79-13263R

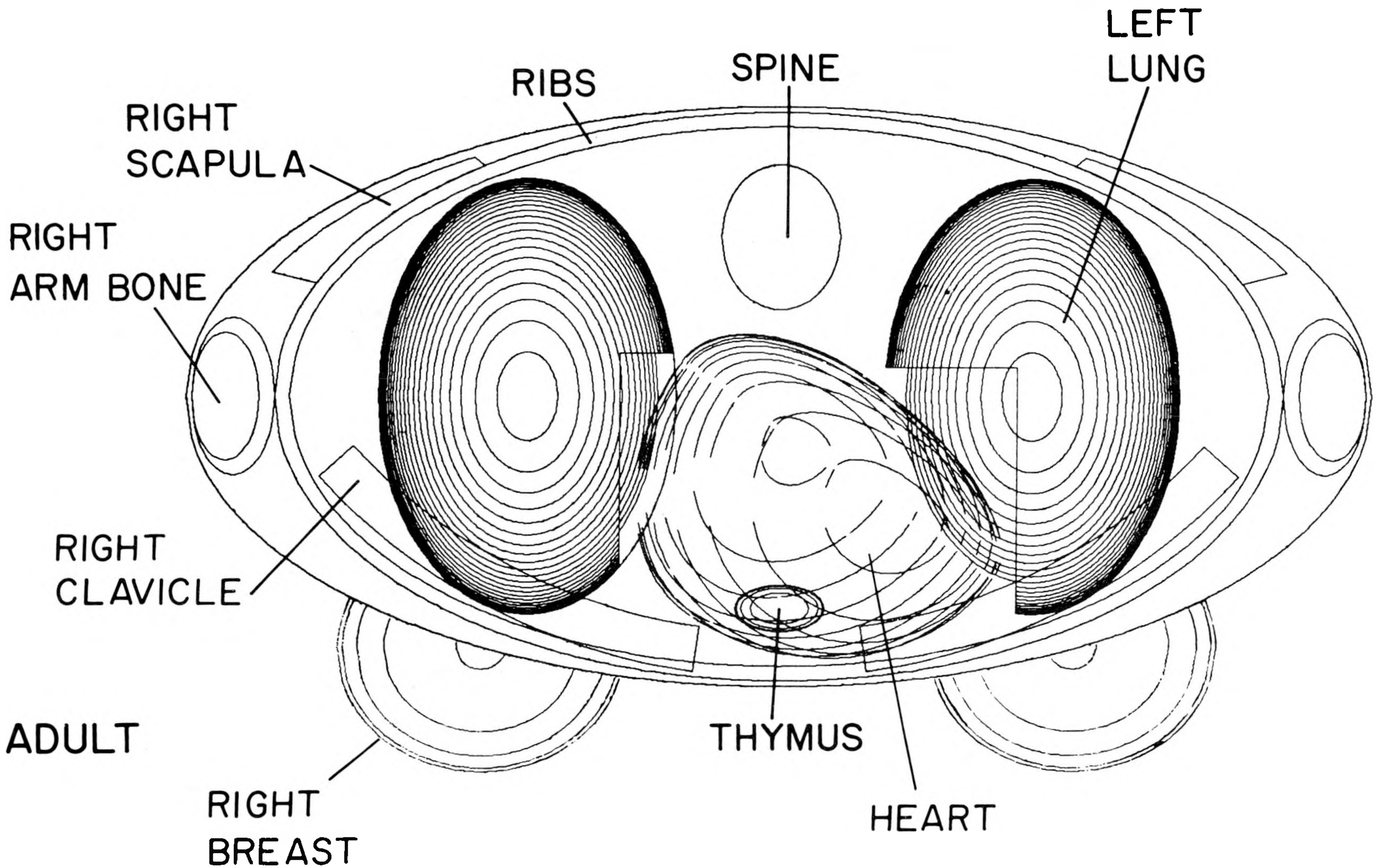

Fig. 11. Superimposed cross-sections within the upper trunk region of the phantom representing the adult. See. Fig. 6.

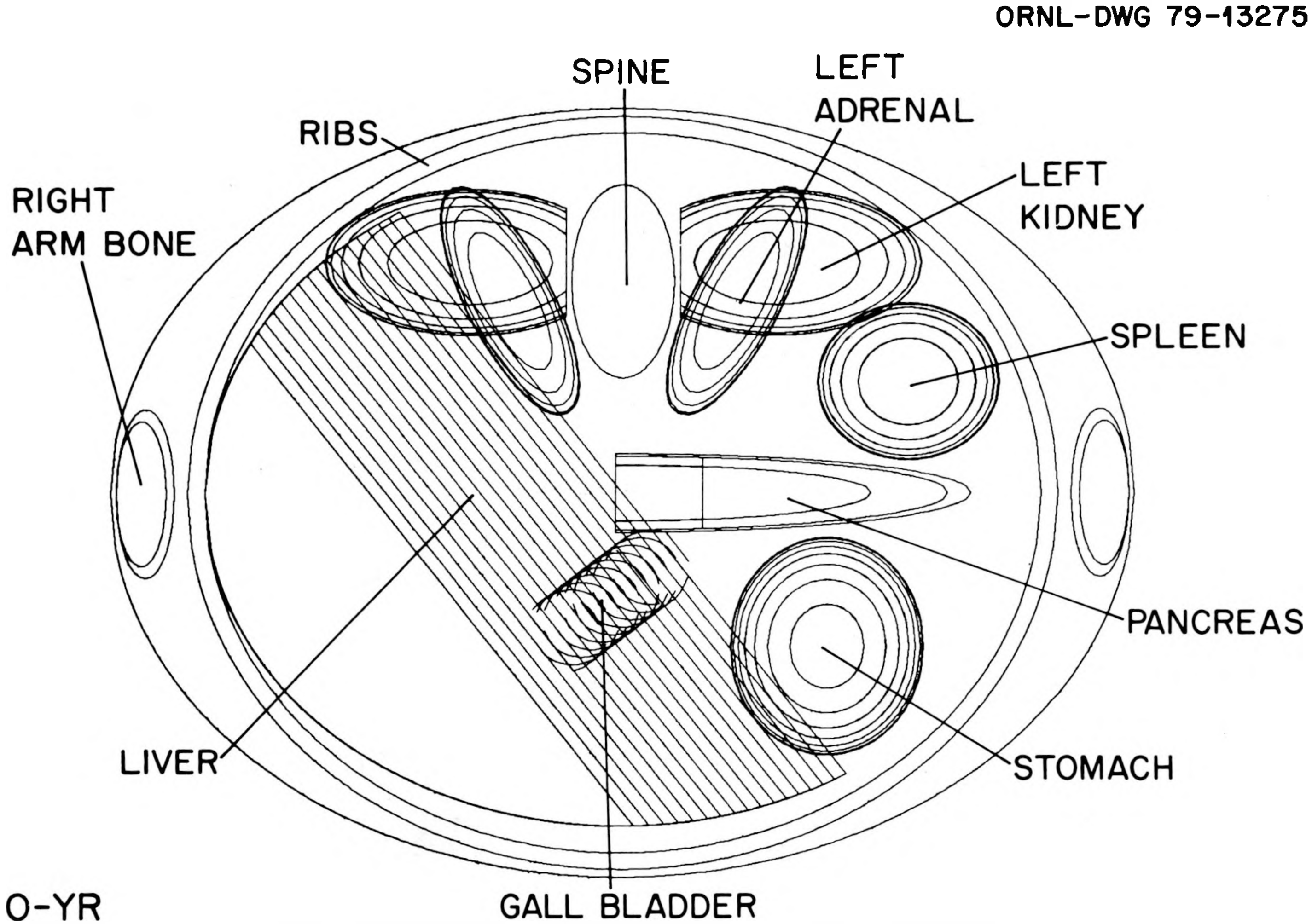

Fig. 12. Superimposed cross-sections within the middle trunk of the newborn phantom. Figs. 12-17 depict the middle trunk of each phantom, defined here as the space from the bottom of the liver to the top of the liver. For the adult (Fig. 17), cross-sections of the organs are drawn at 1-cm intervals. For the other phantoms, cross-sections are drawn at intervals designed to give the same number of superimposed cross-sections as in the adult. Additional cross-sections of individual organs are drawn as necessary to incorporate the largest cross-section of that organ.

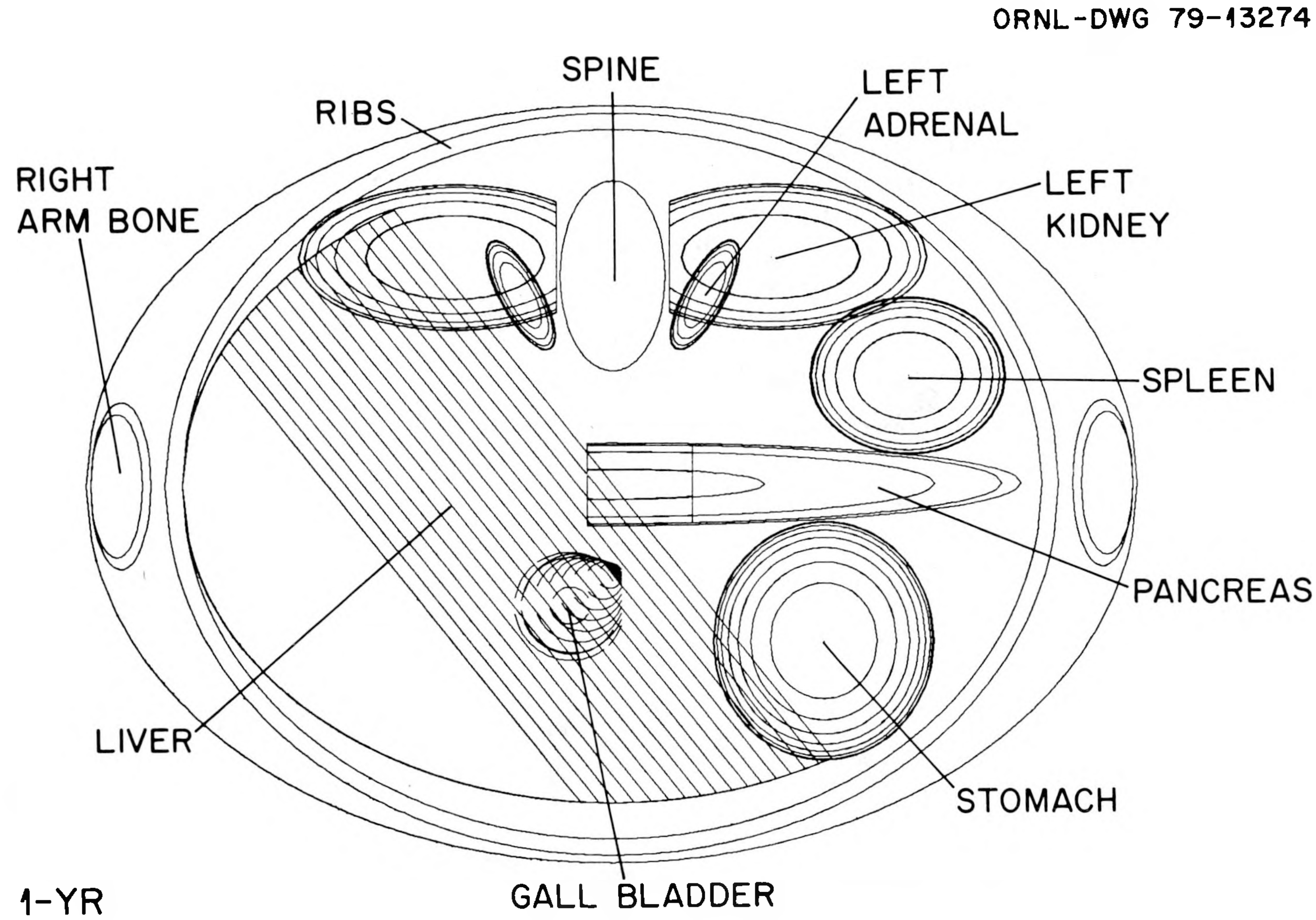

Fig. 13. Superimposed cross-sections within the middle trunk region of the phantom representing the 1-year old. See Fig. 12.

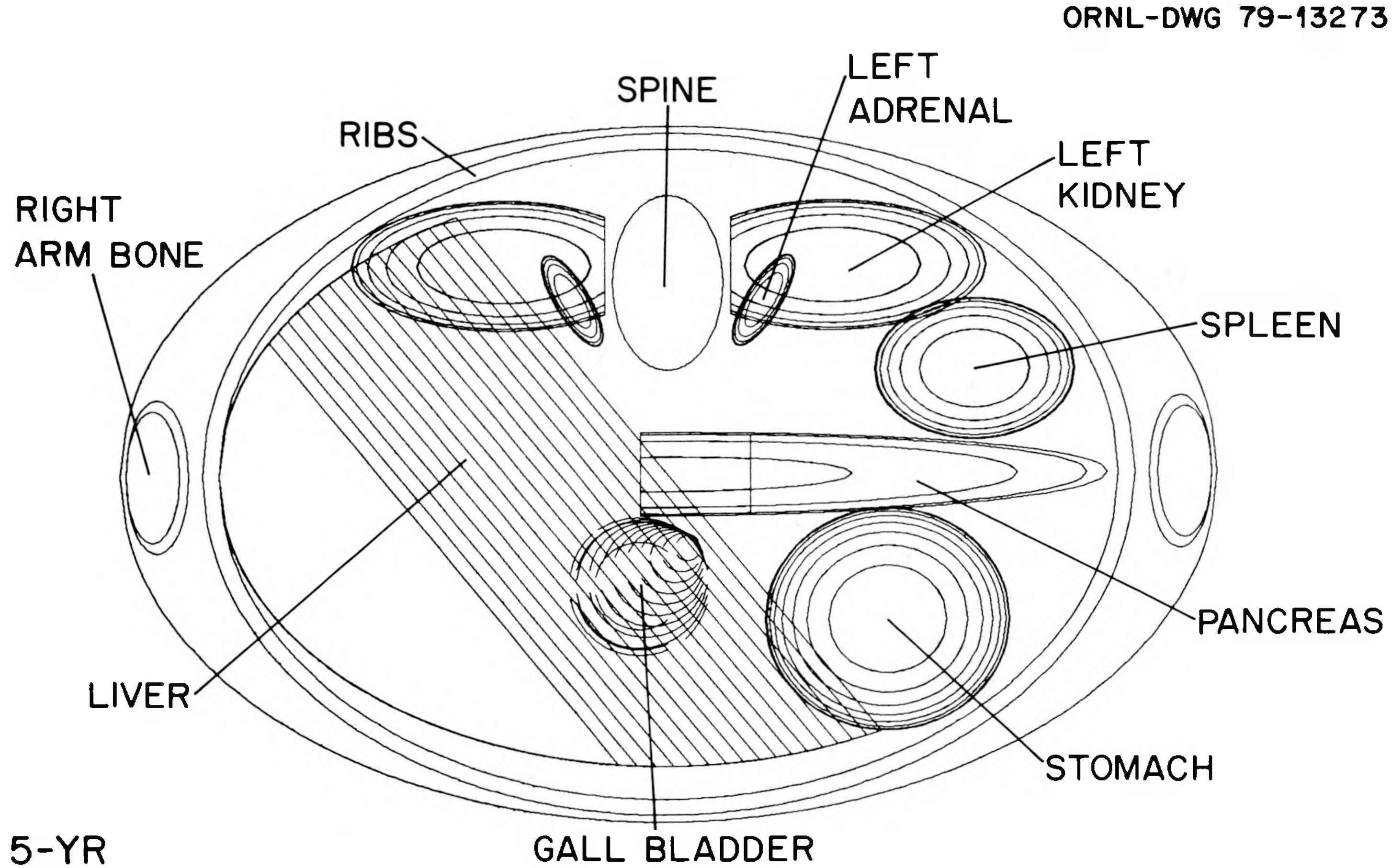

Fig. 14. Superimposed cross-sections within the middle trunk region of the phantom representing the 5-year old. See Fig. 12.

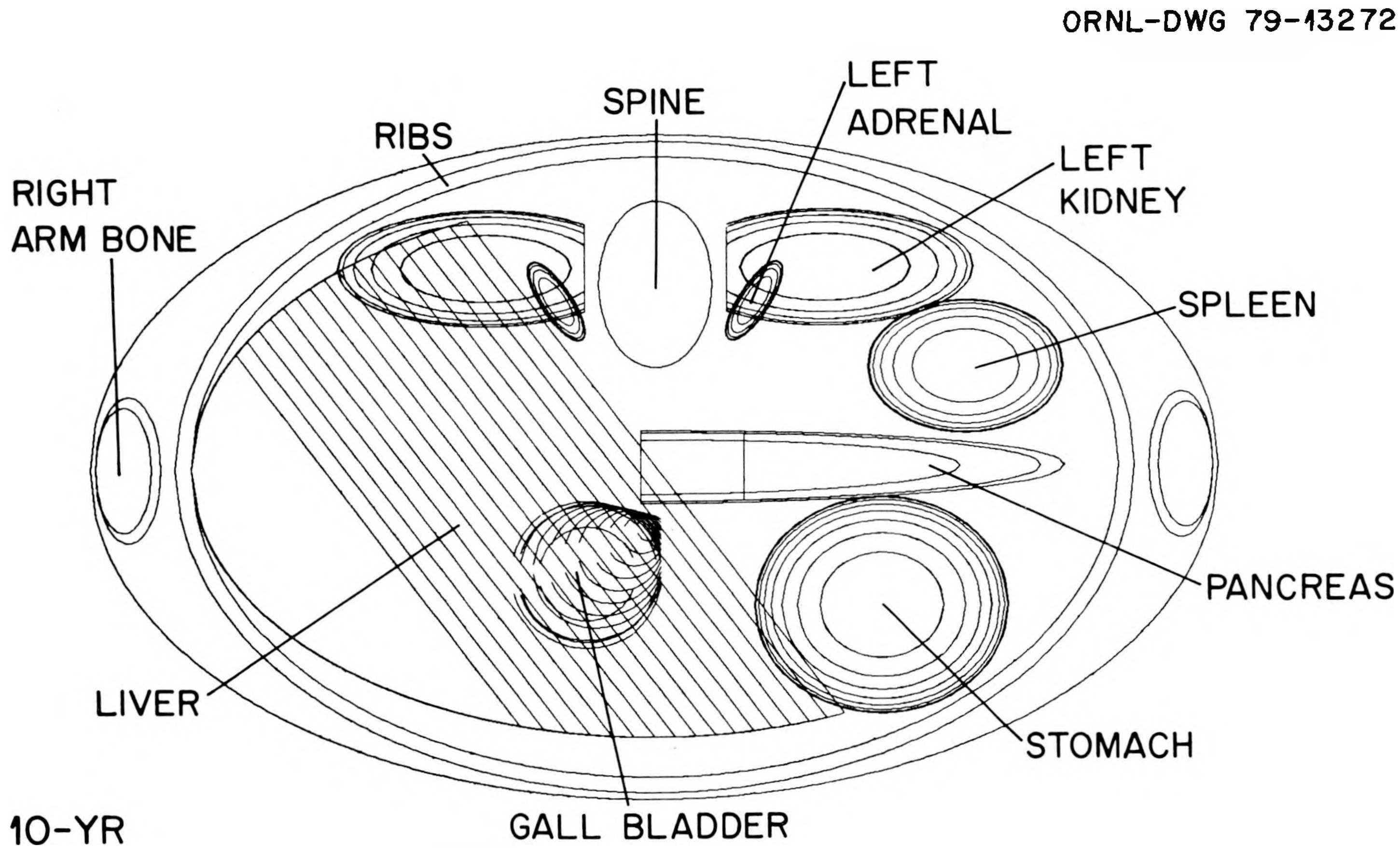

Fig. 15. Superimposed cross-sections within the middle trunk region of the phantom representing the 10-year old. See Fig. 12.

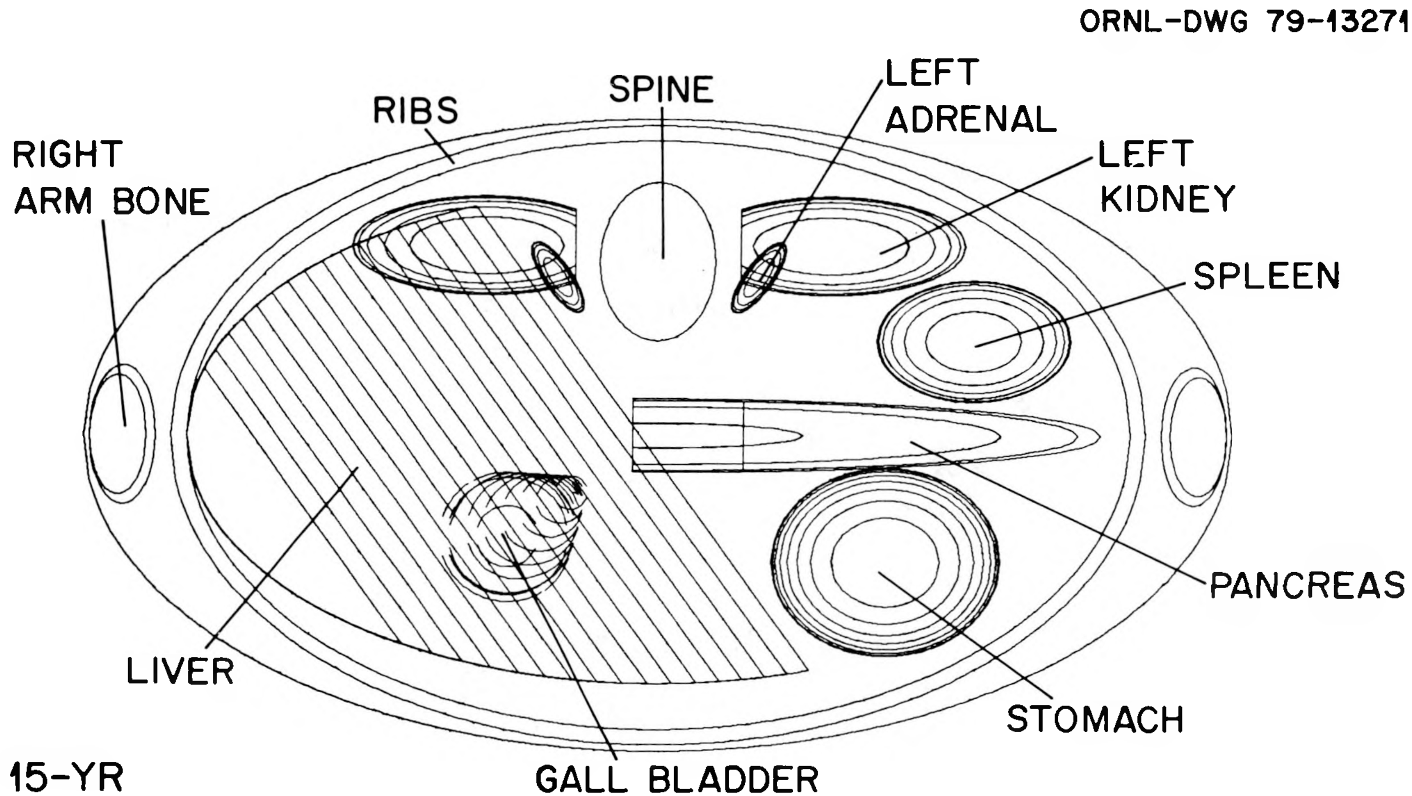

Fig. 16. Superimposed cross-sections within the middle trunk region of the phantom representing the 15-year old. See Fig. 12.

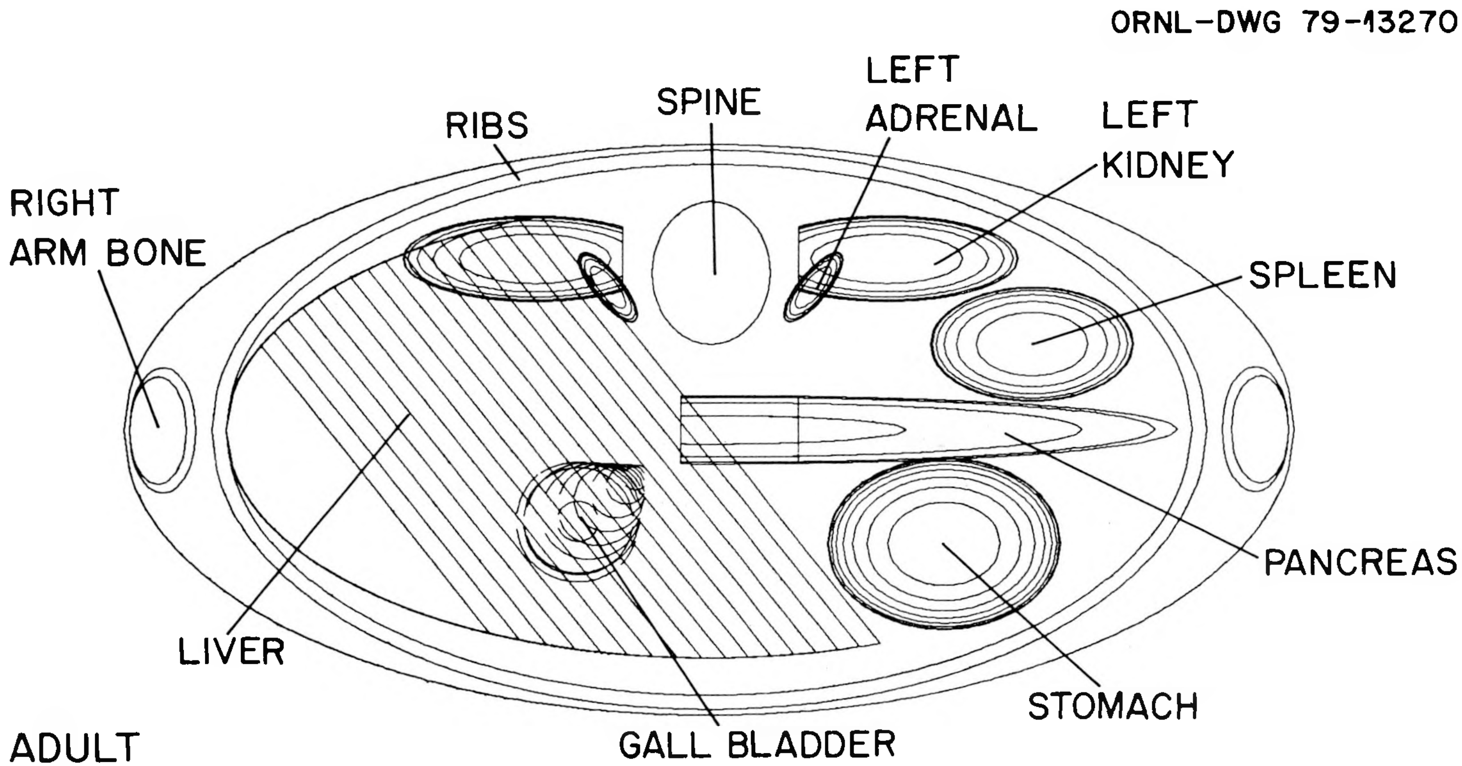

Fig. 17. Superimposed cross-sections within the middle trunk region of the phantom representing the adult. See Fig. 12.

ORNL-DWG 79-13281

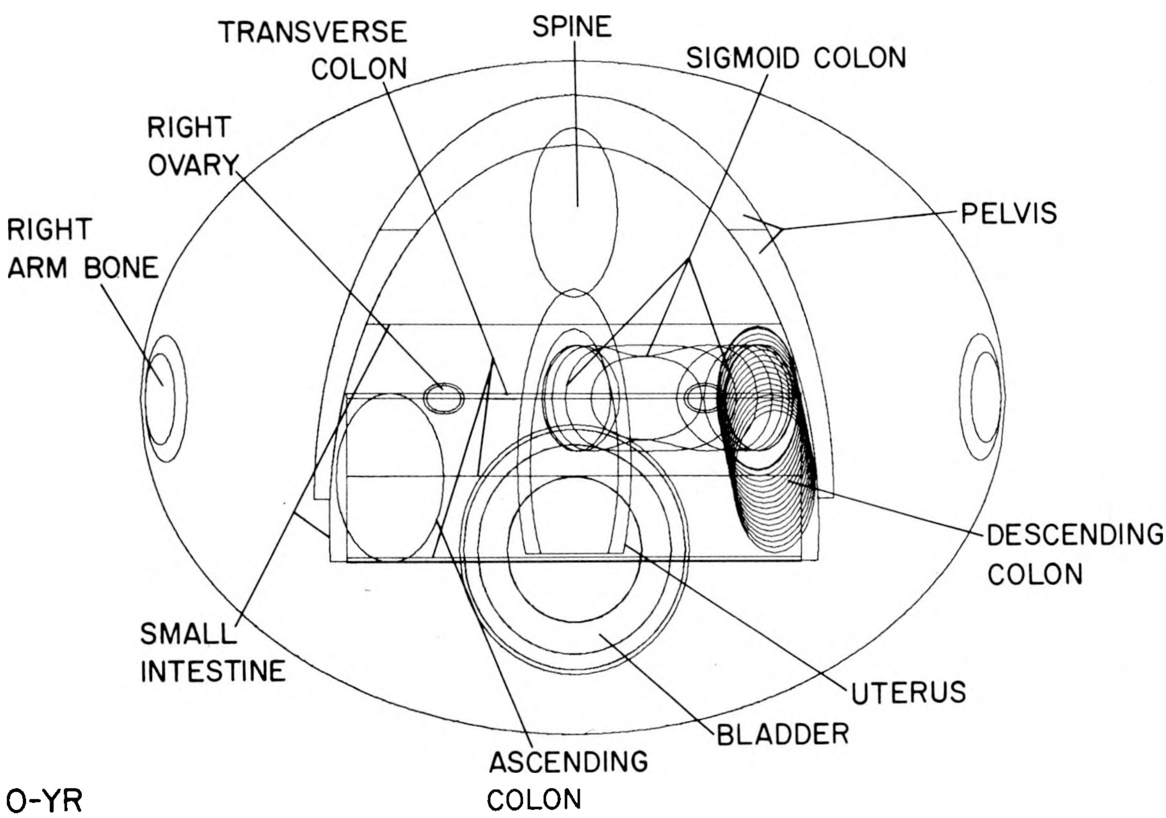

O-YR

Fig. 18. Superimposed cross-sections within the lower trunk of the newborn phantom. Figs. 18-23 depict the lower trunk of each phantom, defined here as the space from the bottom of the trunk to the bottom of the liver. For the adult (Fig. 23), cross-sections of the organs are drawn at 1-cm intervals. For the other phantoms, cross-sections are drawn at intervals designed to give the same number of superimposed cross-sections as in the adult. Additional cross-sections of individual organs are drawn as necessary to incorporate the largest cross-section of that organ.

ORNL-DWG 79-13280

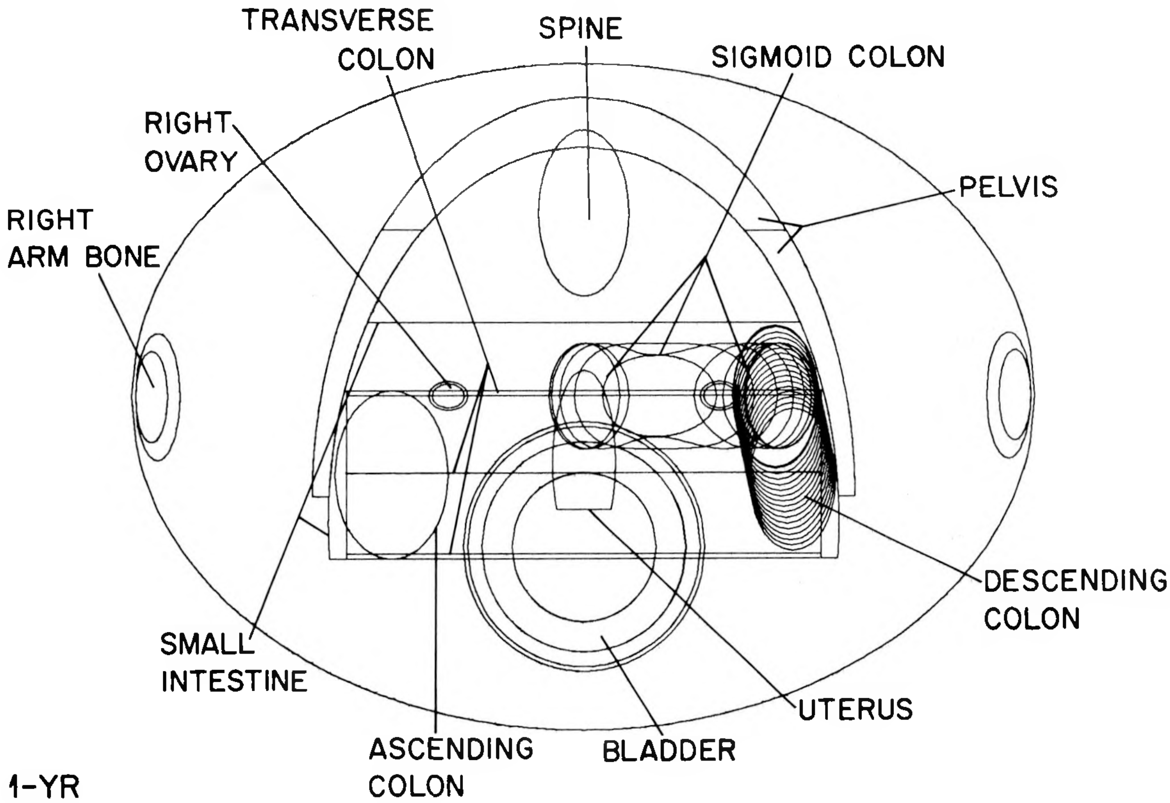

Fig. 19. Superimposed cross-sections within the lower trunk region of the phantom representing the 1-year old. See Fig. 18.

ORNL-DWG 79-13279

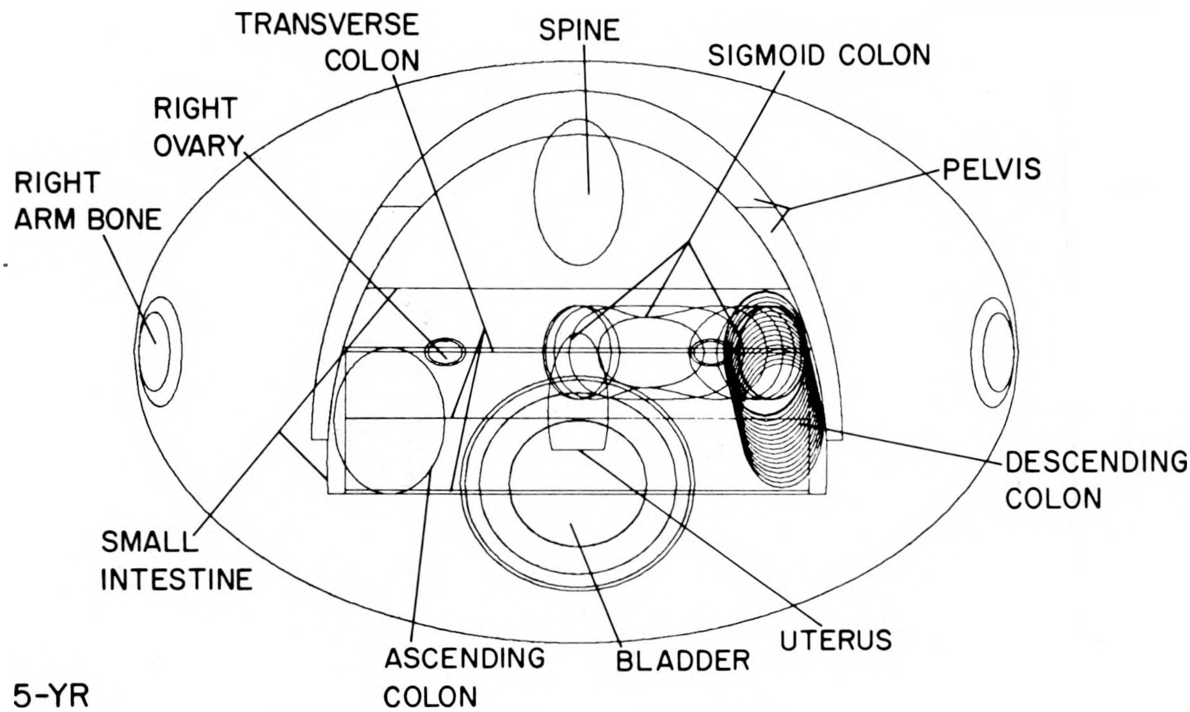

Fig. 20. Superimposed cross-sections within the lower trunk region of the phantom representing the 5-year old. See Fig. 18.

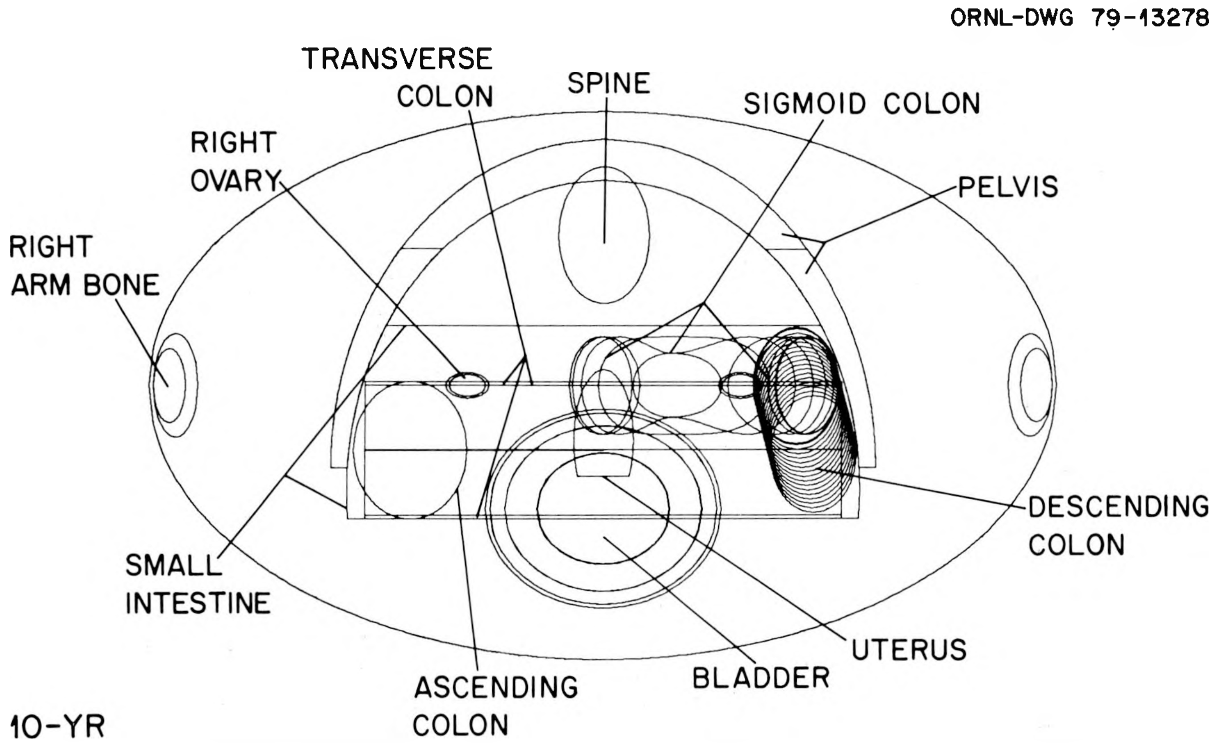

Fig. 21. Superimposed cross-sections within the lower trunk region of the phantom representing the 10-year old. See Fig. 18.

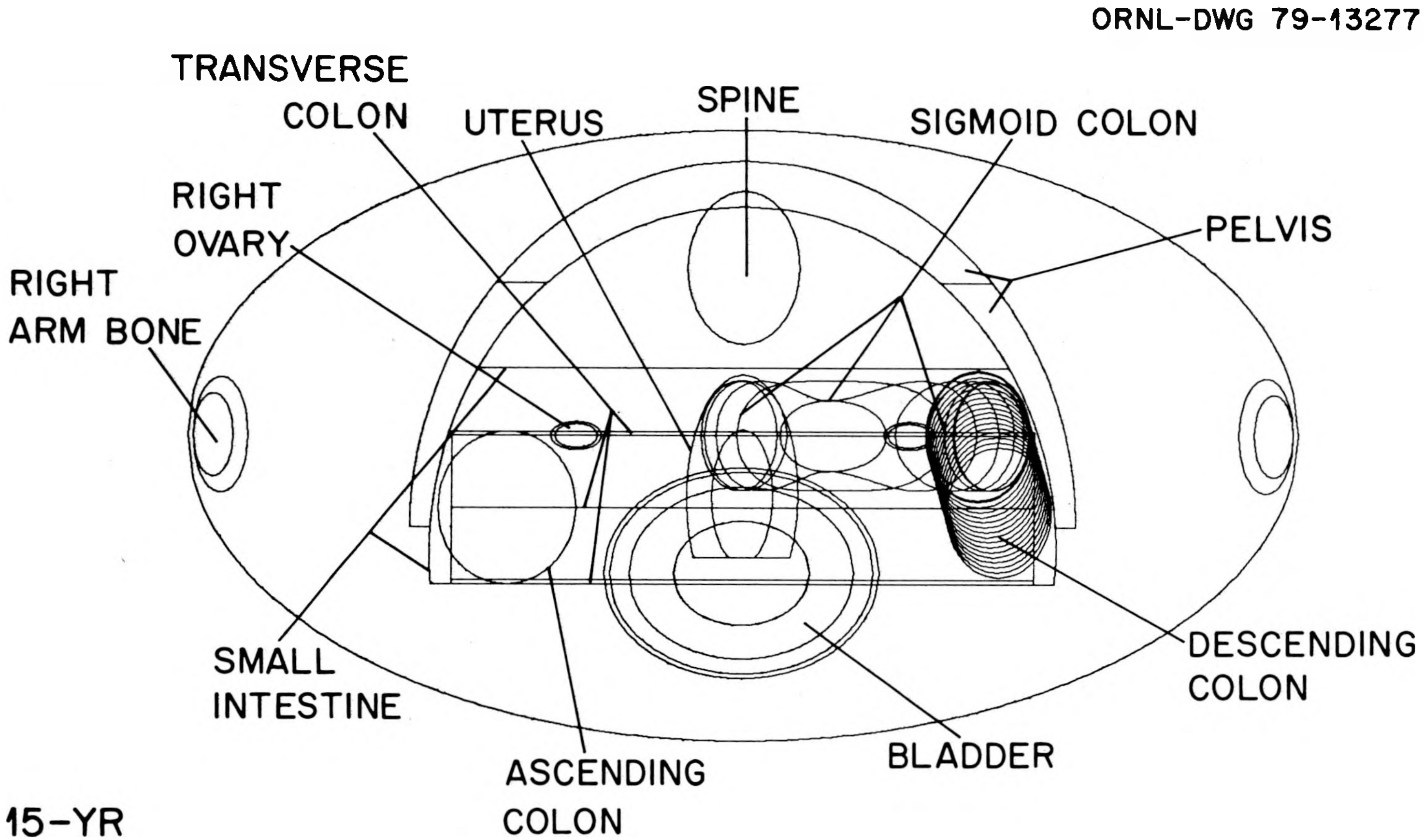

Fig. 22. Superimposed cross-sections within the lower trunk region of the phantom representing the 15-year old. See Fig. 18.

ORNL-DWG 79-13276

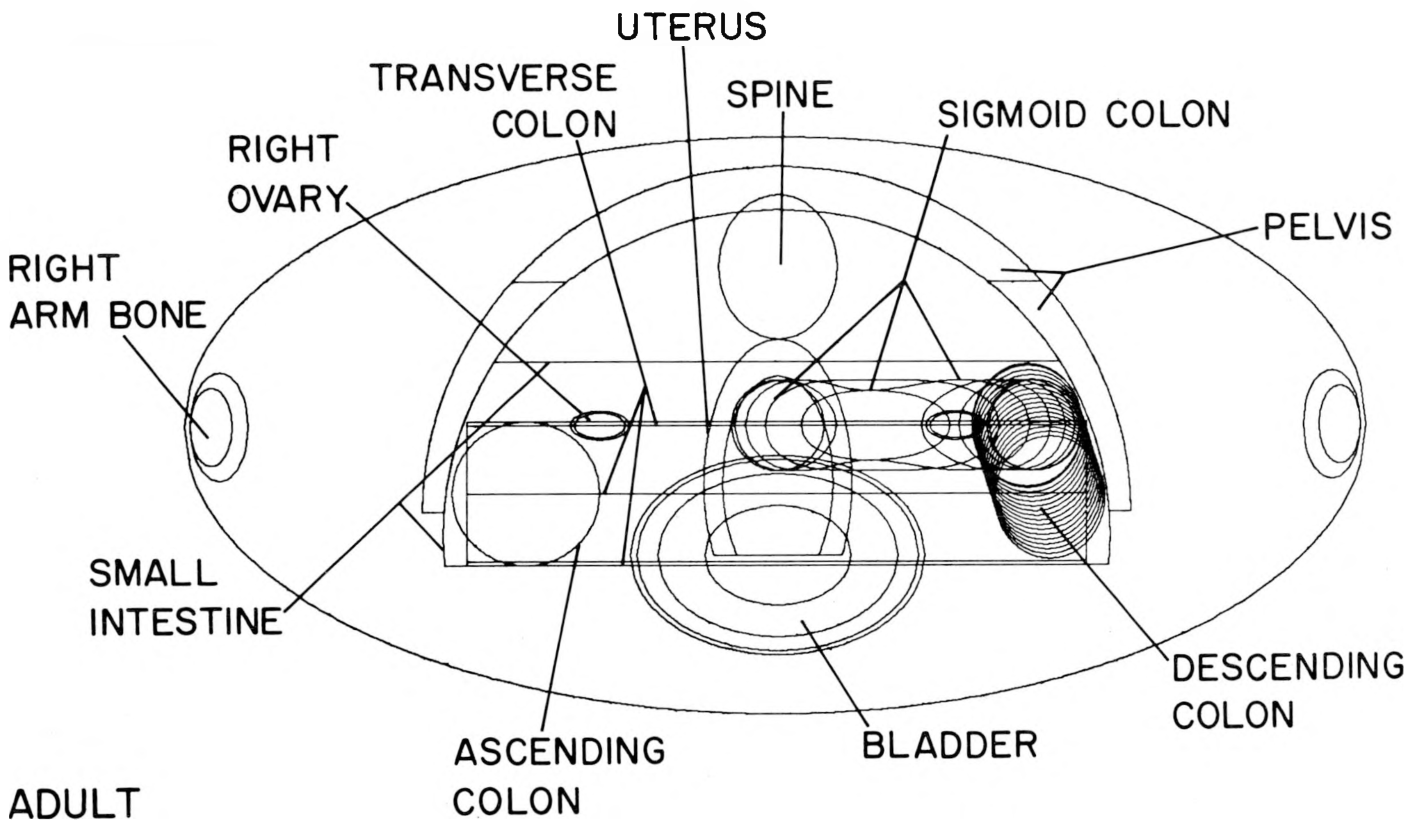

Fig. 23. Superimposed cross-sections within the lower trunk region of the phantom representing the adult. See Fig. 18.

Age (years)	Length (cm) A_T	B_T	C_T	Volume[a] (cm³)	Mass (g)
0	6.35	4.90	21.60	2,110	2,040
1	8.80	6.50	30.70	5,520	5,320
5	11.45	7.50	40.80	11,000	10,600
10	13.90	8.40	50.80	18,600	18,000
15	17.25	9.80	63.10	33,500	32,800
Adult	20.00	10.00	70.00	44,000	42,700

[a]Volume = $\pi A_T B_T C_T$.

The trunk section includes the arms and the pelvic region to the crotch. The female breasts are appended to the outside of the trunk section. The volumes and masses for the trunk given above do not include the breasts.

<u>Head</u>. The head section is a right elliptical cylinder topped by half an ellipsoid. The locus is specified by

$$\left(\frac{x}{A_H}\right)^2 + \left(\frac{y}{B_H}\right)^2 \leq 1 \text{ and } C_T \leq z \leq C_T + C_{H1} ,$$

or

$$\left(\frac{x}{A_H}\right)^2 + \left(\frac{y}{B_H}\right)^2 + \left(\frac{z - [C_T + C_{H1}]}{C_{H2}}\right)^2 \leq 1 \text{ and } z > C_T + C_{H1} .$$

Age (years)	Length (cm) A_H	B_H	C_{H1}	C_{H2}	Volume[a] (cm³)	Mass (g)
0	4.52	5.78	9.10	3.99	965	987
1	6.13	7.84	12.35	5.41	2410	2470
5	7.13	9.05	13.91	6.31	3670	3880
10	7.43	9.40	15.19	6.59	4300	4580
15	7.77	9.76	15.97	6.92	4900	5280
Adult	8.00	10.00	16.85	7.15	5430	5910

[a]Volume = $\pi A_H B_H (C_{H1} + \frac{2}{3} C_{H2})$.

The values of C_T have been given previously in the table of trunk values.

The shape of the adult head has been modified from that given by Snyder et al. (1974) in order to fit the data on head shape (Krogman 1941) more closely and to accommodate the new skull design.

Legs. The legs region of each phantom consists of the frustrums of two circular cones specified by

$$x^2 + y^2 \leq \pm\, x \left(A_T + \frac{A_T}{C_L'} z\right)$$

$$\text{and} \quad -C_L \leq z \leq 0 \quad ,$$

where the "±" sign is taken as plus for the left leg and minus for the right leg.

Age (years)	Length (cm) C_L	Length (cm) C_L'	Volume[a] (cm^3)	Mass (g)
0	16.8	21.6	451	476
1	26.5	37.1	1,470	1,550
5	48.0	65.0	4,380	4,630
10	66.0	90.0	8,930	9,440
15	78.0	100.0	15,400	16,300
Adult	80.0	100.0	20,800	21,900

$$^{a}\text{Volume} = \frac{1}{6}\pi C_L A_T^2 \left[1 + \left(\frac{C_L' - C_L}{C_L'}\right) + \left(\frac{C_L' - C_L}{C_L'}\right)^2\right] \quad .$$

The values of A_T have been given previously in the table of trunk values.

Male genitalia. The male genitalia region of each phantom consists of the region specified by

$$z_1 \leq z \leq 0 \ ,$$
$$-r \leq x \leq r \ ,$$
$$-r \leq y \leq 0 \ ,$$

and

$$(x \pm r)^2 + y^2 \geq r^2 \ .$$

The last inequality must hold for either choice of sign (i.e., the genitalia region lies outside both legs). The value of r is given by the expression $\frac{1}{2}A_T(1 + \frac{z}{C_L'})$, where A_T is the trunk dimension and C_L' is the legs dimension defined previously. The value of z_1 is given by the expression $-(2c + S)$, where c is the value defined for the testes and S is the skin thickness. Thus, all of the parametric values are defined elsewhere, and only the volumes are given here.

Age (years)	Volume[a] (cm³)
0	5.48
1	12.1
5	23.2
10	36.2
15	109
Adult	196

[a]Volume $= \frac{1}{6}|z_1|A_T^2(1 - \frac{\pi}{4})\left[3\left(1 + \frac{z_1}{C_L'}\right) + \left(\frac{z_1}{C_L'}\right)^2\right]$.

Mass of total body. The total body mass of each phantom is given in the following table. The male genitalia and the female breasts are included, and the different densities of lung, skeleton, and remaining tissues have been taken into account. For comparison, the mass of a human of corresponding age is also tabulated (from Watson and Lowrey, 1967).

Age (years)	Mass (g)	
	Phantom total body	Human total body
0	3,510	3,400
1	9,360	9,900
5	19,100	18,600
10	32,100	32,400
15	54,500	55,600
Adult	71,100	71,700

Note: In the equations of the organs, which follow, the body section parameters A_T, B_T, C_T, A_H, B_H, C_H, C_{H1}, C_{H2}, C_L, and C_L' and the skin thickness S will be used without further explanation or denotation. Symbols for other parameters, usually lower case letters, will have meaning only for the organ being defined. The symbol "a," for example, is used in defining many different organs.

Organs

In the text below, each organ is explicitly defined and the volume is given. The mass determined by this volume and the appropriate density is given in the Appendix.

Skeletal system. The skeletal system consists of the 13 parts described below. A view of the total skeleton is shown in Fig. 24.

Except for the skull, little information was available on weights of individual bones as a function of age during childhood. However, for the skeleton as a whole, Scammon (1953, p. 37) does make this statement: "Its postnatal growth apparently proceeds with that of the body as a whole, the total increase in weight between birth and maturity being about twenty-fold." Consequently, for the bones in the trunk and legs, the Similitude Rule was used for determining volumes as well as shape and position. This is similar to the procedure used by Hwang et al. (1976). The data used for the skull design are documented in the relevant section below.

ORNL–DWG 70-4810R2A

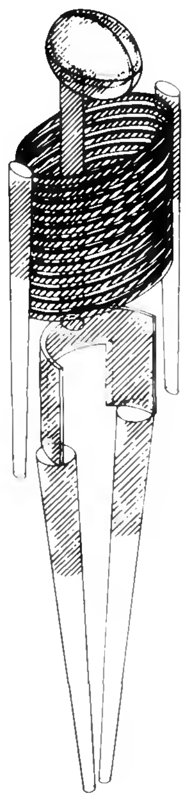

SKELETAL REGION DEFINED IN PHANTOM	DISTRIBUTION OF ACTIVE MARROW IN ADULT PHANTOM – OF SNYDER et al. (1974)	– OF THIS REPORT
SKULL	13.1%	8.3%
SPINE	28.4	29.9
RIBS	10.2	19.2
SCAPULAE	4.8	2.9
ARM BONES – UPPER PORTION	1.9	2.3
CLAVICLES	1.6	0.8
LEG BONES – UPPER PORTION	3.8	3.4
PELVIS	36.2	33.3
TOTAL AMOUNT OF ACTIVE BONE MARROW:	1500g	1120g

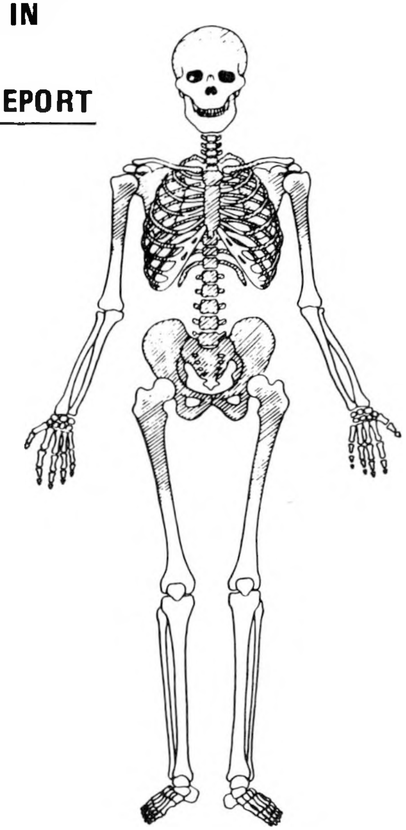

ACTIVE BONE MARROW

Fig. 24. For the adult of Snyder et al. (1974), the idealized model of the skeleton for computer calculations is shown on the left and a more realistic representation is shown on the right. The shaded areas indicate where the active bone marrow is located in the adult (from Hashimoto, 1960). The amount of active marrow in given bones, expressed as the percentage of the active marrow in the body, is also given for the adult. The values given in this report differ from those given by Snyder et al. (1974), and both sets of values are given above for comparison. Clavicles and scapulae are not shown in the phantom. The skull has been changed from that shown here to include a separate facial skeleton.

Leg bones. Each leg bone is the frustrum of a circular cone. In the defining inequalities below, the "±" sign is taken as minus for the left leg bone and plus for the right:

$$\left(x \pm \left[\frac{A_T}{2} + \frac{kz}{C_L - S}\right]\right)^2 + y^2 \leq \left(R_1 + \left[\frac{R_1 - R_2}{C_L - S}\right] z\right)^2 ,$$

and $-(C_L - S) \leq z \leq 0$, in which

$$k = \frac{A_T}{2}\left(1 - \frac{C'_L - C_L}{C'_L}\right) ,$$

$$R_1 = 0.175\, A_T ,$$

and $R_2 = \dfrac{A_T}{4}\left(\dfrac{C'_L - C_L}{C'_L}\right)$.

Age (years)	Volume (both)[a] (cm^3)
0	61.4
1	207
5	610
10	1250
15	2100
Adult	2800

[a]Volume (both) $= \frac{2}{3}\pi(C_L - S)(R_1^2 + R_2^2 + R_1R_2)$.

Arm bones. Each arm bone is the frustrum of an elliptical cone, and is defined by

$$\left[\frac{\left(\frac{a}{2z_2}\right)(z - z_2) + (x - x_0)}{a}\right]^2 + \left(\frac{y}{b}\right)^2 \leq \left[\frac{2z_2 + (z - z_2)}{2z_2}\right]^2 ,$$

and $0 \leq z \leq z_2$.

In the table below, positive values of x_0 are used for the left arm bone, and negative for the right.

Age (years)	a	b	x_0	z_2	Volume (both)[a] (cm^3)
0	0.44	1.32	± 5.84	21.29	45.3
1	0.62	1.76	± 8.10	30.26	121
5	0.80	2.03	±10.53	40.22	239
10	0.97	2.27	±12.79	50.07	404
15	1.21	2.65	±15.87	62.20	731
Adult	1.40	2.70	±18.40	69.00	956

[a]Volume (both) = $\frac{7}{6} z_2 \pi ab$.

Pelvis. The pelvis is a portion of the volume between two nonconcentric elliptical cylinders. The inequalities defining the pelvis are

$$\left(\frac{x}{a_2}\right)^2 + \left(\frac{y - y_{02}}{b_2}\right)^2 \le 1 ,$$

$$\left(\frac{x}{a_1}\right)^2 + \left(\frac{y - y_{01}}{b_1}\right)^2 \ge 1 ,$$

$$y \ge y_{02} ,$$

$$0 \le z \le z_2 ,$$

and $y \le y_1$ if $z \le z_1$.

Age (years)	a_1	b_1	a_2	b_2	y_{01}	y_{02}	y_1	z_1	z_2	Volume[a] (cm^3)
0	3.59	5.54	3.81	5.88	-1.86	-1.47	2.45	4.32	6.79	28.9
1	4.97	7.35	5.28	7.80	-2.47	-1.95	3.25	6.14	9.65	76.0
5	6.47	8.48	6.87	9.00	-2.85	-2.25	3.75	8.16	12.82	151
10	7.85	9.49	8.34	10.08	-3.19	-2.52	4.20	10.16	15.97	258
15	9.75	11.07	10.35	11.76	-3.72	-2.94	4.90	12.62	19.83	460
Adult	11.30	11.30	12.00	12.00	-3.80	-3.00	5.00	14.00	22.00	606

[a]Volume $= \frac{a_2}{b_2}\left[\frac{\pi}{2}b_2^2(z_2 - z_1) + z_1\left\{(y_1 - y_{02})\sqrt{b_2^2 - (y_1 - y_{02})^2} + b_2^2 \sin^{-1}\left(\frac{y_1 - y_{02}}{b_2}\right)\right\}\right] - \left[\frac{a_1}{b_1}\ \frac{\pi}{2}b_1^2(z_2 - z_1) - z_2\left\{(y_{02} - y_{01})\sqrt{b_1^2 - (y_{02} - y_{01})^2} + b_1^2 \sin^{-1}\left(\frac{y_{02} - y_{01}}{b_1}\right)\right\} + z_1\left\{(y_1 - y_{01})\sqrt{b_1^2 - (y_1 - y_{02})^2} + b_1^2 \sin^{-1}\left(\frac{y_1 - y_{01}}{b_1}\right)\right\}\right]$.

Spine. The spine is an elliptical cylinder given by

$$\left(\frac{x}{a}\right)^2 + \left(\frac{y - y_0}{b}\right)^2 \leq 1 \text{ and } z_1 \leq z \leq z_4 \ .$$

It is divided into 3 portions — an upper, middle, and lower — such that dose and absorbed fractions can be estimated separately for each portion. These divisions are formed by the planes $z = z_2$ and $z = z_3$.

Age (years)	a	b	y_0	z_1	z_2	z_3	z_4	Volume[a] (cm^3)
0	0.64	1.23	2.70	6.79	10.83	21.60	27.02	50.0
1	0.88	1.63	3.58	9.65	15.39	30.70	38.01	128
5	1.15	1.88	4.13	12.82	20.46	40.80	48.83	245
10	1.39	2.10	4.62	15.97	25.47	50.80	59.89	403
15	1.73	2.45	5.39	19.83	31.64	63.10	72.91	707
Adult	2.00	2.50	5.50	22.00	35.10	70.00	80.54	920

[a]Volume $= \pi ab(z_4 - z_1)$.

The value of z_4 is determined by skull position. All others are similitude values.

Skull. The skull has been redesigned to include separate cranium and facial skeleton, following the ideas of Hwang, Shoup, and Poston (1976b).

In designing the cranium and facial skeleton, the designs of the head, brain, and skeletal parts had to be considered together. The following information was used as a guideline: the size of the head as a function of age (Bardeen 1920), the cephalic index as a function of age (Krogman 1941), skull weight for newborn and adult (ICRP 1975), general statements on growth of the skull (Scammon 1953, p. 54; Watson and Lowrey 1967, pp. 376-381), relative skull dimensions and ratio of cranium volume to facial skeleton volume as a function of age (Watson and Lowrey 1967, p. 380), skull thickness at lambda as a function of age (Hansman 1966), and brain size as a function of age (ICRP 1975).

The cranium is represented by the volume between two concentric ellipsoids defined by

$$\left(\frac{x}{a}\right)^2 + \left(\frac{y}{b}\right)^2 + \left(\frac{z - [C_T + C_{H1}]}{c}\right)^2 \geq 1$$

and $$\left(\frac{x}{a + d}\right)^2 + \left(\frac{y}{b + d}\right)^2 + \left(\frac{z - [C_T + C_{H1}]}{c + d}\right)^2 \leq 1 \ .$$

The values a, b, and c are the same as the values a, b, and c given in the statements and table for the brain.

Age (years)	d	Volume[a] (cm^3)
0	0.20	49.8
1	0.30	139
5	0.56	339
10	0.67	434
15	0.76	508
Adult	0.90	618

[a]Volume $= \frac{4}{3}\pi[(a + d)(b + d)(c + d) - abc]$.

The facial skeleton is represented by a portion of the volume between two concentric elliptical cylinders (Fig. 25). The portion of the volume that intersects the cranium and brain is excluded. The inequalities are

$$\left(\frac{x}{a_1}\right)^2 + \left(\frac{y}{b_1}\right)^2 \leq 1 ,$$

$$\left(\frac{x}{a_1 - d}\right)^2 + \left(\frac{y}{b_1 - d}\right)^2 \geq 1 ,$$

$$y \leq 0 ,$$

$$C_T + z_1 \leq z \leq C_T + z_5 ,$$

$$\text{and} \left(\frac{x}{a_2}\right)^2 + \left(\frac{y}{b_2}\right)^2 + \left(\frac{z - [C_T + C_{H1}]}{c_2}\right)^2 > 1 .$$

The variables a_2, b_2, and c_2 correspond in numerical value with the variable expressions (a + b), (b + d), and (c + d), respectively, in the statements defining the cranium and hence are not given below.

Age (years)	a_1	b_1	d	z_1	z_5	Volume[a] (cm^3)
0	4.17	5.43	0.07	2.16	8.18	6.13
1	5.73	7.44	0.14	2.93	11.18	22.8
5	6.68	8.60	0.58	3.30	12.57	114
10	6.93	8.90	0.74	3.61	13.73	161
15	6.92	8.91	1.10	3.79	14.05	234
Adult	7.00	9.00	1.40	4.00	14.73	305

[a]Volume $= \frac{\pi}{2}(z_2 - z_1)[a_1 b_1 - (a_1 - d)(b_1 - d)]$

$$+ \int_{z_2}^{z_3} \left\{ \frac{\pi}{2}[a_1 b_1 - (a_1 - d)(b_1 - d)] \right.$$

ORNL-DWG 76-1947R

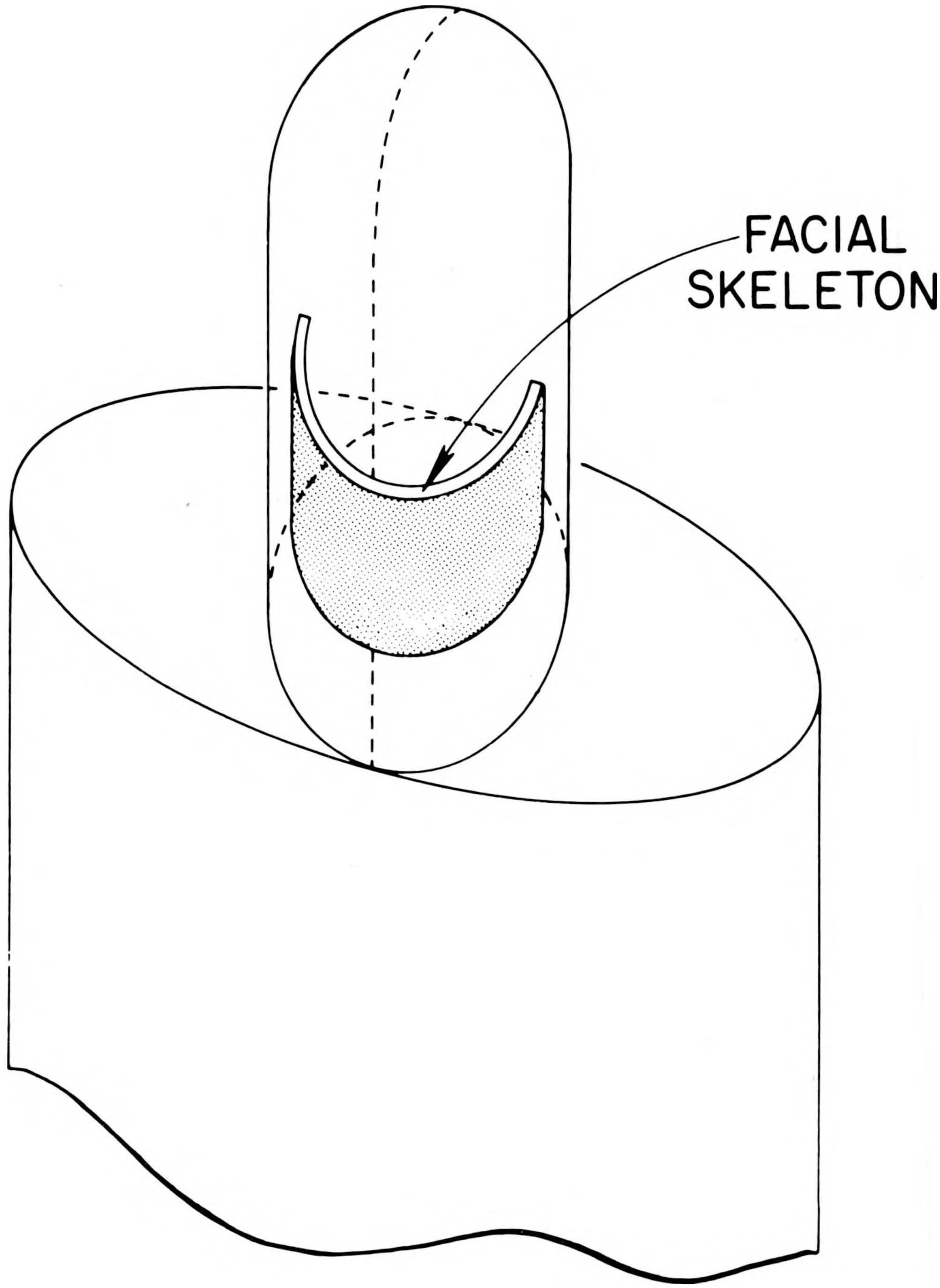

Fig. 25. Model of the facial skeleton, modified from Hwang, Shoup, and Poston (1976a).

$$- \frac{a_2}{b_2}\left[y_3\sqrt{b_2^2\left\{1 - \left(\frac{z - z_0}{c_2}\right)^2\right\} - y_3^2}\right.$$

$$\left. + b_2^2\left\{1 - \left(\frac{z - z_0}{c_2}\right)^2\right\}\sin^{-1}\left(\frac{y_3}{b_2\sqrt{1 - \left(\frac{z - z_0}{c_2}\right)^2}}\right)\right]$$

$$+ \frac{a_1 - d}{b_1 - d}\left[y_3\sqrt{(b_1 - d)^2 - y_3^2} + (b_1 - d)^2 \sin^{-1}\left(\frac{y_3}{b_1 - d}\right)\right]\Bigg\} dz$$

$$+ \frac{\pi}{2}(z_4 - z_3)(a_1b_1 - a_2b_2)$$

$$- \frac{\pi a_2b_2}{6c_2^2}\left[(z_3 - z_0)^3 - (z_4 - z_0)^3\right]$$

$$+ \int_{z_4}^{z_5}\Bigg\{\frac{b_1}{a_1}\left[x_1\sqrt{a_1^2 - x_1^2} + a_1^2 \sin^{-1}\frac{x_1}{a_1}\right]$$

$$- \frac{b_2}{a_2}\left[x_1\sqrt{a_2^2\left\{1 - \left(\frac{z - z_0}{c_2}\right)^2\right\} - x_1^2}\right.$$

$$\left. + a_2^2\left\{1 - \left(\frac{z - z_0}{c_2}\right)^2\right\}\sin^{-1}\left(\frac{x_1}{a_2\sqrt{1 - \left(\frac{z - z_0}{c_2}\right)^2}}\right)\right]\Bigg\} dz ,$$

where $z_0 = C_T + C_{H1}$,

$$z_2 = z_0 - c_2\sqrt{1 - \left(\frac{a_1 - d}{a_2}\right)^2},$$

$$z_3 = z_0 - c_2\sqrt{1 - \left(\frac{b_1 - d}{b_2}\right)^2},$$

$$z_4 = z_0 - c_2\sqrt{1 - \left(\frac{a_1}{a_2}\right)^2},$$

$$x_1 = \sqrt{\frac{b_2^2 - b_1^2 - \dfrac{b_2^2}{c_2^2}(z - z_0)^2}{\dfrac{b_2^2}{a_2^2} - \dfrac{b_1^2}{a_1^2}}} ,$$

$$x_2 = a_2\sqrt{1 - \left(\frac{z - z_0}{c_2}\right)^2} ,$$

$$\text{and } y_3 = \sqrt{\frac{a_2^2 - (a_1 - d)^2 - \left[\dfrac{a_2}{c_2}(z - z_0)\right]^2}{\left(\dfrac{a_2}{b_2}\right)^2 - \left(\dfrac{a_1 - d}{b_1 - d}\right)^2}} .$$

The integrations in the volume formula were performed numerically with the Gaussian quadrature method.

Rib cage. The rib volume is a series of bands between two concentric, right-vertical, elliptical cylinders. This region is sliced by a series of equispaced horizontal planes into slabs, every other slice being a rib. The statements that must be satisfied are

$$\left(\frac{x}{a}\right)^2 + \left(\frac{y}{b}\right)^2 \leq 1 ,$$

$$\left(\frac{x}{a - d}\right)^2 + \left(\frac{y}{b - d}\right)^2 \geq 1 ,$$

$$z_1 \leq z \leq z_2 ,$$

and Integer $\left(\frac{z - z_1}{c}\right)$ is even.

The function Integer (u) is the integral part of u [e.g., Integer (3.67) = 3]. Thus, the statement "Integer $\left(\frac{z - z_1}{c}\right)$ is even" amounts to requiring that

$$0 \leq \frac{z - z_1}{c} < 1 \text{ or } 2 \leq \frac{z - z_1}{c} \leq 3 \text{ or } 4 \leq \frac{z - z_1}{c} < 5, \text{ etc.}$$

Age (years)	a	b	d	z_1	z_2	c	Volume[a] (cm^3)
0	5.40	4.80	0.21	10.86	20.75	0.43	34.0
1	7.48	6.37	0.28	15.44	29.47	0.61	87.4
5	9.73	7.35	0.34	20.53	39.16	0.81	174
10	11.82	8.23	0.39	25.43	48.89	1.02	295
15	14.66	9.60	0.47	31.67	60.65	1.26	531
Adult	17.00	9.80	0.50	35.10	67.30	1.40	694

[a]Volume = $12\pi c[ab - (a - d)(b - d)]$.

Clavicles. The clavicles are represented as two portions of a torus which lies along the circular arc $x^2 + (y - y_0)^2 = R^2$ at $z = z_1$ and has a smaller radius of r. The clavicles include only the portion of the torus between the planes $y_0 - y = |x| \cot \theta_1$ and $y_0 - y = |x| \cot \theta_2$. (The absolute value sign on x allows for both a right and a left clavicle.) These equations can be reduced to the form

$$(z - z_1)^2 + (R - \sqrt{x^2 + (y - y_0)^2})^2 \leq r^2 ,$$

$$\cot \theta_2 \leq \frac{y_0 - y}{|x|} \leq \cot \theta_1, \text{ and } y < 0 .$$

Age (years)	y_0	z_1	R	r	$\cot \theta_1$	$\cot \theta_2$	Volume (both)[a] (cm^3)
0	0.73	21.06	5.07	0.2833	5.5868	0.38510	2.62
1	1.38	29.93	7.14	0.3930	5.6814	0.43161	6.85
5	3.14	39.78	9.80	0.4991	5.9977	0.56391	13.7
10	4.93	49.53	12.40	0.5981	6.2581	0.65708	23.2
15	7.22	61.52	15.93	0.7274	6.4852	0.73137	41.6
Adult	11.10	68.25	20.00	0.7883	7.0342	0.89415	54.7

[a]Volume (both) = $2\pi r^2(\theta_2 - \theta_1) R$.

The clavicles lie slightly inside the cylinder defining the rib cage and just above the top rib (Fig. 26).

ORNL-DWG 74-957

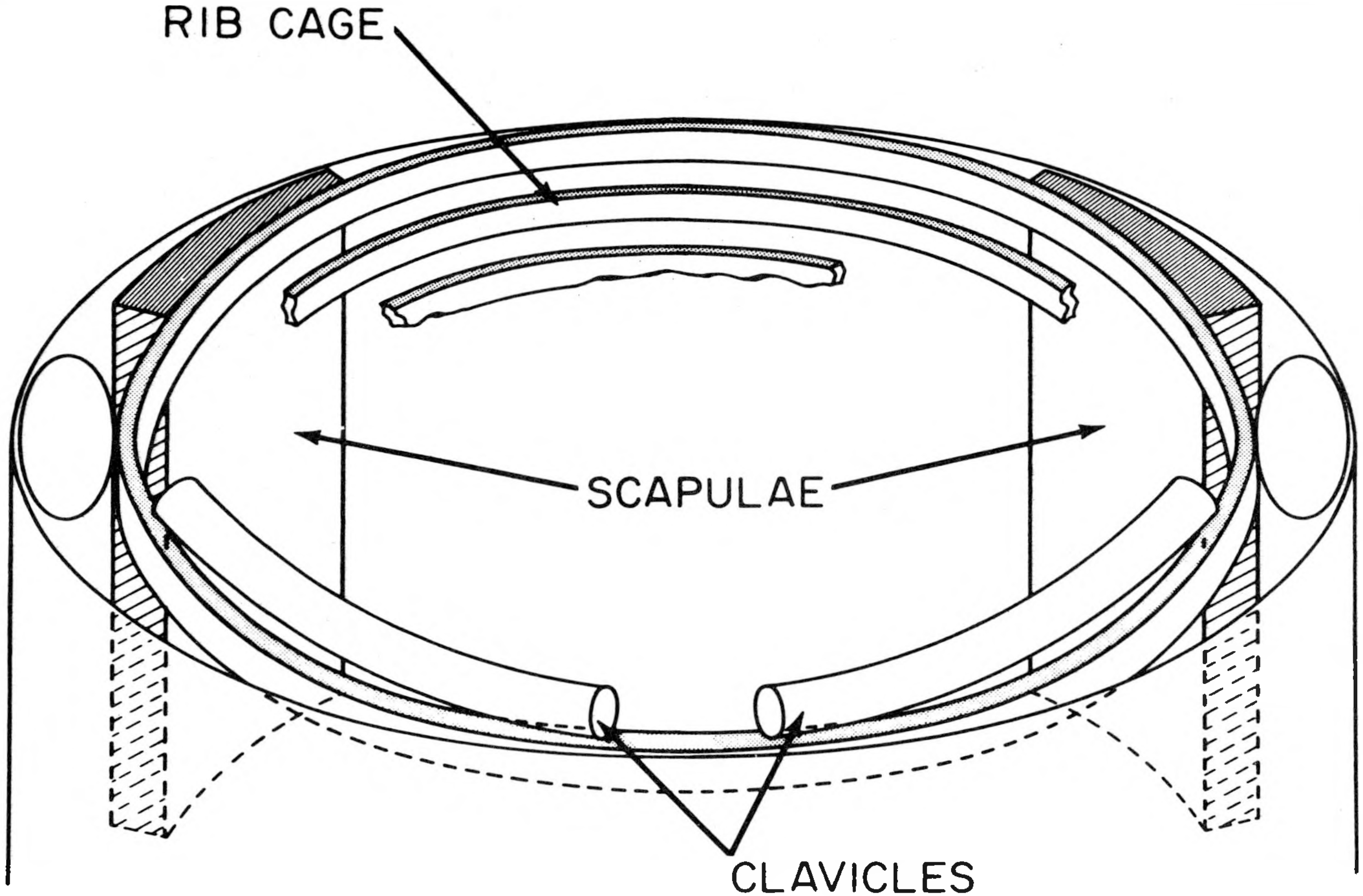

Fig. 26. Detailed view of scapulae and clavicles, drawn for the adult (from Snyder et al., 1974).

Scapulae. The scapulae are defined as part of the volume between two concentric elliptical cylinders. For each scapula, the volume is bounded by the planes $z = z_1$, $z = z_2$, $y = m_1|x|$, and $y = m_2|x|$. (The absolute value sign on x allows for both a right and a left scapula.) The defining inequalities are

$$\left(\frac{x}{a_2}\right)^2 + \left(\frac{y}{b}\right)^2 \leq 1 ,$$

$$\left(\frac{x}{a_1}\right)^2 + \left(\frac{y}{b}\right)^2 > 1 ,$$

$$z_1 \leq z \leq z_2 ,$$

$$y > 0 ,$$

$$\text{and } m_1 < \frac{y}{|x|} < m_2 .$$

Age (years)	a_1	a_2	b	z_1	z_2	m_1	m_2	Volume (both)[a] (cm^3)
0	5.40	6.04	4.80	15.71	20.77	0.39	1.23	9.64
1	7.48	8.36	6.37	22.32	29.52	0.37	1.18	25.3
5	9.73	10.88	7.35	29.67	39.23	0.33	1.05	50.4
10	11.82	13.20	8.23	36.94	48.84	0.30	0.97	85.7
15	14.66	16.36	9.60	45.88	60.67	0.28	0.91	154
Adult	17.00	19.00	9.80	50.90	67.30	0.25	0.80	202

[a]Volume (both) $= b(z_2 - z_1)\left\{a_2\left[\tan^{-1}\frac{a_2 m_2}{b} - \tan^{-1}\frac{a_2 m_1}{b}\right] - a_1\left[\tan^{-1}\frac{a_1 m_2}{b} - \tan^{-1}\frac{a_1 m_1}{b}\right]\right\}.$

Bone marrow. On the right in Fig. 24 is shown an adult skeleton, with the areas containing active marrow cross-hatched. On the left is shown the idealized skeleton used for the adult phantom with the corresponding areas cross-hatched.

The regional distributions of the active (hematopoietic) bone marrow and the inactive (fatty) marrow vary greatly with age. The regional distributions were calculated by the method of Cristy (1980). The approximate weights of the total (active plus inactive) marrow, the active marrow, and the inactive marrow as a function of age are given in Table 3. Data from Hudson (1965), Custer (1974), ICRP (1975), and Woodard and Holodny (1960) were used to estimate the weight of the total marrow. The weights of active and inactive marrow in Table 3 were calculated from the total marrow values using the method of Cristy (1980).

The active marrow in individual bones, parts of bones, or bone groups of the phantoms, expressed as the percentage of active marrow in the body, are given in Table 4. The weight of active marrow in a given bone or bone group may be found by using Tables 3 and 4 together. Similarly, in Table 5 are given the inactive (fatty) marrow percentages, and the weights of inactive marrow may be found by using Tables 3 and 5 together. The weights of active and inactive marrow in individual bones are given in the Appendix.

The marrow, active or inactive, is assumed to be distributed uniformly in the bone regions defined. In calculating an absorbed fraction for active and for inactive marrow in these regions, it is assumed that the marrow absorbs energy per gram as efficiently as does bone. This assumption is not grossly in error at energies of 200 keV or more; but it is increasingly inaccurate at energies below 100 keV, where the photoelectric effect dominates the photon interaction process. The effect is to overestimate the dose to marrow and to underestimate the dose to the bone mineral component of the mixture. It is difficult to program the intricate microscopic intermixture of bone and marrow spaces in a more realistic fashion in the macroscopic characterization used in photon transport. The composition of the skeleton (Table 2) has a density of approximately 1.5 g/cm^3 and thus is to be regarded as a homogeneous mixture of true bone and marrow and other organic constituents of the skeleton.

The marrow from the lumbar vertebra L_5 and 50% of the upper half of the femora were assigned to the pelvis of each phantom (Tables 4 and 5).

Table 3. Weights of total marrow, active marrow, and inactive marrow in the body as a function of age

Age (years)	Total marrow (g)	Active marrow (g)	Inactive marrow (g)
0	47	47	0
1	170	150	20
5	460	320	140
10	1200	610	590
15	2600	1050	1550
Adult	3500	1120	2380

Table 4. Active marrow in individual bones, parts of bones, or bone groups expressed as the percentage of active marrow in the body (derived from Cristy, 1980)

Phantom skeletal region	Corresponding skeletal region(s)	Percentage at various ages: 0	1	5	10	15	Adult[a]
Skull (cranium + facial skeleton)[b]	Skull (cranium + mandible)[b]	29.50	27.47	17.44	12.72	10.12	8.32
Scapulae	Scapulae	2.70	2.73	2.72	2.89	3.26	2.85
Clavicles	Clavicles	0.80	0.83	0.85	0.89	0.98	0.79
Ribs	Ribs + sternum	9.20	9.61	10.58	13.02	16.27	19.22
Spine (upper portion[c])	Cervical vertebrae C_1-C_5	2.30	1.88	1.46	1.80	2.25	2.66
Spine (middle portion[c])	Cervical vertebrae C_6-C_7 + all thoracic vertebrae	9.40	9.27	9.58	11.79	14.75	17.41
Spine (lower portion[c])	Lumbar vertebrae L_1-L_4	1.90	3.37	5.39	6.63	8.29	9.79
Pelvis	Sacrum + os coxae + lumbar vertebra L_5 + 50% of upper 1/2 femora	11.66	16.47	23.33	28.73	33.60	33.31
Leg bones (upper portion[d])	50% of upper 1/2 femora	1.87	2.07	3.41	4.72	4.60	3.35
Leg bones (middle portion[d])	Lower 1/2 femora	3.73	3.88	6.28	6.14	2.04	0
Leg bones (lower portion[d])	Tibiae, fibulae, patellae + ankle and foot bones	16.24	13.40	11.55	5.51	0	0
Arm bones (upper portion[e])	Upper 1/2 humeri	2.32	2.41	2.36	2.49	3.14	2.29
Arm bones (middle portion[e])	Lower 1/2 humeri	2.32	2.25	2.18	1.62	0.70	0
Arm bones (lower portion[e])	Radii and ulnae + wrist and hand bones	6.07	4.36	2.88	1.06	0	0

[a]Age 40 values from Cristy (1980) were used for the adult phantom.

[b]In column 1, cranium does not include the facial skeleton, but in column 2, cranium includes all the facial skeleton except the mandible.

[c]The upper, middle, and lower portions of the spine are defined in the section on the spine.

[d]The upper portion of the leg bones is defined as the upper 14% of the length of the bones; the lower portion is defined as the lower 57%; and the middle portion is the rest. The unevenness of these numbers results from the assignment of part of the marrow in the upper femora to the pelvis.

[e]The upper portion of the arm bones is defined as the upper 25% of the length of the bones; the lower portion is defined as the lower 50%; and the middle portion is the rest.

Table 5. Inactive marrow in individual bones, parts of bones, or bone groups expressed as the percentage of inactive marrow in the body (derived from Cristy, 1980)

Phantom skeletal region	Corresponding skeletal region(s)	Percentage at various ages					
		0	1	5	10	15	Adult[a]
Skull (cranium + facial skeleton)[b]	Skull (cranium + mandible)[b]		11.33	10.17	7.16	5.63	6.35
Scapulae	Scapulae		1.06	1.60	1.64	1.82	2.17
Clavicles	Clavicles		0.35	0.53	0.53	0.61	0.75
Ribs	Ribs + sternum		3.90	4.32	3.42	3.70	3.86
Spine (upper portion[c])	Cervical vertebrae C_1-C_5		0.78	0.61	0.47	0.51	0.53
Spine (middle portion[c])	Cervical vertebrae C_6-C_7 + all thoracic vertebrae		3.82	3.95	3.10	3.34	3.50
Spine (lower portion[c])	Lumbar vertebrae L_1-L_4		1.40	2.21	1.74	1.90	1.97
Pelvis	Sacrum + os coxae + lumbar vertebra L_5 + 50% of upper 1/2 femora		6.79	13.28	11.87	13.28	16.07
Leg bones (upper portion[d])	50% of upper 1/2 femora		0.84	2.36	3.31	3.83	4.70
Leg bones (middle portion[d])	Lower 1/2 femora		3.72	5.95	10.08	12.53	12.53
Leg bones (lower portion[d])	Tibiae, fibulae, patellae + ankle and foot bones		45.35	39.29	40.05	36.66	32.05
Arm bones (upper portion[e])	Upper 1/2 humeri		0.97	1.63	1.74	2.62	3.21
Arm bones (middle portion[e])	Lower 1/2 humeri		2.21	2.06	2.64	4.29	4.29
Arm bones (lower portion[e])	Radii and ulnae + wrist and hand bones		17.45	12.04	12.25	9.28	8.02

[a] Age 40 values from Cristy (1980) were used for the adult phantom.

[b] In column 1, cranium does not include the facial skeleton, but in column 2, cranium includes all the facial skeleton except the mandible.

[c] The upper, middle, and lower portions of the spine are defined in the section on the spine.

[d] The upper portion of the leg bones is defined as the upper 14% of the length of the bones; the lower portion is defined as the lower 57%; and the middle portion is the rest. The unevenness of these numbers results from the assignment of part of the marrow in the upper femora to the pelvis.

[e] The upper portion of the arm bones is defined as the upper 25% of the length of the bones; the lower portion is defined as the lower 50%; and the middle portion is the rest.

This assignment occurs because of the simplicity of the skeleton in the phantoms. For example, approximately the upper quarter of the femora is adjacent to the os coxae of the pelvis in humans, but in the phantom the leg bones begin below the pelvis.

The total mass of the skeleton in each phantom is given in the following table.

Age (years)	Mass of entire skeleton (g)
0	428
1	1,210
5	2,880
10	4,920
15	8,120
Adult	10,600

Adrenals. Each adrenal is half an ellipsoid atop a kidney, defined by

$$\left(\frac{x_1}{a}\right)^2 + \left(\frac{y_1}{b}\right)^2 + \left(\frac{z_1}{c}\right)^2 \leq 1 \text{ and } z_1 \geq 0 ,$$

where the (x_1,y_1,z_1)-coordinate system is related to the phantom's (x,y,z)-coordinate system by the following rotation-translation equations, given in matrix form:

$$\begin{bmatrix} x_1 \\ y_1 \\ z_1 \end{bmatrix} = \begin{bmatrix} \cos\theta & \sin\theta & 0 \\ -\sin\theta & \cos\theta & 0 \\ 0 & 0 & 1 \end{bmatrix} \begin{bmatrix} x - x_0 \\ y - y_0 \\ z - z_0 \end{bmatrix} .$$

In the following table of parametric values, x_0 and θ are both taken as positive for the left adrenal, and both negative for the right. The position of the adrenals in the adult has been changed for consistency with the pediatric phantom design. Drawings of the mathematical models for the adrenals and other selected organs are shown in Fig. 27.

ORNL–DWG 79-20294

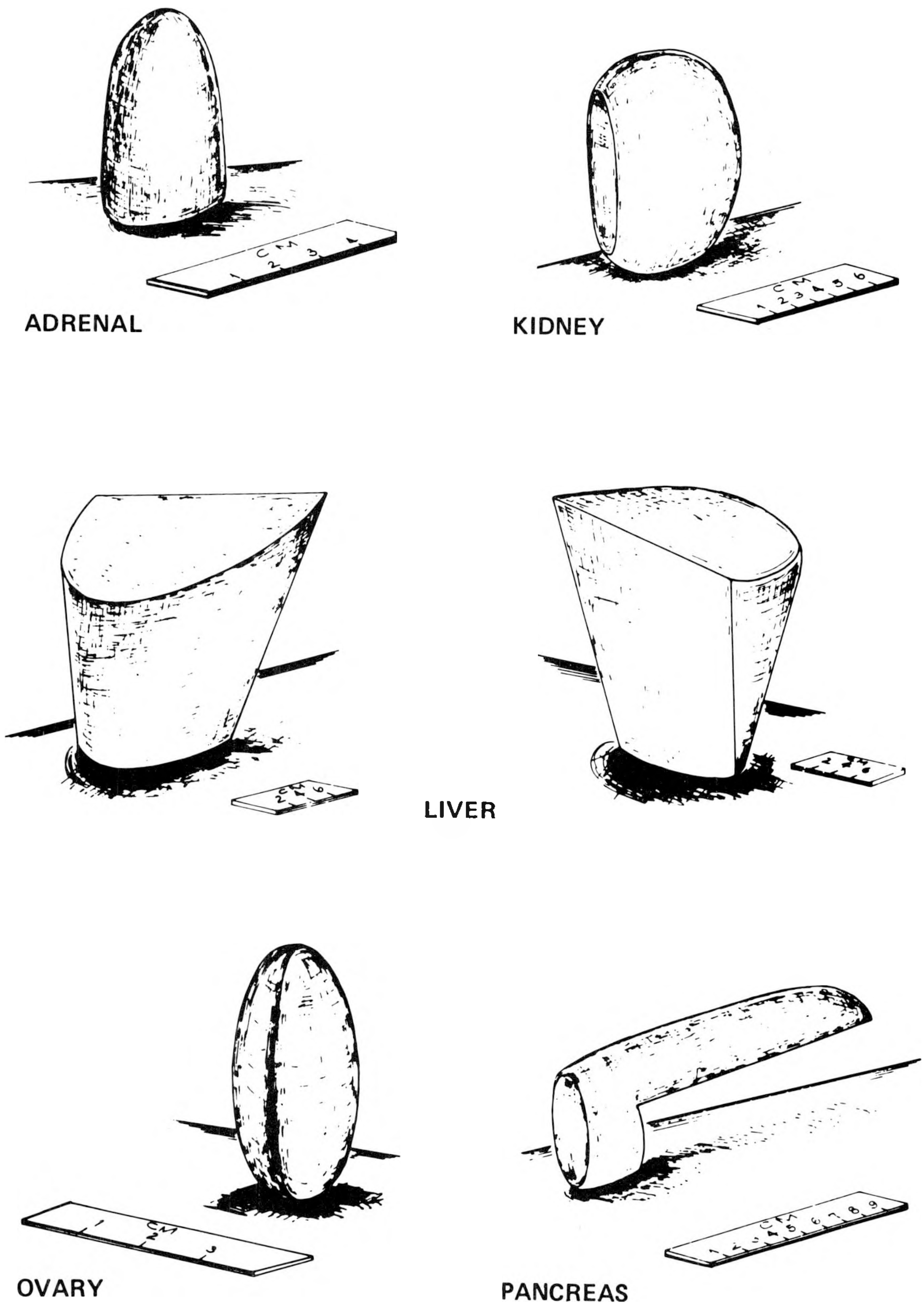

Fig. 27. Mathematical models for the adrenals, kidneys, liver, ovaries, and pancreas, as drawn for the adult (from Snyder et al., 1974).

Age (years)	a	b	c	x_0	y_0	z_0	θ	Volume (both)[a] (cm^3)	Targeted volume[b] (cm^3)
0	1.61	0.54	1.54	±1.41	2.45	11.73	±63.3°	5.61	5.59
1	1.05	0.35	2.20	±1.54	3.25	16.66	±62.2	3.39	3.40
5	1.12	0.37	2.92	±2.00	3.75	22.14	±59.3	5.07	5.08
10	1.17	0.39	3.63	±2.43	4.20	27.58	±57.2	6.94	6.93
15	1.30	0.43	4.30	±3.02	4.90	34.26	±55.6	10.1	10.1
Adult	1.50	0.50	5.00	±3.50	5.00	38.00	±52.0	15.7	13.4

[a]Volume (both) = $\frac{4}{3}\pi abc$.
[b]Derived from ICRP Publication 23 (1975).

Brain. The brain is an ellipsoid given by

$$\left(\frac{x}{a}\right)^2 + \left(\frac{y}{b}\right)^2 + \left(\frac{z - [C_T + C_{H1}]}{c}\right)^2 \leq 1 \ .$$

Age (years)	a	b	c	Volume[a] (cm^3)	Targeted volume[b] (cm^3)
0	4.14	5.40	3.61	338	338
1	5.63	7.34	4.91	850	850
5	6.34	8.26	5.52	1210	1210
10	6.51	8.48	5.67	1310	1310
15	6.58	8.57	5.73	1350	1350
Adult	6.60	8.60	5.75	1370	1370

[a]Volume = $\frac{4}{3}\pi abc$.
[b]Derived from ICRP Publication 23 (1975).

The adult brain has been modified to fit into the new skull.

Breasts. The female breasts are represented by portions of two ellipsoids attached to the trunk, given by

$$\left(\frac{x - x_0}{a}\right)^2 + \left(\frac{y - y_0}{b}\right)^2 + \left(\frac{z - z_0}{c}\right)^2 \leq 1$$

and $\left(\frac{x}{A_T}\right)^2 + \left(\frac{y}{B_T}\right)^2 > 1$,

where $y_0 = -B_T\sqrt{1 - \left(\frac{x_0}{A_T}\right)^2}$.

The positive values of x_0 in the table below are taken for the left breast; and the negative values, for the right breast.

Since the outer thickness S is counted as skin, the breast tissue is represented by

$$\left(\frac{x - x_0}{a - S}\right)^2 + \left(\frac{y - y_0}{b - S}\right)^2 + \left(\frac{z - z_0}{c - S}\right)^2 \leq 1$$

and $\left(\frac{x}{A_T}\right)^2 + \left(\frac{y}{B_T}\right)^2 > 1$.

The risk to females after puberty associated with radiation absorbed in the breasts before puberty is uncertain (UNSCEAR 1977, pp. 385-394). For prudence' sake, female breast tissue has been included for all ages.

In the designing of the female breasts, the data in ICRP Publication 23 (ICRP 1975, p. 195) were used. For the adult, the dimensions of the breast and the weight of the breast given therein do not correspond. Consequently, the dimensions were reduced by a constant factor to yield the targeted size. For the adolescent breast (15-year-old phantom), the adult dimensions were reduced by half, following the example of Boice, Rosenstein, and Trout (1978). For the earlier ages, a hemispherical form was adopted and the size was estimated by scaling down the adult male breast.

Age						Volume (both)[a] (cm^3)	
(years)	a	b	c	x_0	z_0	Including skin	Excluding skin
0	0.36	0.36	0.36	3.18	16.05	0.197	0.103
1	0.63	0.63	0.63	4.40	22.81	1.06	0.704
5	0.79	0.79	0.79	5.73	30.31	2.09	1.45
10	0.94	0.94	0.94	6.95	37.73	3.51	2.50
15	2.42	2.13	2.03	8.63	46.87	44.8	35.1
Adult	4.83	4.26	4.06	10.00	52.00	362	314

[a]Volume (both breasts, including skin) =

$$2\left\{\frac{2}{3}\pi abc + \int_{z=z_0-c}^{z=z_0+c}\int_{y=y_1(z)}^{y=y_0} t(y,z)\ dy\ dz\right.$$

$$\left. - \int_{z=z_0-c}^{z=z_0+c}\int_{y=y_0}^{y=y_2(z)} u(y,z)\ dy\ dz\right\},$$

$$\text{where } t(y,z) = x_0 + a\sqrt{1-\left(\frac{y - y_0}{b}\right)^2 - \left(\frac{z - z_0}{c}\right)^2} - A_T\sqrt{1 - \left(\frac{y}{B_T}\right)^2},$$

$$u(y,z) = A_T\sqrt{1 - \left(\frac{y}{B_T}\right)^2} - x_0 + a\sqrt{1-\left(\frac{y - y_0}{b}\right)^2 - \left(\frac{z - z_0}{c}\right)^2},$$

$y_1(z)$ is the zero of the function $t(y,z)$ in the interval $(y_0 - b, y_0)$, and $y_2(z)$ is the zero of the function $u(y,z)$ in the interval $(y_0, y_0 + b)$. The integrations were performed numerically using the Gaussian quadrature method.

The volume of the breast tissue (excluding the skin) can be found using the same formula, but substituting a - S, b - S, and c - S for a, b, and c, respectively, throughout.

Gall bladder and contents. For the adult and ages 1, 5, 10, and 15 years, the gall bladder is represented by the frustrum of a cone capped with a hemisphere. For the newborn phantom, the gall bladder is cylindrical. The gall bladder is defined as a walled organ.

The equations are given below in (x_1,y_1,z_1)-coordinates which are related to the (x,y,z)-coordinate system by the following rotation-translation equations:

$$\begin{bmatrix} x_1 \\ y_1 \\ z_1 \end{bmatrix} = \begin{bmatrix} \alpha_1 & \beta_1 & \gamma_1 \\ \alpha_2 & \beta_2 & \gamma_2 \\ \alpha_3 & \beta_3 & \gamma_3 \end{bmatrix} \begin{bmatrix} x - x_0 \\ y - y_0 \\ z - z_0 \end{bmatrix} .$$

The walls are specified as follows:

(hemispherical part)

$$x_1^2 + y_1^2 + z_1^2 \leq r_2^2 ,$$

$$x_1^2 + y_1^2 + z_1^2 \geq r_1^2 ,$$

and $z_1 < 0$;

and (conical part)

$$x_1^2 + y_1^2 \leq (r_2 - sz_1)^2 ,$$

$$x_1^2 + y_1^2 \geq (r_1 - sz_1)^2 ,$$

and $0 \leq z_1 \leq h$.

The contents are specified as follows:

(hemispherical part)

$$x_1^2 + y_1^2 + z_1^2 < r_1^2$$

and $z_1 < 0$;

and (conical part)

$$x_1^2 + y_1^2 < (r_1 - sz_1)^2$$

and $0 \leq z_1 \leq h$.

To obtain the equations for the newborn gall bladder wall and contents, set s = 0 and ignore the hemispherical part.

The newborn and adult gall bladders are those designed by Hwang, Shoup, and Poston (1976a,b), with slight modifications.

Age (years)	α_1	β_1	γ_1	α_2	β_2	γ_2	α_3	β_3	γ_3
0	0.9292	0.0000	-0.3695	-0.1018	0.9613	-0.2559	0.3553	0.2754	0.8933
1	0.9770	0.0000	-0.2132	-0.0348	0.9866	-0.1594	0.2105	0.1632	0.9639
5	0.9814	0.0000	-0.1921	-0.0291	0.9884	-0.1490	0.1898	0.1518	0.9700
10	0.9722	0.0000	-0.2342	-0.0400	0.9853	-0.1661	0.2307	0.1709	0.9579
15	0.9550	0.0000	-0.2964	-0.0606	0.9789	-0.1952	0.2903	0.2044	0.9349
Adult	0.9615	0.0000	-0.2748	-0.0574	0.9779	-0.2008	0.2687	0.2090	0.9403

Age (years)	r_1	r_2	s	h	x_0	y_0	z_0
0	0.458	0.500	0	3.10	-0.67	-1.75	8.68
1	0.884	0.937	0.2275	3.54	-0.71	-2.08	13.16
5	1.414	1.499	0.2275	5.66	-0.59	-2.40	17.49
10	1.768	1.874	0.2275	7.07	-1.69	-2.69	21.77
15	1.916	2.031	0.2275	7.66	-4.48	-3.14	27.04
Adult	2.000	2.120	0.2275	8.00	-4.50	-3.20	30.00

Age	Volume (cm^3)			Targeted volume-[a]
(years)	Wall	Contents	Wall + Contents	wall + contents (cm^3)
0	0.392	2.04	2.43	2.5-3
1	0.875	4.62	5.50	5.5
5	3.59	18.9	22.5	22.5
10	7.00	37.0	44.0	44
15	8.92	47.1	56.0	56
Adult	10.1	53.6	63.7	50-65

[a]Derived from ICRP Publication 23 (1975).

For newborn,

$$\text{Volume (wall)} = \pi(r_2^2 - r_1^2)h$$

and $$\text{Volume (contents)} = \pi r_1^2 h \ .$$

For all other ages,

$$\text{Volume (wall)} = \frac{2}{3}\pi(r_2^3 - r_1^3) + \pi h[r_2^2 - r_1^2 + sh(r_1 - r_2)]$$

and $$\text{Volume (contents)} = \frac{2}{3}\pi r_1^3 + \frac{1}{3}\pi h[r_1^2 + (r_1 - sh)^2 + r_1(r_1 - sh)] \ .$$

With lack of data on separate wall and contents volumes, the ratio of wall to contents volumes in the adult was assumed for the other ages.

Gastrointestinal tract and contents. Stomach. The stomach wall is represented by the volume between two concentric ellipsoids. The contents are represented by the volume within the inner ellipsoid. The wall is defined by

$$\left(\frac{x - x_0}{a}\right)^2 + \left(\frac{y - y_0}{b}\right)^2 + \left(\frac{z - z_0}{c}\right)^2 \leq 1$$

and $$\left(\frac{x - x_0}{a - d}\right)^2 + \left(\frac{y - y_0}{b - d}\right)^2 + \left(\frac{z - z_0}{c - d}\right)^2 \geq 1 \ .$$

The contents are defined by

$$\left(\frac{x - x_0}{a - d}\right)^2 + \left(\frac{y - y_0}{b - d}\right)^2 + \left(\frac{z - z_0}{c - d}\right)^2 < 1 \ .$$

Age (years)	a	b	c	d	x_0	y_0	z_0
0	1.20	1.39	2.34	0.22	2.54	-1.96	10.80
1	1.85	2.05	3.51	0.33	3.52	-2.70	15.35
5	2.55	2.40	4.66	0.45	4.58	-3.15	20.40
10	3.14	2.74	5.81	0.53	5.56	-3.51	25.40
15	3.43	2.92	7.16	0.56	6.90	-3.92	31.55
Adult	4.00	3.00	8.00	0.613	8.00	-4.00	35.00

Age (years)	Volume-wall[a] (cm^3)	Targeted volume-wall[b] (cm^3)	Volume-contents[c] (cm^3)
0	6.17	6.18	10.2
1	20.9	21.0	34.8
5	47.2	47.1	72.2
10	81.8	81.9	128
15	113	113	187
Adult	152	143	250

[a]Volume (wall) = $\frac{4}{3}\pi[abc - (a - d)(b - d)(c - d)]$.

[b]Derived from ICRP Publication 23 (1975).

[c]Volume (contents) = $\frac{4}{3}\pi(a - d)(b - d)(c - d)$.

The stomach represented here is a "full" stomach, and the average dose rate, even for the same activity present, probably varies greatly depending on the degree of extension of the stomach, presence of air spaces, etc.

Small intestine. The small intestine does not seem to remain in any "standard position" except the ends, which are relatively fixed. Thus, the small intestine is to be regarded as occupying a volume within which it is free to move. No attempt to determine a specific configuration is made here, and thus the wall and contents are not distinguished for estimation of photon dose.

The small intestine and contents are represented by a section of an elliptical cylinder, defined by

$$\left(\frac{x}{a}\right)^2 + \left(\frac{y - y_0}{b}\right)^2 \leq 1 ,$$

$$y_1 \leq y \leq y_2 ,$$

and $z_1 \leq z \leq z_2$.

The portion of the large intestine within this region is excluded.

Age (years)	a	b	y_0	y_1	y_2	z_1	z_2	Volume[a] (cm^3)
0	3.59	5.54	-1.86	-2.38	1.08	5.25	8.33	50.9
1	4.97	7.35	-2.47	-3.16	1.43	7.46	11.84	132
5	6.47	8.48	-2.85	-3.65	1.65	9.91	15.74	265
10	7.85	9.49	-3.19	-4.08	1.85	12.34	19.59	447
15	9.75	11.07	-3.72	-4.76	2.16	15.32	24.34	806
Adult	11.30	11.30	-3.80	-4.86	2.20	17.00	27.00	1060

[a]Volume = $(z_2 - z_1)ab\left[\left(\frac{y - y_0}{b}\right)\sqrt{1 - \left(\frac{y - y_0}{b}\right)^2} + \sin^{-1}\left(\frac{y - y_0}{b}\right)\right]_{y=y_1}^{y=y_2}$.

- ascending colon contribution
- transverse colon contribution
- descending colon contribution,

in which the expression within the brackets is evaluated between the limits $y=y_1$ and $y=y_2$; and

$$\text{ascending colon contribution} = [z_2 - z_1(\text{sm.int.})]\pi ab ,$$

where z_2, a, and b are the variables defined for the ascending colon and z_1(sm.int.) is the z_1 value for the small intestine; and

$$\text{transverse colon contribution} = 2\pi bcx_1 ,$$

where b, c, and x_1 are the variables defined for the transverse colon; and

$$\text{descending colon contribution} = [z_2 - z_1(\text{sm.int.})]\pi ab ,$$

where z_2, a, and b are the variables defined for the descending colon and z_1(sm.int.) is the z_1 value for the small intestine.

Upper large intestine. The upper large intestine consists of an ascending colon and a transverse colon.

The ascending colon wall is defined by the space between two coaxial elliptical cylinders:

$$\left(\frac{x - x_0}{a}\right)^2 + \left(\frac{y - y_0}{b}\right)^2 \leq 1 ,$$

$$\left(\frac{x - x_0}{a - d}\right)^2 + \left(\frac{y - y_0}{b - d}\right)^2 \geq 1 ,$$

and $z_1 \leq z \leq z_2$.

The contents are defined by the space within the inner cylinder,

$$\left(\frac{x - x_0}{a - d}\right)^2 + \left(\frac{y - y_0}{b - d}\right)^2 < 1$$

and $z_1 \leq z \leq z_2$.

Age (years)	a	b	d	x_0	y_0	z_1	z_2	Volume (cm^3) Wall[a]	Contents[b]
0	0.79	1.23	0.27	-2.70	-1.16	4.46	7.41	4.38	4.63
1	1.10	1.63	0.37	-3.74	-1.53	6.34	10.53	11.5	12.1
5	1.43	1.88	0.46	-4.87	-1.77	8.42	13.99	22.9	24.1
10	1.74	2.10	0.54	-5.91	-1.98	10.49	17.42	38.8	40.8
15	2.16	2.45	0.65	-7.33	-2.31	13.03	21.63	69.5	73.4
Adult	2.50	2.50	0.7085	-8.50	-2.36	14.45	24.00	91.2	96.3

[a]Volume (wall) = $\pi(z_2 - z_1)[ab - (a - d)(b - d)]$.

[b]Volume (contents) = $\pi(z_2 - z_1)(a - d)(b - d)$.

The transverse colon wall is also defined by the space between two coaxial elliptical cylinders:

$$\left(\frac{y - y_0}{b}\right)^2 + \left(\frac{z - z_0}{c}\right)^2 \leq 1 ,$$

$$\left(\frac{y - y_0}{b - d}\right)^2 + \left(\frac{z - z_0}{c - d}\right)^2 \geq 1 ,$$

and $- x_1 \leq x \leq x_1$.

The contents are defined by the space within the inner cylinder,

$$\left(\frac{y - y_0}{b - d}\right)^2 + \left(\frac{z - z_0}{c - d}\right)^2 < 1$$

and $-x_1 \leq x \leq x_1$.

Age (years)	b	c	d	y_0	z_0	x_1	Volume (cm^3) Wall[a]	Contents[b]
0	1.23	0.46	0.18	-1.16	7.87	3.33	5.69	6.15
1	1.63	0.65	0.26	-1.53	11.18	4.62	15.2	15.5
5	1.88	0.87	0.33	-1.77	14.86	6.01	30.2	31.6
10	2.10	1.08	0.40	-1.98	18.51	7.30	51.0	53.0
15	2.45	1.35	0.49	-2.31	22.99	9.06	92.3	96.0
Adult	2.50	1.50	0.527	-2.36	25.50	10.50	121	127

[a]Volume (wall) = $2\pi x_1[bc - (b - d)(c - d)]$.

[b]Volume (contents) = $2\pi x_1(b - d)(c - d)$.

Lower large intestine. The lower large intestine consists of a descending colon and a sigmoid colon.

The descending colon wall is defined by the space between two coaxial elliptical cylinders. The axis of the cylinders is at a slight angle with the z-axis of the phantom, but the ends of the descending colon are defined by horizontal planes ($z = z_1$ and $z = z_2$). The wall is specified by

$$\left(\frac{x - x_0}{a}\right)^2 + \left(\frac{y - y_0}{b}\right)^2 \leq 1 ,$$

$$\left(\frac{x - x_0}{a - d}\right)^2 + \left(\frac{y - y_0}{b - d}\right)^2 \geq 1 ,$$

and $z_1 \leq z \leq z_2$,

where $x_0 = x_1 + \dfrac{m_x(z - z_2)}{z_2 - z_1}$

and $y_0 = \dfrac{m_y(z_1 - z)}{z_2 - z_1}$.

The contents of the descending colon are defined by the space within the inner cylinder, i.e.,

$$\left(\frac{x - x_0}{a - d}\right)^2 + \left(\frac{y - y_0}{b - d}\right)^2 < 1$$

and $z_1 \leq z \leq z_2$.

Age (years)	a	b	d	x_1	m_x	m_y	z_1	z_2	Volume (cm^3) Wall[a]	Contents[b]
0	0.60	1.04	0.20	2.94	0.2477	1.225	2.69	7.41	4.27	4.98
1	0.83	1.38	0.27	4.07	0.3432	1.625	3.82	10.53	11.0	13.1
5	1.08	1.60	0.34	5.30	0.4466	1.875	5.08	13.99	22.3	26.1
10	1.31	1.79	0.40	6.43	0.5421	2.100	6.33	17.42	37.6	44.1
15	1.62	2.09	0.49	7.98	0.6728	2.450	7.86	21.63	68.3	78.2
Adult	1.88	2.13	0.54	9.25	0.7800	2.500	8.72	24.00	89.9	102

[a]Volume (wall) = $\pi[ab - (a - d)(b - d)](z_2 - z_1)$.

[b]Volume (contents) = $\pi(a - d)(b - d)(z_2 - z_1)$.

The sigmoid colon plus contents is represented by portions of two flattened tori; that is, the axis of each torus is circular but the cross-section is elliptical. The wall is defined as follows:

(portion of upper torus)

$$\left(\frac{\sqrt{(x - x_0)^2 + (z - z_0)^2} - R_1}{a}\right)^2 + \left(\frac{y}{b}\right)^2 \leq 1 ,$$

$$\left(\frac{\sqrt{(x - x_0)^2 + (z - z_0)^2} - R_1}{a - d}\right)^2 + \left(\frac{y}{b - d}\right) \geq 1 ,$$

$x \geq x_0$, and $z \leq z_0$;

and (portion of lower torus)

$$\left(\frac{\sqrt{(x - x_0)^2 + z^2} - R_2}{a}\right)^2 + \left(\frac{y}{b}\right)^2 \leq 1 ,$$

$$\left(\frac{\sqrt{(x - x_0)^2 + z^2} - R_2}{a - d}\right)^2 + \left(\frac{y}{b - d}\right)^2 \geq 1 ,$$

$x \leq x_0$, and $z \geq 0$.

The contents of the sigmoid colon are defined as follows:

(portion of upper torus)

$$\left(\frac{\sqrt{(x - x_0)^2 + (z - z_0)^2} - R_1}{a - d}\right)^2 + \left(\frac{y}{b - d}\right)^2 < 1 ,$$

$x \geq x_0$, and $z \leq z_0$;

and (portion of lower torus)

$$\left(\frac{\sqrt{(x - x_0) + z^2} - R_2}{a - d}\right)^2 + \left(\frac{y}{b - d}\right)^2 < 1 ,$$

$x \leq x_0$, and $z \geq 0$.

Age (years)	a	b	d	x_0	z_0	R_1	R_2	Volume (cm^3)	
								Wall[a]	Contents[b]
0	0.50	0.77	0.25	0.95	2.69	1.77	0.92	3.39	1.73
1	0.69	1.02	0.34	1.32	3.82	2.51	1.31	8.78	4.49
5	0.88	1.21	0.42	1.72	5.08	3.33	1.75	17.6	9.11
10	0.96	1.50	0.48	2.09	6.33	4.15	2.18	29.7	15.3
15	1.18	1.76	0.59	2.59	7.86	5.16	2.70	53.8	26.8
Adult	1.57	1.57	0.66	3.00	8.72	5.72	3.00	70.4	35.6

[a]Volume (wall) = $\frac{1}{2}\pi^2[ab - (a - d)(b - d)](R_1 + R_2)$.

[b]Volume (contents) = $\frac{1}{2}\pi^2(a - d)(b - d)(R_1 + R_2)$.

The mathematical model of the entire gastrointestinal tract is sketched in Fig. 28.

ORNL-DWG 73-12124

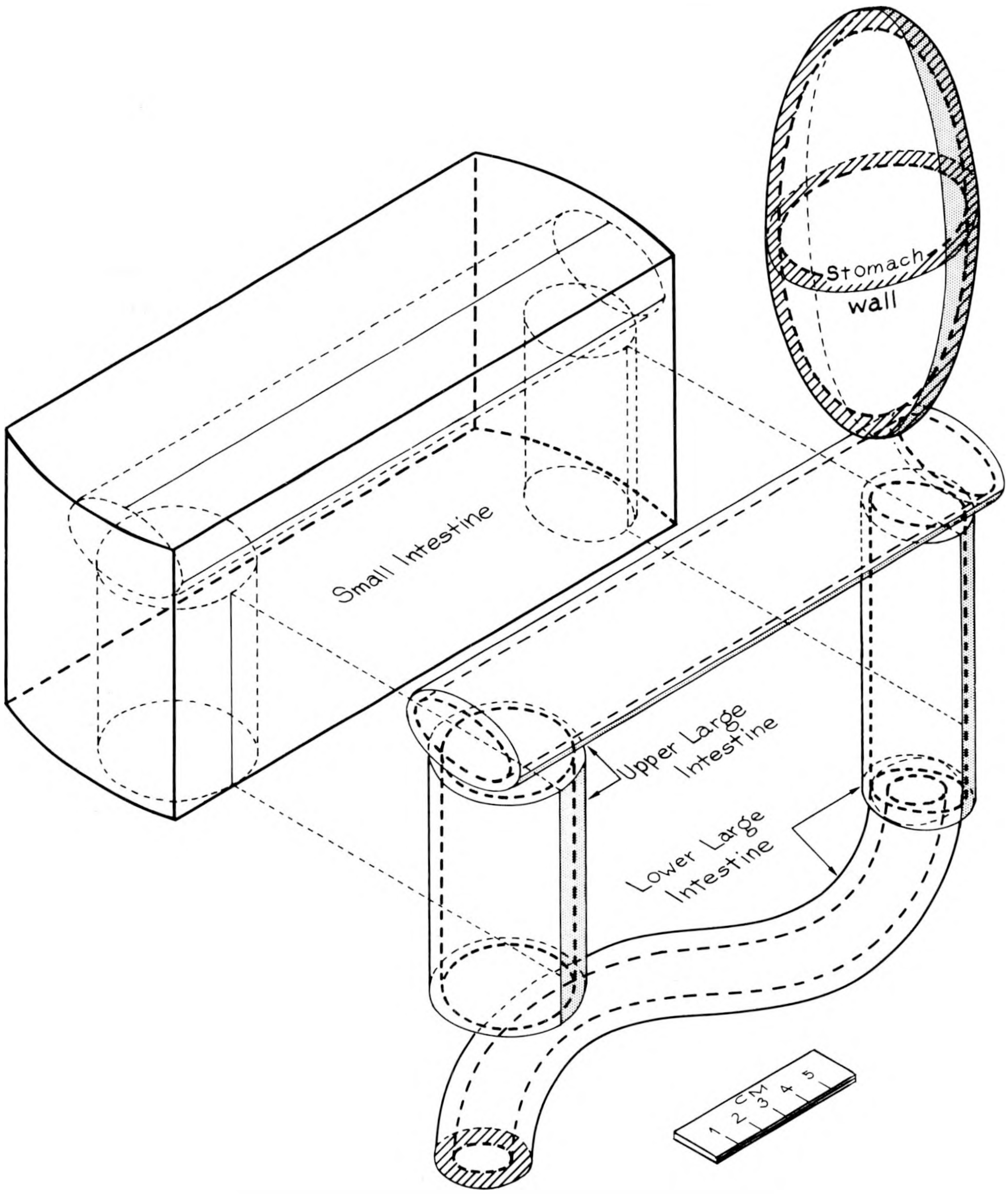

Fig. 28. Mathematical model for the gastrointestinal tract, as drawn for the adult by Snyder et al. (1974).

Heart and contents. The heart model developed by Coffey (1978) for the adult phantom has been employed (see Figs. 29-31). The outer surface of the heart is represented by four quarter-ellipsoids. Within this space, the heart is divided into regions representing the muscular walls and the four chambers. The equations are given below in (x_1, y_1, z_1)-coordinates, which are related to the (x,y,z)-coordinate system by the following rotation-translation equations:

$$\begin{bmatrix} x_1 \\ y_1 \\ z_1 \end{bmatrix} = \begin{bmatrix} \alpha_1 & \beta_1 & \gamma_1 \\ \alpha_2 & \beta_2 & \gamma_2 \\ \alpha_3 & \beta_3 & \gamma_3 \end{bmatrix} \begin{bmatrix} x - x_0 \\ y - y_0 \\ z - z_0 \end{bmatrix} .$$

In the equations below, the variable names VX, AVY, LAVZ, RAVZ, AX, TLVW, TRVW, and TAW are acronyms in which the letters L and R refer to left and right, A and V to atrium and ventricle, T to thickness, W to wall, and X, Y, and Z to dimensions in the x_1, y_1, and z_1 directions. Thus, AVY is a dimension common to the atria and ventricles in the y_1 direction.

The left ventricle (wall + contents) is represented by half an ellipsoid. The wall is defined by the inequalities

$$\left(\frac{x_1}{VX}\right)^2 + \left(\frac{y_1}{AVY}\right)^2 + \left(\frac{z_1}{LAVZ}\right)^2 \leq 1 ,$$

$$\left(\frac{x_1}{VX - TLVW}\right)^2 + \left(\frac{y_1}{AVY - TLVW}\right)^2 + \left(\frac{z_1}{LAVZ - TLVW}\right)^2 \geq 1 ,$$

and $x_1 \geq 0$.

The contents of the left ventricle are defined by the volume within the inner of the two half-ellipsoids given above, i.e.,

$$\left(\frac{x_1}{VX - TLVW}\right)^2 + \left(\frac{y_1}{AVY - TLVW}\right)^2 + \left(\frac{z_1}{LAVZ - TLVW}\right)^2 < 1$$

and $x_1 \geq 0$.

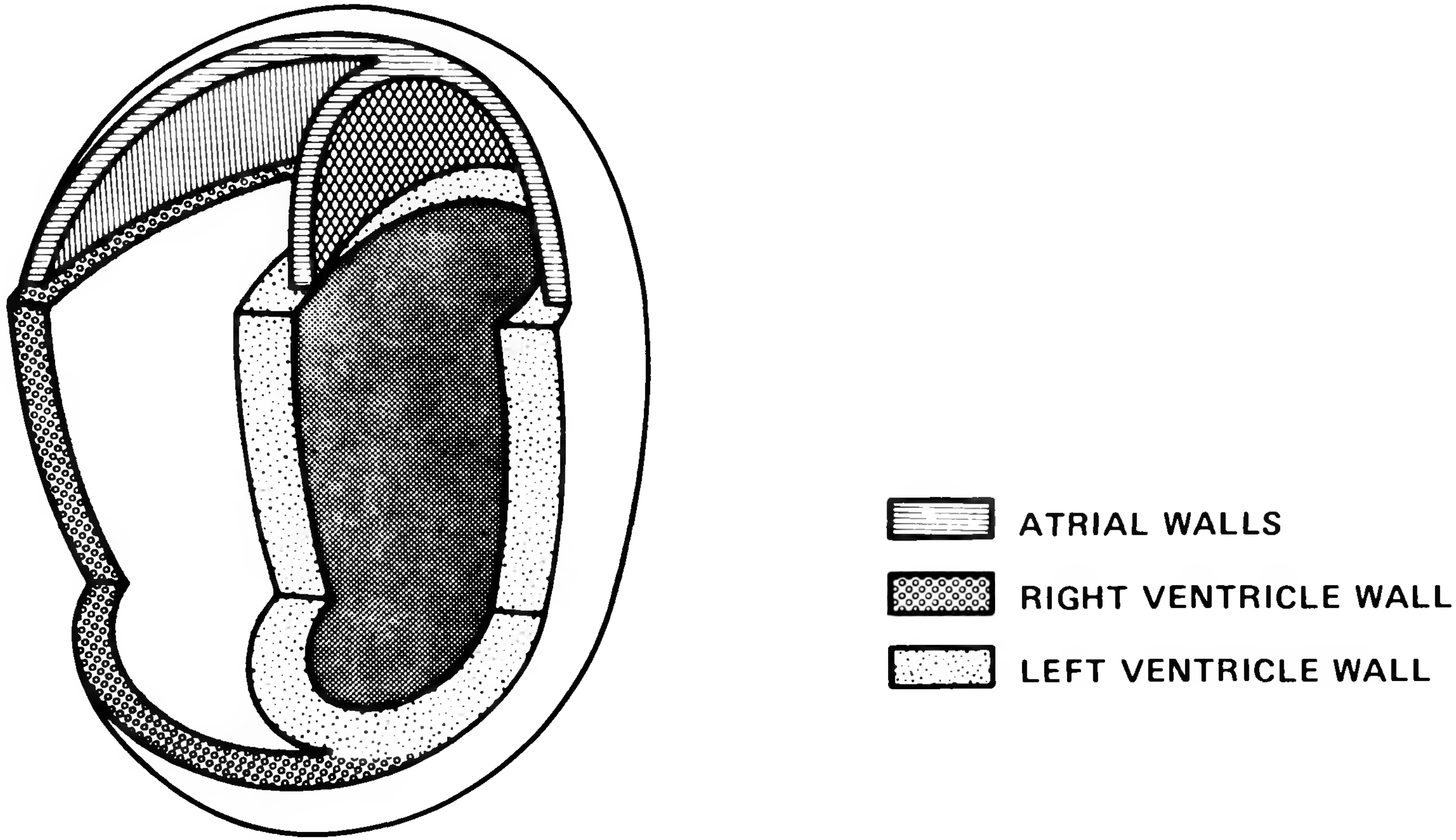

Fig. 29. Artist's drawing of adult heart model. Source: Coffey, Cristy, and Warner (1980).

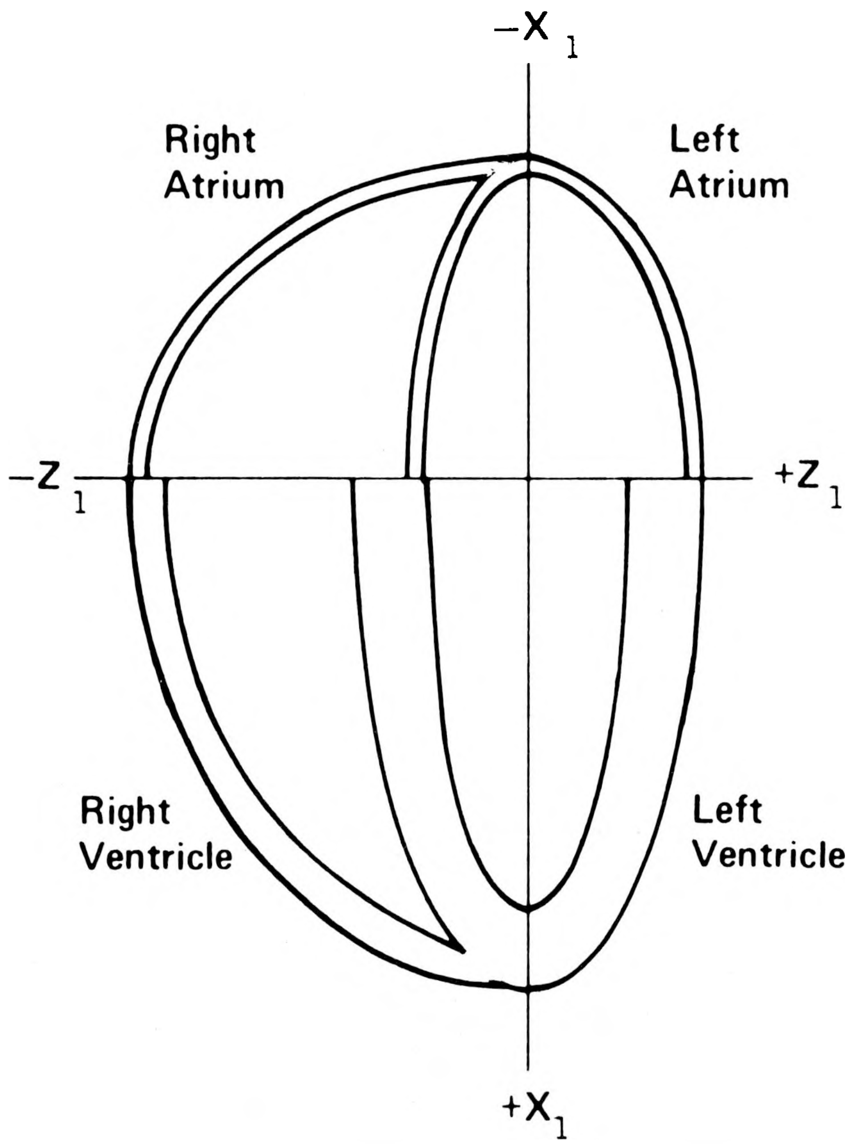

Fig. 30. Frontal section of the adult heart model through the center of the model. Source: Coffey (1978), modified.

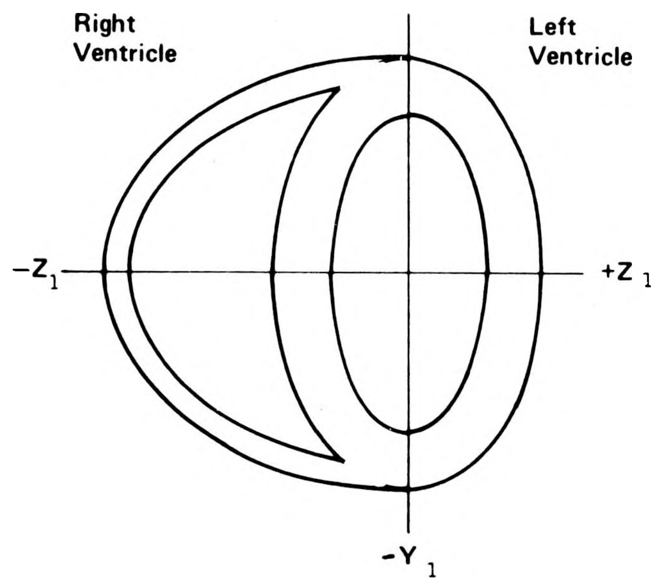

Fig. 31. Cross-section through the top of the ventricles of the adult heart model. Source: Coffey (1978), modified.

The right ventricle (wall + contents) is represented by a quarter-ellipsoid that wraps around half of the left ventricle. The wall is defined by the inequalities

$$\left(\frac{x_1}{VX}\right)^2 + \left(\frac{y_1}{AVY}\right)^2 + \left(\frac{z_1}{RAVZ}\right)^2 \leq 1 \ ,$$

$$\left(\frac{x_1}{VX - TRVW}\right)^2 + \left(\frac{y_1}{AVY - TRVW}\right)^2 + \left(\frac{z_1}{RAVZ - TRVW}\right)^2 \geq 1 \ ,$$

$x_1 \geq 0$, and $z_1 < 0$.

The volume common to the left and right ventricle walls is considered part of the left ventricle wall and is excluded here.

The contents of the right ventricle are defined by the inequalities

$$\left(\frac{x_1}{VX - TRVW}\right)^2 + \left(\frac{y_1}{AVY - TRVW}\right)^2 + \left(\frac{z_1}{RAVZ - TRVW}\right)^2 < 1 \ ,$$

$x_1 \geq 0$, and $z_1 < 0$.

The portion of the left ventricle within this space is excluded, i.e., the inequality

$$\left(\frac{x_1}{VX}\right)^2 + \left(\frac{y_1}{AVY}\right)^2 + \left(\frac{z_1}{LAVZ}\right)^2 > 1$$

must also hold.

The left atrium (wall + contents) is represented by two adjacent quarter-ellipsoids. The left atrial wall is defined as follows:

(part 1)

$$\left(\frac{x_1}{AX}\right)^2 + \left(\frac{y_1}{AVY}\right)^2 + \left(\frac{z_1}{LAVZ}\right)^2 \leq 1 \ ,$$

$$\left(\frac{x_1}{AX - TAW}\right)^2 + \left(\frac{y_1}{AVY - TAW}\right)^2 + \left(\frac{z_1}{LAVZ - TAW}\right)^2 \geq 1 \ ,$$

$x_1 < 0$, and $z_1 \geq 0$;

and (part 2)

$$\left(\frac{x_1}{AX}\right)^2 + \left(\frac{y_1}{AVY}\right)^2 + \left(\frac{z_1}{LAVZ - TLVW + TAW}\right)^2 \leq 1 ,$$

$$\left(\frac{x_1}{AX - TAW}\right)^2 + \left(\frac{y_1}{AVY - TAW}\right)^2 + \left(\frac{z_1}{LAVZ - TLVW}\right)^2 \geq 1 ,$$

$x_1 < 0$, and $z_1 < 0$.

The contents of the left atrium are represented by the volume within these walls, i.e., by

(part 1)

$$\left(\frac{x_1}{AX - TAW}\right)^2 + \left(\frac{y_1}{AVY - TAW}\right)^2 + \left(\frac{z_1}{LAVZ - TAW}\right)^2 < 1 ,$$

$x_1 < 0$, and $z_1 \geq 0$;

and (part 2)

$$\left(\frac{x_1}{AX - TAW}\right)^2 + \left(\frac{y_1}{AVY - TAW}\right)^2 + \left(\frac{z_1}{LAVZ - TLVW}\right)^2 < 1 ,$$

$x_1 < 0$, and $z_1 < 0$.

The right atrium (wall + contents) is represented by a quarter-ellipsoid that wraps around part of the left atrium. The wall is defined by the inequalities

$$\left(\frac{x_1}{AX}\right)^2 + \left(\frac{y_1}{AVY}\right)^2 + \left(\frac{z_1}{RAVZ}\right)^2 \leq 1 ,$$

$$\left(\frac{x_1}{AX - TAW}\right)^2 + \left(\frac{y_1}{AVY - TAW}\right)^2 + \left(\frac{z_1}{RAVZ - TAW}\right)^2 \geq 1 ,$$

$x_1 < 0$, and $z_1 < 0$.

The volume common to the left and right atrial walls is considered part of the left atrial wall and is excluded here.

The contents of the right atrium are defined by the inequalities

$$\left(\frac{x_1}{AX - TAW}\right)^2 + \left(\frac{y_1}{AVY - TAW}\right)^2 + \left(\frac{z_1}{RAVZ - TAW}\right)^2 < 1 ,$$

$x_1 < 0$, and $z_1 < 0$.

The portion of the left atrium within this space is excluded, i.e., the inequality

$$\left(\frac{x_1}{AX}\right)^2 + \left(\frac{y_1}{AVY}\right)^2 + \left(\frac{z_1}{LAVZ - TLVW + TAW}\right)^2 > 1$$

must also hold.

The age-dependent values of all the heart parameters are given in the tables below. The ages are given in years, and the volumes are given in cubic centimeters. Targeted volumes were derived from ICRP Publication 23 (1975).

Age	α_1	β_1	γ_1	α_2	β_2	γ_2	α_3	β_3	γ_3
0	0.5942	-0.6421	-0.4845	-0.3291	0.3556	-0.8748	0.7340	0.6792	0.0000
1	0.6009	-0.6216	-0.5025	-0.3493	0.3613	-0.8646	0.7190	0.6950	0.0000
5	0.6237	-0.5721	-0.5327	-0.3926	0.3601	-0.8463	0.6760	0.7369	0.0000
10	0.6345	-0.5370	-0.5559	-0.4243	0.3591	-0.8312	0.6460	0.7633	0.0000
15	0.6453	-0.5134	-0.5658	-0.4428	0.3523	-0.8245	0.6226	0.7825	0.0000
Adult	0.6751	-0.4727	-0.5664	-0.4640	0.3249	-0.8241	0.5736	0.8191	0.0000

Age	VX	AVY	LAVZ	RAVZ	AX	TLVW	TRVW	TAW	x_0	y_0	z_0
0	3.71	2.16	1.34	3.02	2.33	0.56	0.26	0.13	0.42	-1.08	16.05
1	4.67	2.72	1.68	3.80	2.93	0.71	0.33	0.16	0.54	-1.67	22.43
5	5.72	3.33	2.06	4.66	3.59	0.86	0.40	0.20	0.77	-1.70	29.60
10	6.73	3.92	2.43	5.48	4.23	1.02	0.47	0.23	0.80	-1.70	36.60
15	7.86	4.57	2.83	6.40	4.94	1.19	0.55	0.27	0.86	-2.10	45.10
Adult	8.60	5.00	3.10	7.00	5.40	1.30	0.60	0.30	1.00	-1.80	50.00

	Volume			
	Left ventricle		Right ventricle	
Age	Wall	Contents	Wall	Contents
0	14.3	8.23	5.42	8.68
1	28.5	16.2	10.9	17.3
5	52.0	30.2	19.8	32.0
10	85.4	48.9	32.3	52.0
15	135	77.4	51.4	82.9
Adult	177	102	67.2	108

	Volume			
	Left atrium		Right atrium	
Age	Wall	Contents	Wall	Contents
0	2.55	9.31	2.21	8.91
1	4.96	18.5	4.32	18.0
5	9.31	34.0	8.09	32.7
10	14.9	55.8	12.9	53.8
15	23.7	88.3	20.7	85.5
Adult	31.6	115	27.4	111

Age	Volume-total heart walls	Targeted volume-total heart walls	Volume-total heart contents
0	24.4	24.3	35.1
1	48.7	48.6	69.9
5	89.3	89.3	129
10	145	146	210
15	231	232	334
Adult	303	320	437

Volume (left ventricle wall) =

$$\frac{2}{3}\pi[(VX)(AVY)(LAVZ) - (VX - TLVW)(AVY - TLVW)(LAVZ - TLVW)] .$$

Volume (left ventricle contents) =

$$\frac{2}{3}\pi[(VX - TLVW)(AVY - TLVW)(LAVZ - TLVW)] .$$

Volume (right ventricle wall) =

$$\frac{\pi}{3}[(VX)(AVY)(RAVZ) - (VX - TRVW)(AVY - TRVW)(RAVZ - TRVW)]$$

$$- \text{ overlap volume (of ventricles)}.$$

Volume (right ventricle contents) =

$$\frac{\pi}{3}[(VX - TRVW)(AVY - TRVW)(RAVZ - TRVW) - (VX)(AVY)(LAVZ)]$$

$$+ \text{ overlap volume (of ventricles)}.$$

Volume (left atrium wall) =

$$\frac{\pi}{3}[(AX)(AVY)(LAVZ) - (AX - TAW)(AVY - TAW)(LAVZ - TAW) + (AX)(AVY)(LAVZ - TLVW + TAW) - (AX - TAW)(AVY - TAW)(LAVZ - TLVW)] .$$

Volume (left atrium contents) =

$$\frac{\pi}{3}(AX - TAW)(AVY - TAW)[(LAVZ - TAW) + (LAVZ - TLVW)] .$$

Volume (right atrium wall) =

$$\frac{\pi}{3}[(AX)(AVY)(RAVZ) - (AX - TAW)(AVY - TAW)(RAVZ - TAW)]$$

- overlap volume (of atria).

Volume (right atrium contents) =

$$\frac{\pi}{3}[(AX - TAW)(AVY - TAW)(RAVZ - TAW) - (AX)(AVY)(LAVZ - TLVW + TAW)] + \text{overlap volume (of atria)}.$$

In the equations above, the overlap volume (of ventricles or atria) is given by the expression

$$2\int_{x=0}^{x=d}\int_{z=0}^{z=h(x)} r(x,z)\,dz\,dx + \left[\frac{\pi}{3}a_2b_2c_2 - \frac{\pi}{2}b_2c_2\left(d - \frac{d^3}{3a_2^2}\right)\right]$$

$$- \left[\frac{\pi}{3}a_1b_1c_1 - \frac{\pi}{2}b_1c_1\left(d - \frac{d^3}{3a_1^2}\right)\right] ,$$

in which $d = \left[\frac{1}{a_1^2} + \frac{\left(\frac{1}{a_2^2} - \frac{1}{a_1^2}\right)}{c_1^2\left(\frac{1}{c_1^2} - \frac{1}{c_2^2}\right)}\right]^{-\frac{1}{2}}$,

$$h(x) = \left[\frac{1 - x^2\left[\frac{1}{a_1^2} + \frac{\left(\frac{1}{a_2^2} - \frac{1}{a_1^2}\right)}{b_1^2\left(\frac{1}{b_1^2} - \frac{1}{b_2^2}\right)}\right]}{\frac{1}{c_1^2} + \frac{\left(\frac{1}{c_2^2} - \frac{1}{c_1^2}\right)}{b_1^2\left(\frac{1}{b_1^2} - \frac{1}{b_2^2}\right)}}\right]^{\frac{1}{2}} ,$$

and $r(x,z) = b_2\sqrt{1 - \left(\frac{z}{c_2}\right)^2 - \left(\frac{x}{a_2}\right)^2} - b_1\sqrt{1 - \left(\frac{z}{c_1}\right)^2 - \left(\frac{x}{a_1}\right)^2}$.

For the ventricles, the values of a_1, b_1, c_1, a_2, b_2, and c_2 are

$$a_1 = VX - TRVW ,$$

$$b_1 = AVY - TRVW ,$$

$$c_1 = RAVZ - TRVW ,$$

$$a_2 = VX ,$$

$$b_2 = AVY ,$$

and $c_2 = LAVZ$;

for the atria, the values are

$$a_1 = AX - TAW ,$$

$$b_1 = AVY - TAW ,$$

$$c_1 = RAVZ - TAW ,$$

$$a_2 = AX ,$$

$$b_2 = AVY ,$$

and $c_2 = LAVZ - TLVW + TAW$.

The double integral is evaluated numerically using the Gaussian quadrature method.

Kidneys. Each kidney is an ellipsoid cut by a plane, given by the following:

$$\left(\frac{x - x_0}{a}\right)^2 + \left(\frac{y - y_0}{b}\right)^2 + \left(\frac{z - z_0}{c}\right)^2 \leq 1$$

and $|x| \geq x_1$.

In the following table, x_0 is taken as positive for the left kidney, and negative for the right.

Age (years)	a	b	c	x_0	y_0	z_0	x_1	Volume (both)[a] (cm^3)	Targeted Volume (both)[b] (cm^3)
0	1.79	0.93	1.70	±1.91	2.94	10.03	0.71	22.0	22.0
1	2.61	1.25	2.41	±2.64	3.90	14.25	0.95	60.5	63.5
5	3.20	1.40	3.20	±3.44	4.50	18.94	1.31	111	111
10	3.66	1.47	3.99	±4.17	5.04	23.59	1.74	166	166
15	4.05	1.53	4.96	±5.18	5.88	29.30	2.48	238	239
Adult	4.50	1.50	5.50	±6.00	6.00	32.50	3.00	288	295

[a]Volume (both) = $2\pi bc\left[\frac{2}{3}a + (|x_0| - x_1) - \frac{(|x_0| - x_1)^3}{3a^2}\right]$.

[b]Derived from ICRP Publication 23 (1975).

Liver. The liver is defined by an elliptical cylinder cut by a plane as follows:

$$\left(\frac{x}{a}\right)^2 + \left(\frac{y}{b}\right)^2 \leq 1 ,$$

$$\frac{x - k}{x_m} + \frac{y}{y_m} - \frac{z}{z_m} \leq - 1 ,$$

and $z_1 \leq z \leq z_2$.

Age (years)	a	b	x_m	y_m	z_m	k	z_1	z_2
0	5.19	4.25	8.45	10.90	13.27	0	8.33	13.27
1	7.20	5.47	12.83	16.55	18.86	0	11.84	18.86
5	9.39	6.30	16.27	20.34	25.06	0	15.74	25.06
10	11.43	6.83	21.98	29.67	31.21	0	19.59	31.21
15	14.19	7.70	31.51	44.75	38.76	-0.50	24.34	38.76
Adult	16.50	8.00	35.00	45.00	43.00	0	27.00	43.00

Age (years)	Volume[a] (cm^3)	Targeted volume[b] (cm^3)
0	117	132
1	281	281
5	562	562
10	853	854
15	1230	1230
Adult	1830	1780

[a]Volume $= \frac{abz_m}{x_m}\sqrt{a^2 + \left(\frac{bx_m}{y_m}\right)^2} \left[-\frac{1}{3}(1 - u^2)^{3/2} + u \sin^{-1}u + \sqrt{1 - u^2} + \frac{\pi}{2}u \right]_{u=f(z_1)}^{u=f(z_2)}$,

where

$$f(z) = \frac{x_m\left(\frac{z}{z_m} - 1\right) + k}{\sqrt{a^2 + \left(\frac{bx_m}{y_m}\right)^2}} ,$$

and the expression within the brackets is evaluated between the limits $u=f(z_1)$ and $u=f(z_2)$.

[b]Derived from ICRP Publication 23 (1975).

Lungs. Each lung is represented by half an ellipsoid with a section removed. Note that the section removed from the left lung is larger than that removed from the right lung because of the position of the heart. The adult lungs have been modified from those given by Snyder et al. (1974) to accommodate the new heart design. The right lung is defined as follows:

$$\left(\frac{x + x_0}{a}\right)^2 + \left(\frac{y}{b}\right)^2 + \left(\frac{z - z_0}{c}\right)^2 \leq 1$$

and $z \geq z_0$;

if $z_{1R} \leq z \leq z_{2R}$ and $y < y_{2R}$, then $x \leq x_{1R}$

must also hold.

The statements for the left lung are similar, but replace $(x + x_0)$ with $(x - x_0)$, and z_{1R}, z_{2R}, and y_{2R} with z_0, z_{2L}, and y_{2L}, respectively; and replace the inequality $(x \leq x_{1R})$ with $(x \geq x_{1L})$. The letters R and L refer to right and left.

Age (years)	a	b	c	x_0	z_0
0	1.89	3.68	7.41	2.70	13.42
1	2.68	4.88	10.53	3.74	19.08
5	3.47	5.63	13.99	4.87	25.35
10	3.82	6.30	17.42	5.91	31.57
15	4.09	6.98	20.55	7.33	39.21
Adult	5.00	7.50	24.00	8.50	43.50

Age (years)	x_{1R}	y_{1R}	z_{1R}	z_{2R}	x_{1L}	y_{1L}	z_{2L}
0	-2.30	0.75	14.15	17.85	+3.00	0.30	17.90
1	-2.90	0.70	20.10	24.60	+3.90	0.40	24.80
5	-3.50	1.00	26.90	32.30	+5.00	0.50	32.60
10	-4.10	1.30	33.40	39.60	+5.90	0.75	40.00
15	-5.00	1.20	41.60	48.50	+7.00	0.70	49.00
Adult	-5.40	1.50	46.00	54.00	+8.00	1.00	55.00

Age	Volume (cm^3)			Targeted volume[a]
(years)	Left lung	Right lung	Both lungs	both lungs (cm^3)
0	79.1	91.9	171	171
1	225	259	484	490
5	454	526	980	1070
10	709	821	1530	1530
15	1020	1180	2200	2200
Adult	1560	1810	3380	3400

[a]Derived from ICRP Publication 23 (1975).

$$\text{Volume of each lung} = \frac{2}{3}\pi abc$$

$$- \int_{z_1}^{z_2} \left[(x_1 - x_0)y + \frac{a}{2b} \left\{ y\sqrt{b^2 g(z) - y^2} + b^2 g(z) \sin^{-1}\left(\frac{y}{b\sqrt{g(z)}}\right) \right\} \right]_{y=y_1(z)}^{y=y_2} dz$$

$$- \int_{z_1}^{z_2} \left[y_2(x_1 - x_0) + \frac{b}{2a}\left\{(x_1 - x_0)\sqrt{a^2 g(z) - (x_1 - x_0)^2} + a^2 g(z) \sin^{-1}\left(\frac{x_1 - x_0}{a\sqrt{g(z)}}\right)\right\}\right] dz ,$$

in which $g(z) = 1 - \left(\frac{z - z_0}{c}\right)^2$

and $y_1(z) = - b\sqrt{g(z) - \left(\frac{x_1 - x_0}{a}\right)^2}$.

To obtain the volume of the left lung, set $x_1 = x_{1L}$, $y_2 = y_{2L}$, $z_1 = z_0$, and $z_2 = z_{2L}$. To obtain the volume of the right lung, set $x_1 = |x_{1R}|$, $y_2 = y_{2R}$, $z_1 = z_{1R}$, and $z_2 = z_{2R}$.

If $x_1 > x_0$, which is true for the left lung in the 0, 1, and 5-year-old phantoms, set $x_1 = x_0$ in the second term only [including the formula for $y_1(z)$ used in the second term]. (The second term is the first integration.) If $x_1 \leq x_0$, ignore the entire third term (the second integration).

The expression within the brackets in the second term is evaluated between the limits $y = y_1(z)$ and $y = y_2$ before the integration is done. Both integrations are done numerically using the Gaussian quadrature method.

After Scammon (1953) was consulted, some compromise with the Similitude Rule was made for ages 0-5 in order to make the shape of the lungs more realistic.

The right lung is approximately 16% larger than the left lung in the adult (ICRP 1975). This relationship was assumed for the other ages as well.

Ovaries. Each ovary is an ellipsoid and is given by

$$\left(\frac{x - x_0}{a}\right)^2 + \left(\frac{y}{b}\right)^2 + \left(\frac{z - z_0}{c}\right)^2 \leq 1 .$$

The values of x_0 in the table below are taken as positive for the left ovary, and negative for the right ovary.

Age (years)	a	b	c	x_0	z_0	Volume (both)[a] (cm^3)	Targeted volume (both)[b] (cm^3)
0	0.30	0.22	0.57	±1.91	4.63	0.315	0.31
1	0.38	0.28	0.77	±2.64	6.58	0.686	0.69
5	0.53	0.35	1.07	±3.44	8.74	1.66	1.66
10	0.66	0.40	1.36	±4.17	10.89	3.01	3.01
15	0.80	0.45	1.65	±5.18	13.52	4.98	4.96
Adult	1.00	0.50	2.00	±6.00	15.00	8.38	10.2

[a]Volume (both) = $\frac{8}{3}\pi abc$.
[b]Derived from ICRP Publication 23 (1975).

Pancreas. The pancreas is half an ellipsoid with a section removed. It is defined by

$$\left(\frac{x - x_0}{a}\right)^2 + \left(\frac{y}{b}\right)^2 + \left(\frac{z - z_0}{c}\right)^2 \leq 1 ,$$

$$x \geq x_0 ,$$

and $z \geq z_0$ if $x > x_1$.

The pancreas of the Fisher-Snyder adult phantom has been enlarged to be consistent with the sizes chosen for the pediatric series.

Age (years)	a	b	c	x_0	z_0	x_1	Volume[a] (cm^3)	Targeted volume[b] (cm^3)
0	4.32	0.50	0.87	-0.09	11.42	0.99	2.69	2.7
1	6.85	0.71	1.41	-0.43	16.23	1.32	9.87	10.5
5	9.16	0.90	1.92	-0.57	21.57	1.72	22.7	22.5
10	10.09	0.92	2.17	-0.38	26.85	2.15	28.9	28.7
15	13.32	1.14	2.87	-0.72	33.35	2.61	62.4	62.2
Adult	16.00	1.20	3.30	-1.00	37.00	3.00	90.7	92.0

[a]Volume = $\pi bc\left\{\frac{1}{3}a + \frac{1}{2}\left[(x_1 - x_0) - \frac{(x_1 - x_0)^3}{3a^2}\right]\right\}$.
[b]Derived from ICRP Publication 23 (1975).

Skin. Skin is represented as a layer of thickness S extending over the exterior of the phantom, including the exposed top of the trunk and the bottom of the legs, but excluding the exposed bottom of the trunk, top of the legs, and bottom of the head. The part of the legs covered by the male genitalia region has skin, but the part of the trunk covered by the female breasts does not.

This layer corresponds to the dermis as well as the epidermis. Greater thicknesses in places such as the back have been ignored. Skin thicknesses were derived from Southwood (1955).

Age		Volume of skin (cm^3)				
(years)	S	Head[a]	Trunk[b]	Legs[c]	Male Genitalia[d]	Total
0	0.07	30.2	54.6	28.3	0.741	114
1	0.08	63.6	121	75.0	1.48	261
5	0.09	94.3	225	195	2.64	517
10	0.10	117	370	363	4.05	854
15	0.17	217	958	866	13.5	2050
Adult	0.20	274	1410	1190	23.4	2890

[a]Volume of head skin =

$$\pi A_H B_H (C_{H1} + \frac{2}{3} C_{H2}) - \pi (A_H - S)(B_H - S)[C_{H1} + \frac{2}{3}(C_{H2} - S)] \quad .$$

[b]Volume of trunk skin (disregarding the female breasts, for the moment) =

$$\begin{aligned} &\pi A_T B_T C_T - \pi (A_T - S)(B_T - S) C_T \\ &+ 2S \left\{ \left(\frac{A_T - S}{B_T - S}\right) \left[y_1 \sqrt{(B_T - S)^2 - y_1^2} + (B_T - S)^2 \sin^{-1}\left(\frac{y_1}{B_T - S}\right) \right] \right. \\ &\left. - \frac{A_H}{B_H} \left[y_1 \sqrt{B_H^2 - y_1^2} + B_H^2 \sin^{-1}\left(\frac{y_1}{B_H}\right) \right] \right\} , \end{aligned}$$

$$\text{where } y_1 = \sqrt{\frac{(A_T - S)^2 - A_H^2}{\left(\frac{A_T - S}{B_T - S}\right)^2 - \left(\frac{A_H}{B_H}\right)^2}} \quad .$$

The volume of skin covering the breasts is added to the above, and the volume of trunk skin covered by the breasts is subtracted. The term to be added is given by (volume of breasts, including skin) minus (volume of breast tissue, excluding skin); these volumes are given with the description of the breasts. The term to be subtracted is given by

$$4cS\int_{x_1}^{x_2} \sqrt{t(x)\cdot u(x)}\,dx ,$$

$$\text{where } t(x) = 1 - \left(\frac{x - x_0}{a}\right)^2 - \left[\frac{B_T\sqrt{1 - \left(\frac{x}{A_T}\right)^2} - y_0}{b}\right]^2 ,$$

$$u(x) = 1 + \frac{B_T^2 x^2}{A_T^2(A_T^2 - x^2)} ,$$

x_1 is the zero of $t(x)$ in the interval $(x_0 - a, x_0)$,
x_2 is the zero of $t(x)$ in the interval $(x_0, x_0 + a)$,
and a, b, c, x_0, and y_0 are the values defined for the breasts.

The integration was done numerically using the Gaussian quadrature method.

[c]Volume of legs skin =

$$\frac{2}{3}\pi C_L\{(R_1^2 + R_2^2 + R_1R_2) - [(R_1 - S)^2 + (R_2 - S)^2$$

$$+ (R_1 - S)(R_2 - S)]\} + 2\pi(R_2 - S)^2 S ,$$

$$\text{where } R_1 = \frac{A_T}{2} \text{ and } R_2 = \frac{A_T}{2}\left(\frac{C_L' - C_L}{C_L'}\right) .$$

[d]Volume of male genitalia skin =

$$2cSA_T\left(1 - \frac{c}{C_L'}\right)$$

$$-2\int_{z=-2c}^{z=0}\int_{x=-r}^{x=-r+\sqrt{2rS-S^2}} \left[-r + S + \sqrt{r^2-(x + r)^2}\right] dx\, dz$$

$$+ \left(2 - \frac{\pi}{2}\right)\left(\frac{A_T}{2}\right)^2 \left[z + \frac{z^2}{C_L'} + \frac{z^3}{3C_L'^2}\right]_{z=-(2c+S)}^{z=-2c} ,$$

where $r = \frac{A_T}{2}\left(1 + \frac{z}{C_L'}\right)$,

and c is the testis c value.

The integration was done numerically using the Gaussian quadrature method.

Spleen. The spleen is represented by the ellipsoid

$$\left(\frac{x - x_0}{a}\right)^2 + \left(\frac{y - y_0}{b}\right)^2 + \left(\frac{z - z_0}{c}\right)^2 \leq 1 .$$

Age (years)	a	b	c	x_0	y_0	z_0	Volume[a] (cm^3)	Targeted volume[b] (cm^3)
0	1.13	1.00	1.85	3.54	1.42	11.42	8.76	8.8
1	1.65	1.35	2.63	4.94	1.85	16.23	24.5	25.4
5	2.09	1.52	3.49	6.40	2.25	21.57	46.4	48.0
10	2.43	1.68	4.35	7.65	2.52	26.85	74.4	74.3
15	2.90	1.88	5.19	9.49	2.94	33.35	119	119
Adult	3.50	2.00	6.00	11.00	3.00	37.00	176	181

[a]Volume = $\frac{4}{3}\pi abc$.

[b]Derived from ICRP Publication 23 (1975).

Testes. The testes are represented by the ellipsoids

$$\left(\frac{x \pm a}{a}\right)^2 + \left(\frac{y - y_0}{b}\right)^2 + \left(\frac{z + c}{c}\right)^2 \leq 1 ,$$

where the "±" sign is taken as positive for the right testis and negative for the left testis.

Age (years)	a	b	c	y_0	Volume (both)[a] (cm^3)	Targeted volume (both)[b] (cm^3)
0	0.36	0.42	0.64	-2.58	0.811	0.81
1	0.41	0.47	0.72	-3.73	1.16	1.15
5	0.45	0.52	0.80	-4.98	1.57	1.58
10	0.47	0.55	0.84	-6.15	1.82	1.82
15	0.96	1.10	1.69	-7.10	15.0	14.9
Adult	1.30	1.50	2.30	-8.00	37.6	33.2

[a]Volume (both) = $\frac{8}{3}\pi abc$.

[b]Derived from ICRP Publication 23 (1975).

Thymus. The thymus is represented by an ellipsoid, given by

$$\left(\frac{x}{a}\right)^2 + \left(\frac{y - y_0}{b}\right)^2 + \left(\frac{z - z_0}{c}\right)^2 \leq 1 .$$

Age (years)	a	b	c	y_0	z_0	Volume[a] (cm^3)	Targeted Volume[b] (cm^3)
0	1.76	0.70	2.10	-3.60	19.30	10.8	12.4
1	1.75	1.00	3.00	-4.75	27.00	22.0	22.0
5	1.85	1.05	3.50	-5.48	35.00	28.5	28.5
10	1.85	1.00	3.90	-6.13	43.00	30.2	30.1
15	1.75	0.93	4.00	-7.15	52.00	27.3	27.3
Adult	1.50	0.80	4.00	-7.30	57.00	20.1	19.5

[a]Volume = $\frac{4}{3}\pi abc$.

[b]Derived from ICRP Publication 23 (1975).

The position and shape of this organ were determined by consulting Scammon (1953) and ICRP Publication 23 (1975). The Similitude Rule was not used for this organ. The thymus of the adult phantom was changed to fit the data from those sources.

Thyroid. The lobes of the thyroid lie between two concentric cylinders and are formed by a cutting surface (Figs. 32 and 33). The statements defining this organ are

ORNL–DWG 79-20293

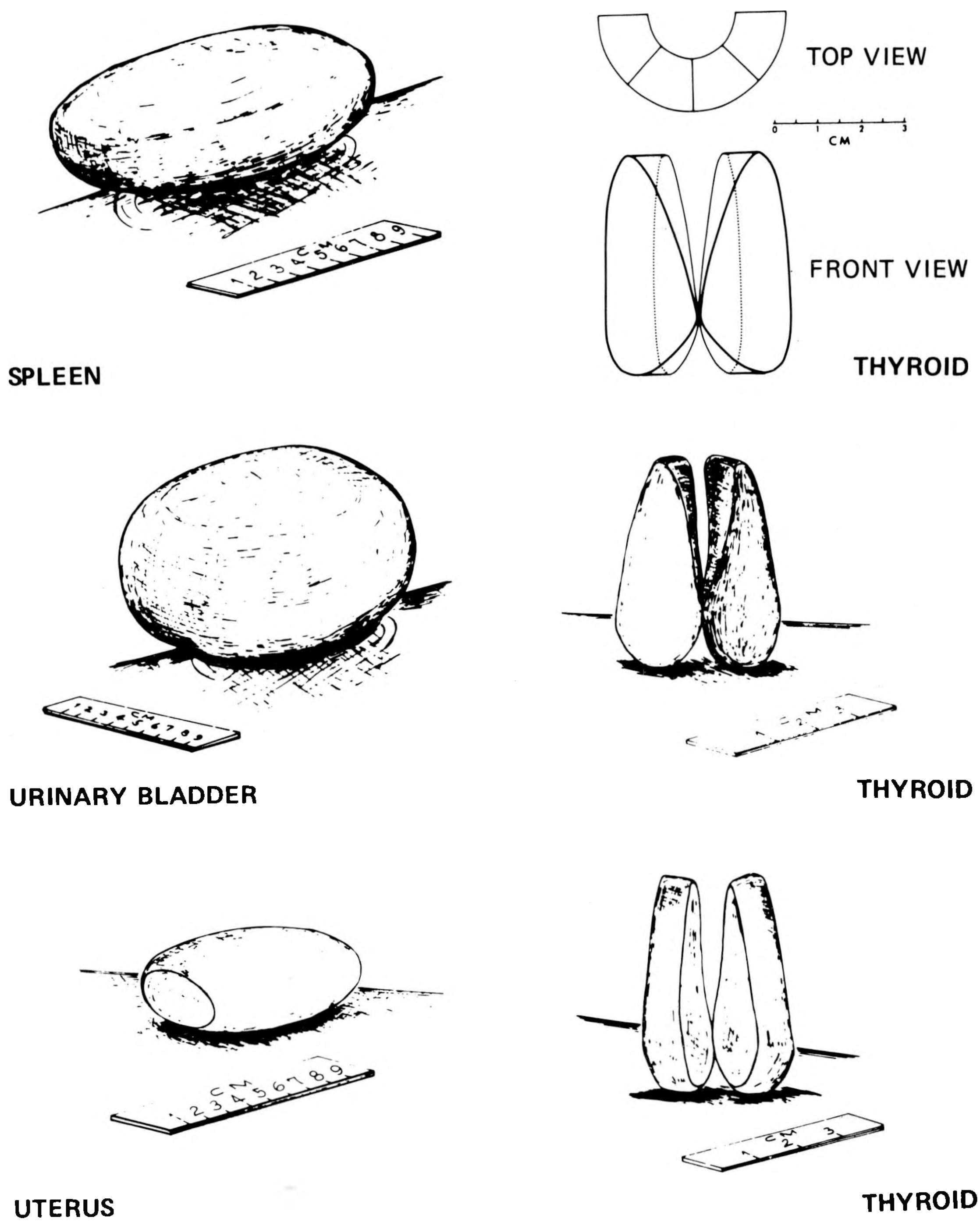

Fig. 32. Mathematical models for the spleen, urinary bladder, uterus, and thyroid, as drawn for the adult by Snyder et al. (1974).

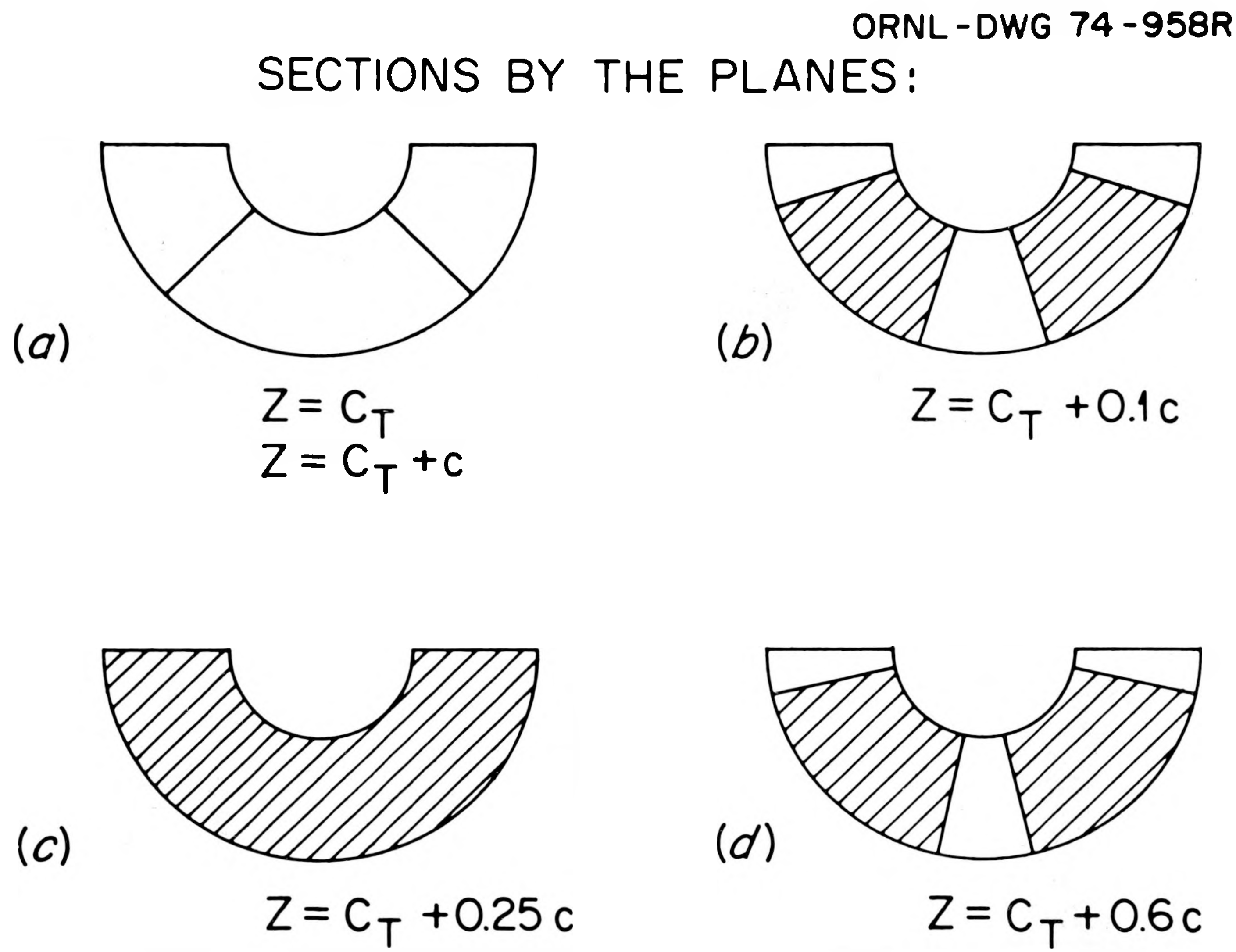

Fig. 33. Sections of the mathematical thyroid at various heights. C_T is the trunk height, and c is the thyroid height. The cross-hatched areas indicate thyroidal tissue (modified from Snyder et al., 1974).

$$x^2 + (y - y_0)^2 \leq R^2 ,$$

$$x^2 + (y - y_0)^2 \geq r^2 ,$$

$$y \leq y_0 ,$$

$$C_T \leq z \leq C_T + c ,$$

and $[(y - y_0) - |x|]^2 \geq 2[x^2 + (y - y_0)^2]\tau^2$,

in which

$$\tau = \left(\frac{\sqrt{2} - 2}{2}\right)\left(\frac{z - C_T}{0.25c}\right) + 1 \text{ for } 0 \leq z - C_T \leq 0.25c$$

and

$$\tau = \left(\frac{2 - \sqrt{2}}{2}\right)\left(\frac{z - C_T}{0.75c}\right) + \frac{2\sqrt{2} - 1}{3} \text{ for } 0.25c \leq z - C_T \leq c .$$

Age (years)	R	r	c	y_0	Volume[a] (cm^3)	Targeted volume[b] (cm^3)
0	0.87	0.40	2.00	-2.14	1.24	1.24
1	0.97	0.44	2.21	-2.87	1.71	1.71
5	1.21	0.55	2.76	-3.31	3.32	3.33
10	1.60	0.73	3.63	-3.56	7.62	7.62
15	1.85	0.83	4.20	-3.91	11.9	11.9
Adult	2.20	1.00	5.00	-4.00	19.9	17.3

[a]Volume = $\frac{2\sqrt{2}c(R^2 - r^2)(1 - \frac{\pi}{4})}{2 - \sqrt{2}}$.

[b]Derived from ICRP Publication 23 (1975).

The shape of the thyroid has been designed to be the same for all ages.

The thyroid has been moved closer to the front surface of the body, after Hwang, Shoup, and Poston (1976b). The thyroid had been located too deeply within the neck-and-head region for external dose calculations (Kerr 1979). The new position is better for external sources anterior to the body, but it will remain unsuitable for external sources from the back or sides until a separate neck region is added to the phantom design. This difficulty is unimportant for internal emitters.

Urinary bladder and contents. The bladder wall is represented by the volume between two concentric ellipsoids. The contents are represented by the volume within the inner ellipsoid. The wall is defined by

$$\left(\frac{x}{a}\right)^2 + \left(\frac{y - y_0}{b}\right)^2 + \left(\frac{z - z_0}{c}\right)^2 \leq 1$$

$$\text{and} \quad \left(\frac{x}{a - d}\right)^2 + \left(\frac{y - y_0}{b - d}\right)^2 + \left(\frac{z - z_0}{c - d}\right)^2 \geq 1 \; .$$

The contents are defined by

$$\left(\frac{x}{a - d}\right)^2 + \left(\frac{y - y_0}{b - d}\right)^2 + \left(\frac{z - z_0}{c - d}\right)^2 < 1 \; .$$

Age (years)	a	b	c	d	y_0	z_0	Volume-wall[a] (cm^3)	Targeted volume-wall[b] (cm^3)	Volume-contents[c] (cm^3)
0	1.69	1.82	1.14	0.10	-2.21	2.47	2.77	2.7	11.9
1	2.35	2.42	1.64	0.14	-2.93	3.51	7.41	7.2	31.7
5	3.04	2.77	2.16	0.17	-3.38	4.66	14.0	14.0	62.2
10	3.61	3.04	2.63	0.20	-3.78	5.81	22.3	22.2	98.6
15	4.27	3.38	3.11	0.23	-4.41	7.21	34.5	34.6	154
Adult	4.958	3.458	3.458	0.252	-4.50	8.00	45.7	45.0	203

[a]Volume (wall) = $\frac{4}{3}\pi[abc - (a - d)(b - d)(c - d)]$.

[b]Derived from ICRP Publication 23 (1975).

[c]Volume (contents) = $\frac{4}{3}\pi(a - d)(b - d)(c - d)$.

Dose to the bladder wall from a photon emitter present in the urine will vary greatly, depending on the degree of filling even for the same concentration or amount of activity present. The specific absorbed fraction, Φ (bladder wall $\leftarrow$ contents), will vary by approximately an order of magnitude in the adult, according to the calculations of Snyder, Ford, and Warner (1970). Thus, the reader should be aware that specific absorbed fractions calculated using these phantoms are appropriate only for one size of bladder. The difference in Φ to bladder walls of different sizes from other source organs outside the bladder is generally small (Snyder 1970).

Uterus. The uterus is an ellipsoid cut by a plane and is given by

$$\left(\frac{x}{a}\right)^2 + \left(\frac{y - y_0}{b}\right)^2 + \left(\frac{z - z_0}{c}\right)^2 \leq 1$$

and $y \geq y_1$.

Age (years)	a	b	c	y_0	z_0	y_1	Volume[a] (cm^3)	Targeted volume[b] (cm^3)
0	0.83	2.57	0.49	-0.98	4.32	-2.27	3.70	3.7
1	0.61	1.80	0.36	-1.30	6.14	-2.20	1.40	1.4
5	0.78	2.00	0.47	-1.50	8.16	-2.51	2.60	2.6
10	0.91	2.17	0.57	-1.68	10.16	-2.78	4.00	4.0
15	1.72	3.91	1.08	-1.96	12.62	-3.92	25.7	25.7
Adult	2.50	5.00	1.50	-2.00	14.00	-4.50	66.3	76.0

[a]Volume $= \pi ac\left[\frac{2}{3}b + |y_1 - y_0| - \frac{|y_1 - y_0|^3}{3b^2}\right]$.

[b]Derived from ICRP Publication 23 (1975).

CONCLUDING REMARKS

The pediatric phantoms presented here are intended to replace the similitude phantoms developed by Snyder and co-workers and the pediatric phantoms designed by Hwang and co-workers for estimating absorbed dose. These phantoms have been designed to form a developmentally consistent family of phantoms with the Fisher-Snyder adult phantom.

The regional distribution of the hematopoietically active bone marrow in children is more accurately portrayed in these phantoms than in previous phantoms, because the method of Cristy (1980), a refinement of the method of Atkinson (1962), was employed.

Organ sizes for each age were chosen to be consistent with age-dependent data presented in ICRP Publication 23 (1975). In most cases, shape and location of organs were determined using the Similitude Rule; but where exceptions to the rule were recognized, appropriate adjustments were made. Since it is important in the Monte Carlo transport computer code that the organs not overlap (i.e., a point in the phantom must be assigned to a single organ), extensive effort was devoted to plotting organ outlines for cross-sections through a phantom to detect potential overlap of organs.

The author encourages readers to inform him of any errors discovered, important data overlooked which could be used to improve the phantoms, or any constructive suggestions about improvement of the phantoms that are consistent with their use in conjunction with the dosimetry of internal emitters.

ACKNOWLEDGMENT

Appreciation is extended to G. G. Warner of the Computer Sciences Division for providing the three-dimensional perspective drawings in Figs. 3-4.

REFERENCES

Atkinson, H. R. 1962. Bone marrow distribution as a factor in estimating radiation to the blood-forming organs. *J. Coll. Radiol. Aust.* 6: 149-154.

Bardeen, C. R. 1920. The height-weight index of build in relation to linear and volumetric proportions and surface-area of the body during post-natal development. *Contributions to Embryology* IX: 483-552.

Boice, J. D., Rosenstein, M., and Trout, E. D. 1978. Estimation of breast doses and breast cancer risk associated with repeated fluoroscopic chest examinations of women with tuberculosis. *Radiat. Res.* 73: 373-390.

Coffey, J. L. 1978. *A revised mathematical model of the heart for use in radiation absorbed dose calculations.* M.S. thesis, Univ. Tenn., Knoxville.

Coffey, J.L., Cristy, M., and Warner, G. G. 1980. *Specific absorbed fraction for photon sources uniformly distributed in the heart contents and heart wall of a heterogeneous phantom.* MIRD Pamphlet No. 13. New York Society of Nuclear Medicine. (In press.)

Cristy, M. 1980. Active bone marrow distribution as a function of age in humans. (Submitted for publication).

Custer, R. P. 1974. *An atlas of the blood and bone marrow.* 2nd ed. Philadelphia: Saunders.

Eycleshymer, A. C., and Schoemaker, D. M. 1911. *A cross-section anatomy.* New York: Appleton.

Fisher, H. L., and Snyder, W. S. 1967. Distribution of dose in the body from a source of gamma rays distributed uniformly in an organ. *Health Phys. Div. Annu. Prog. Rep. July 31, 1967.* ORNL-4168, pp. 245-257.

Fisher, H. L., and Snyder, W. S. 1968. Distribution of dose in the body from a source of gamma rays distributed uniformly in an organ. In *Proc. First Internat. Congr. Radiat. Protection, Rome, Italy, September 5-10, 1966,* pp. 1473-1486. Oxford: Pergamon.

Hansman, C. F. 1966. Growth of interorbital distance and skull thickness as observed in roentgenographic measurements. *Radiol.* 86: 87-96.

Hashimoto, M. 1960. The distribution of active marrow in the bones of normal adult. *Kyushu J. Med. Sci.* 11: 103-111.

Hayes, R. L. 1960. *Standard-man phantoms.* USAEC Report ORINS-35.

Hilyer, M. J. C., Snyder, W. S., and Warner, G. G. 1972. Estimates of dose to infants and children from a photon emitter in the lungs. *Health Phys. Div. Annu. Prog. Rep. July 31, 1972.* ORNL-4811, pp. 91-96.

Hudson, G. 1965. Bone-marrow volume in the human foetus and newborn. *Brit. J. Haemat.* 11: 446-452.

Hwang, J. M. L., Shoup, R. L., and Poston, J. W. 1976a. *Mathematical description of a newborn human for use in dosimetry calculations.* ORNL/TM-5453.

Hwang, J. M. L., Shoup, R. L., and Poston, J. W. 1976b. *Modifications and additions to the pediatric and adult mathematical phantoms.* ORNL/TM-5454.

Hwang, J. M. L. H., Shoup, R. L., Warner, G. G., and Poston, J. W. 1976. *Mathematical descriptions of a one- and five-year-old child for use in dosimetry calculations.* ORNL/TM-5293.

International Commission on Radiological Protection. Publication 23. 1975. *Report of the task group on reference man.* Oxford: Pergamon.

International Commission on Radiological Protection. Publication 26. 1977. *Recommendations of the International Commission on Radiological Protection, annals of the ICRP, Vol. 1, No. 3.* Oxford: Pergamon.

Jones, R. M., Poston, J. W., Hwang, J. L., Jones, T. D., and Warner, G. G. 1976. *The development and use of a fifteen-year-old equivalent mathematical phantom for internal dose calculations.* ORNL/TM-5278.

Kerr, G. D. 1979. Organ dose estimates for the Japanese atomic-bomb survivors. *Health Phys.* 37: 487-508.

Krogman, W. M. 1941. *Growth of man.* Tabulae Biologicae, vol. XX. The Hague: Dr. W. Junk.

Mechanik, N. 1926. Untersuchungen über das Gewicht des Knochenmarkes des Menschen. *Z. Anat. Entwicklungs-Gesch.* 79: 58-99.

Poston, J. W. 1976. The effects of body and organ size on absorbed dose: there is no standard patient. *Radiopharmaceutical Dosimetry Symposium, Oak Ridge, Tenn.* HEW Publication (FDA) 76-8044, pp. 92-109.

Poston, J. W., Snyder, W. S., and Warner, G. G. 1975. Age factors for dose rates from an infinite cloud of a phantom emitter. *Health Phys. Div. Annu. Prog. Rep. June 30, 1975.* ORNL-5046, pp. 249-252.

Scammon, R. E. 1953. Developmental anatomy. In *Morris' human anatomy*, 11th ed., ed. J. P. Schaeffer, pp. 11-62. New York: McGraw-Hill (Blakiston Div.).

Schaeffer, J. P., ed. 1953. *Morris' human anatomy*. 11th ed. New York: McGraw-Hill (Blakiston Div.).

Snyder, W. S. 1970. Estimation of absorbed fraction of energy from photon sources in body organs. In *Medical radionuclides: radiation dose and effects, proc. symp. held at the Oak Ridge Associated Universities, December 8-11, 1969*. CONF-691212, pp. 33-49.

Snyder, W. S. 1977. Private communication to J. K. Poggenburg.

Snyder, W. S., and Cook, M. J. 1971. Preliminary indications of the age variation of the specific absorbed fraction for photons. *Health Phys. Div. Annu. Prog. Rep. July 31, 1971*. ORNL-4720, pp. 116-118.

Snyder, W. S., and Ford, M. R. 1973. Estimates of dose rate to gonads of infants and children from a photon emitter in various organs of the body. *Health Phys. Div. Annu. Prog. Rep. July 31, 1973*. ORNL-4903, pp. 125-129.

Snyder, W. S., Ford, M. R., Poston, J. W., and Warner, G. G. 1976. Estimates of photon dose to the gonads per microcurie-day as a function of the source organ and the age of the individual. *Health Phys. Div. Annu. Prog. Rep. June 30, 1976*. ORNL-5171, pp. 27-40.

Snyder, W. S., Ford, M. R., and Warner, G. G. 1970. Estimation of dose and dose commitment to bladder wall from a radionuclide present in urine. *Health Phys. Div. Annu. Prog. Rep. July 31, 1970*. ORNL-4584, pp. 206-208.

Snyder, W. S., Ford, M. R., Warner, G. G., and Watson, S. B. 1974. *A tabulation of dose equivalent per microcurie-day for source and target organs of an adult for various radionuclides: Part 1*. ORNL-5000.

Southwood, W. F. W. 1955. The thickness of the skin. *Plast. Reconst. Surg*. 15: 423-429.

Tipton, I. H., Snyder, W. S., and Cook, M. J. 1966. Elemental composition of Standard Man. *Health Phys. Div. Annu. Prog. Rep. July 31, 1966*. ORNL-4007, pp. 240-241.

United Nations Scientific Committee on the Effects of Atomic Radiation. 1977. *Sources and effects of ionizing radiation*. General Assembly, Official Records: Thirty-Second Session, Supplement No. 40 (A/32/40). New York.

Warner, G. G., Poston, J. W., and Snyder, W. S. 1974. Absorbed dose in male humanoid phantoms from external sources of photons as a function of age. *Health Phys. Div. Annu. Prog. Rep. July 31, 1974.* ORNL-4979, pp. 40-45.

Watson, E. H., and Lowrey, G. H. 1967. *Growth and development of children.* 5th ed. Chicago: Year Book Medical.

Woodard, H. Q., and Holodny, E. 1960. A summary of the data of Mechanik on the distribution of human bone marrow. *Phys. Med. Biol.* 5: 57-59.

APPENDIX

Summary of Organ Masses in All Phantoms

Table 6. Summary of organ masses in all phantoms

Organ	Mass (g) at various ages					
	0	1	5	10	15	Adult
Skeletal system -- active marrow						
Leg bones -- upper portion[a]	0.879	3.11	10.9	28.8	48.3	37.5
Leg bones -- middle portion[a]	1.75	5.82	20.1	37.5	21.4	0
Leg bones -- lower portion[a]	7.63	20.1	37.0	33.6	0	0
Arm bones -- upper portion[a]	1.09	3.62	7.55	15.2	33.0	25.6
Arm bones -- middle portion[a]	1.09	3.38	6.98	9.88	7.35	0
Arm bones -- lower portion[a]	2.85	6.54	9.22	6.47	0	0
Pelvis	5.48	24.7	74.7	175	353	373
Spine -- upper portion[b]	1.08	2.82	4.67	11.0	23.6	29.8
Spine -- middle portion[b]	4.42	13.9	30.7	71.9	155	195
Spine -- lower portion[b]	0.893	5.06	17.2	40.4	87.0	110
Skull -- cranium	12.3	35.4	41.8	56.6	72.8	62.4
Skull -- facial skeleton	1.52	5.81	14.0	21.0	33.5	30.8
Ribs	4.32	14.4	33.9	79.4	171	215
Clavicles	0.376	1.25	2.72	5.43	10.3	8.85
Scapulae	1.27	4.10	8.70	17.6	34.2	31.9
Skeletal system -- inactive marrow						
Leg bones -- upper portion[a]	0	0.168	3.30	19.5	59.4	112
Leg bones -- middle portion[a]	0	0.744	8.33	59.5	194	298
Leg bones -- lower portion[a]	0	9.07	55.0	236	568	763
Arm bones -- upper portion[a]	0	0.194	2.28	10.3	40.6	76.4
Arm bones -- middle portion[a]	0	0.442	2.88	15.6	66.5	102
Arm bones -- lower portion[a]	0	3.49	16.9	72.3	144	191
Pelvis	0	1.36	18.6	70.0	206	382
Spine -- upper portion[b]	0	0.156	0.854	2.77	7.91	12.6
Spine -- middle portion[b]	0	0.764	5.53	18.3	51.8	83.3
Spine -- lower portion[b]	0	0.280	3.09	10.3	29.5	46.9
Skull -- cranium	0	1.95	10.7	30.8	59.8	101
Skull -- facial skeleton	0	0.320	3.57	11.4	27.5	50.0

Table 6 (continued)

Organ	Mass (g) at various ages					
	0	1	5	10	15	Adult
Ribs	0	0.780	6.05	20.2	57.4	91.9
Clavicles	0	0.070	0.742	3.13	9.46	17.9
Scapulae	0	0.212	2.24	9.68	28.2	51.6
Skeletal system -- bone						
Leg bones -- upper portion[a]	23.6	72.0	216	419	733	1010
Leg bones -- middle portion[a]	34.7	111	325	622	1034	1390
Leg bones -- lower portion[a]	22.6	85.0	231	396	461	555
Arm bones -- upper portion[a]	24.3	64.0	124	201	336	434
Arm bones -- middle portion[a]	18.0	47.2	91.0	145	234	301
Arm bones -- lower portion[a]	20.0	51.0	94.6	125	225	291
Pelvis	37.4	86.9	131	137	126	145
Spine -- upper portion[b]	18.8	46.0	75.5	110	163	204
Spine -- middle portion[b]	35.2	87.9	169	255	416	536
Spine -- lower portion[b]	14.0	33.1	56.8	78.8	117	149
Skull -- cranium	61.7	169	451	557	623	754
Skull -- facial skeleton	7.59	27.7	151	207	286	373
Ribs	46.2	115	218	339	561	724
Clavicles	3.52	8.87	16.9	25.9	42.1	54.5
Scapulae	13.1	33.3	64.0	100	166	217
Skeletal system -- bone + marrow						
Leg bones -- upper portion[a]	24.5	75.3	230	467	841	1154
Leg bones -- middle portion[a]	36.5	118	353	719	1250	1690
Leg bones -- lower portion[a]	30.2	114	323	666	1030	1320
Arm bones -- upper portion[a]	25.4	67.9	134	227	410	536
Arm bones -- middle portion[a]	19.1	51.0	101	170	308	403
Arm bones -- lower portion[a]	22.9	61.0	121	204	369	482
Pelvis	42.9	113	225	383	684	901
Spine -- upper portion[b]	19.9	49.0	81.1	124	194	246

Table 6 (continued)

Organ	Mass (g) at various ages					
	0	1	5	10	15	Adult
Spine -- middle portion[b]	39.6	103	205	345	623	815
Spine -- lower portion[b]	14.8	38.4	77.1	129	234	306
Skull -- cranium	74.0	206	504	644	755	918
Skull -- facial skeleton	9.11	33.9	169	239	347	454
Ribs	50.5	130	258	438	789	1030
Clavicles	3.90	10.2	20.3	34.4	61.9	81.2
Scapulae	14.3	37.6	75.0	127	229	300
Adrenals	5.53	3.34	5.00	6.85	9.94	15.5
Brain	334	839	1200	1290	1340	1350
Breasts -- including skin	0.195	1.05	2.06	3.47	44.2	357
Breasts -- excluding skin	0.102	0.695	1.43	2.47	34.6	310
Gall bladder -- wall	0.387	0.863	3.54	6.91	8.80	10.0
Gall bladder -- contents	2.02	4.56	18.7	36.5	46.5	52.9
Gastrointestinal tract and contents						
-- stomach wall	6.09	20.7	46.6	80.7	112	150
-- stomach contents	10.0	34.4	71.3	126	185	247
-- small intestine, wall and contents	50.2	131	261	441	795	1040
-- upper large intestine wall	9.93	26.4	52.4	88.6	160	209
-- upper large intestine contents	10.6	27.3	55.0	92.5	167	220
-- lower large intestine wall	7.55	19.6	39.3	66.4	120	158
-- lower large intestine contents	6.62	17.4	34.7	58.6	104	136
Heart -- walls	24.1	48.1	88.1	144	228	300
Heart -- contents	34.7	69.0	127	208	330	431
Kidneys	21.7	59.7	110	164	235	284
Liver	115	277	554	842	1220	1810
Lungs	50.6	143	290	453	650	999

Table 6 (continued)

Organ	Mass (g) at various ages					
	0	1	5	10	15	Adult
Ovaries	0.311	0.677	1.64	2.97	4.91	8.27
Pancreas	2.66	9.74	22.4	28.5	61.6	89.5
Skin	112	258	510	843	2030	2860
Spleen	8.64	24.2	45.8	73.4	117	174
Testes	0.800	1.15	1.55	1.80	14.8	37.1
Thymus	10.7	21.7	28.1	29.8	26.9	19.8
Thyroid	1.22	1.69	3.28	7.52	11.7	19.6
Urinary bladder -- wall	2.74	7.31	13.8	22.0	34.0	45.1
Urinary bladder -- contents	11.8	31.2	61.4	97.3	152	200
Uterus	3.65	1.38	2.57	3.94	25.4	65.4

[a]The upper, middle, and lower portions of the leg bones and arm bones are defined in Table 4 of the main text.

[b]The upper, middle, and lower portions of the spine are defined in the section of the main text defining the spine.

NUREG/CR-1159
ORNL/NUREG/TM-367
Dist. Category RH

INTERNAL DISTRIBUTION

1. R. O. Chester
2. D. J. Crawford
3-7. M. Cristy
8. D. E. Dunning, Jr.
9-13. K. F. Eckerman
14. M. R. Ford
15. S. V. Kaye
16. F. F. Knapp
17. R. W. Leggett
18. D. C. Parzyck
19. C. R. Richmond
20. P. S. Rohwer
21. J. C. Ryman
22. P. J. Walsh
23. M. G. Yalcintas
24-28. Internal Dosimetry Information Center, ORNL
29-30. Central Research Library
31-32. Laboratory Records Department
33. Laboratory Records Department-RC
34. ORNL-Patent Office
35. RSIC Library

EXTERNAL DISTRIBUTION

36. J. Coffey, Manpower, Education Research Training, Oak Ridge Associated Universities, Oak Ridge, TN 37830
37. K. Henrichs, Klinikum Steglitz der freien Universität Berlin, Klinik für Radiologie, Nuklearmedizin und Physikalische Therapie, Hindenburgdamm 30, D-1000 Berlin 45, Federal Republic of Germany
38. R. Kramer, Gesellschaft für Strahlen- und Umweltforschung, m.b.H. München, Ingolstadter Landstrasse 1, Institut für Strahlenschutz, 8042 Neuherberg bei Munchen, Fed. Rep. of Germany
39. Katherine A. Lathrop, University of Chicago, Chicago, IL
40. C. Pomroy, Head, Human Monitoring Laboratory, Consumer and Clinical Radiation Hazards Division, Radiation Protection Bureau, Brookfield Road, Ottawa, Ontario, Canada K1A 1C1
41. J. W. Poston, School of Nuclear Engineering, Georgia Institute of Technology, Atlanta, GA 30332
42. H. D. Roedler, Bundesgesundheitsamt, Ingolstadter Landstrasse 1, 8042 Neuherberg bei München, Fed. Rep. of Germany
43. M. Rosenstein, Bureau of Radiological Health, Food and Drug Administration, 12720 Twinbrook Parkway, Rockville, MD 20852
44. B. Schleien, Assistant Director for Scientific Affairs, Bureau of Radiological Health, 5600 Fishers Lane, Rockville, MD 20857
45. R. Simpson, Bureau of Radiological Health, Food and Drug Administration, 12720 Twinbrook Parkway, Rockville, MD 20857
46. R. E. Sullivan, Bioeffects Analysis Branch, Criteria and Standards Division, Office of Radiation Programs, U.S. Environmental Protection Agency, Washington, DC 20460
47. F. Swanberg, Chief, Branch of Health and Environmental Research, U.S. Nuclear Regulatory Commission, Washington, DC 20555
48. G. Tanaka, Division of Radioecology, National Institute of Radiological Sciences, Nakaminato Laboratory, 3609 Isozaki, Nalcaminato, Ibaraki 311-12, Japan

49. E. Walters, Radiation Health Information Project, Environmental Policy Institute, 317 Pennsylvania Avenue, S.E., Washington, DC 20003
50. K. Wise, Australian Radiation Laboratory, Lower Plenty Road, Yallambie, Victoria, Australia 3085
51. Office of Assistant Manager, Energy Research and Development, DOE-ORO, Oak Ridge, TN 37830
52-53. Technical Information Center, Oak Ridge, TN 37830
54-233. Given distribution according to NRC Category RH

☆U.S. GOVERNMENT PRINTING OFFICE: 1980-640-245/111